Methionine Sulfoxide Reductase mediated Redox regulation of mitochondrial GrpE (Mge1), a co-chaperone of Hsp70, during oxidative stress

Thesis submitted for the degree of

DOCTOR OF PHILOSOPHY

By

Praveen Kumar Allu

(10LBPH08)

Department of Biochemistry

School of Life Sciences

University of Hyderabad - 500046

Department of Biochemistry

School of Life Sciences

University of Hyderabad

Hyderabad-500 046

India

CERTIFICATE

This is to certify that this thesis entitled **"Methionine Sulfoxide Reductase mediated redox regulation of mitochondrial GrpE (Mge1), a co-chaperone of Hsp70, during oxidative stress"** submitted to the University of Hyderabad by **Mr. Praveen Kumar Allu**, for the degree of Doctor of Philosophy, is based on the studies carried out by him under my supervision. I declare to the best of my knowledge that this has not been submitted earlier for the award or diploma from any other University or Institution.

Dr. Naresh Babu V. Sepuri

Supervisor

Head

Department of Biochemistry

Dean

School of Life Sciences

Department of Biochemistry

School of Life Sciences

University of Hyderabad

Hyderabad 500 046

India

DECLARATION

I hereby declare that the work presented in my thesis is entirely original and was carried out by me in the Department of Biochemistry, University of Hyderabad, under the supervision of **Dr. Naresh Babu V Sepuri.** I further declare that this work has not been submitted earlier for the award of degree or diploma from any other University or Institution.

Dr. Naresh Babu V Sepuri

Supervisor

Praveen Kumar Allu

Date:

Place: Department of Biochemistry

University of Hyderabad - 500 046

Department of Biochemistry

School of Life Sciences

University of Hyderabad

Hyderabad 500 046

India

DECLARATION

I **Praveen Kumar Allu,** hereby declare that this thesis entitled "**Methionine Sulfoxide Reductase mediated redox regulation of mitochondrial GrpE (Mge1), a co-chaperone of Hsp70, during oxidative stress** " submitted by me under the guidance and supervision of **Dr. Naresh Babu V sepuri** is a bonafide research work which is also free from plagiarism. I also declare that it has not been submitted previously in part or in full to this University or any other University or Institution for the award of any degree or diploma. I hereby agree that my thesis can be deposited in shodganga/INFLIBNET.

A report on plagiarism statistics from the University Librarian enclosed.

Date:

Name: Praveen Kumar Allu

Signature of the student

Reg.No. 10LBPH08

Signature of the supervisor:

Acknowledgments

- First and foremost I offer my sincerest gratitude to my supervisor ***Dr.Naresh Babu V Sepuri*** for his continuous support throughout my research with his motivation, enthusiasm, immense knowledge, invaluable guidance, advice and ideas make my thesis possible here. I could not have imagined having a better advisor and mentor for my Ph.D. thesis. He has been invaluable on both an academic and a personal level, for which I am extremely grateful. His attention, moral support and timely suggestions were useful in the preparation of my thesis. I am always grateful to my supervisor for everything.

- I am always thankful to my doctoral committee members: ***Dr. Krishnaveni Mishra*** and ***Dr. Mrinal Kanti Bhattacharyya*** for their critical comments and invaluable suggestions on my PhD work.

- I would like to thank Heads of Department of Biochemistry **(*Prof. N. Siva Kumar, Prof. O.H. Setty, Prof. K.V.A Ramaiah***) and Deans of School of Life Sciences (***Prof. Pallu Reddanna, Prof. A.S Raghavendra, Prof. R.P. Sharma, Prof. Ramanadham***) for allowing me to use all the central facilities of department and school.

- I express my gratitude to ***Dr. Bramanandam Manavathi, Dr. S. Rajagopal, Dr. A. C. Narayana, Dr. Abhijit Mitra (IIIT-H)*** for moral support, inspiration and encouragement.

- I would like to specially acknowledge ***Dr. Thanuja Krishnamoorthy*** for the invaluable suggestions and sparing her valuable time in patiently reading my manuscripts and PhD thesis.

- I thank all faculty members of school of life sciences, I also thank all the non-teaching staff for their timely help.

- I sincerely acknowledge *Mrs. Monica Kannan* and *Mr. Raghu Tadala* for his help in mass spectrometry and data analysis.
- I also thank my lab mates *Dr. Pulla Reddy*, *Dr. Samuel*, *Dr. Anjaneyulu*, *Dr.Prasad*, *Madhavi*, *Dr. Aadhinarayana*, *Fareed*, *Ramana*, *Srinivas*, *Yerranna*, *Chandrasekhar*, *Viswamitra*, *Naimisha*, *Nilam* and *Narasimha* for making my stay in the lab wonderful. I particularly thank *Prasad*, *Madhavi* and *Fareed* for all their help during my PhD.
- I have been really privileged to have friends; *Dr. Venugopal*, *Sivaramprasad*, *Sai kiran Naville*, *Suresh*, *Vijay N reddy*, *Maruthi*, *Kamu*, *Chava Suresh*, *Sangeetha* and *Subbu*. They literally supported me all through my ups and *downs*. I thank all my Friends for their love and affection.
- I acknowledge CSIR for my financial support through JRF and SRF.
- I also thank all the funding bodies (CSIR, UGC, ICMR, DBT, CREBB, DST, FIST, UPE, PURSE) for their financial assistance to the department and school.
- I would like to thank my family member's *Sujatha* (Mom), *Srinivasuslu* (Dad), *Preethi* and *Naresh* for all the love and support. Their love and care always made me happy and forget the bad times.
- Finally, I thank God Almighty for his blessings throughout.

…… *Praveen Kumar Allu*

Table of contents

Chapter 1: General Introduction

1.1 Mitochondria

1.2 Mechanism of mitochondrial biogenesis

1.3 Protein import into mitochondria

1.4 Quality control in mitochondria

1.5 Electron transport complex

1.6 Iron-Sulfur (Fe/S) cluster biogenesis

1.7 MtDNA

1.8 Cellular sources of reactive oxygen species

1.9 ROS detoxification mechanisms

1.10 Oxidative stress: real culprit for age related diseases

1.11 Redox-regulation of proteins

1.11.1 Regulation of proteins through Cys redox mechanism

1.12 Methionine oxidation and methionine sulfoxide reductases

1.12.1 Catalytic mechanism of methionine sulfoxide reductases

1.12.2 Proteins regulated by Met oxidation

1.13 Mitochondria - the site of redox regulation

1.14 Hsp70 chaperone system in mitochondrial biogenesis

1.15 Structural topology of GrpE

1.16 Scope of the study

Chapter 2: Methionine sulfoxide reductase 2 reversibly regulates Mge1, a co-chaperone of mitochondrial Hsp70, during oxidative stress.

2.1 Introduction

2.2 Methodology

2.2.1 Plasmid construction

2.2.2 Expression and purification of recombinant proteins

2.2.3 Yeast strains and construction

2.2.4 Yeast media - growth conditions

2.2.5 Spotting assay

2.2.6 Isolation of mitochondria

2.2.7 *In vitro* protein import

2.2.8 Preparation of mitoplasts and treatment with proteinase K

2.2.9 Ni pull down assay

2.2.10 Co-immunoprecipitation

2.2.11 Mxr2 enzymatic assay

2.2.12 ATPase assay of Hsp70

2.2.13 ROS measurement

2.2.14 Purification of His-Mge1 from yeast cells

2.2.15 *In vitro* treatment of Mge1 with H_2O_2 and Mxr2 for MALDI-TOF analysis

2.2.16 Mass spectrometry

2.2.17 Protein aggregation assay

2.3 Results

2.3.1 Deletion of MXR2 exacerbates sensitivity to H_2O_2

2.3.2 Mxr2 localized to mitochondrial matrix

2.3.3 Mxr2 interacts with Mge1 in an oxidative stress dependent manner

2.3.4 *In vivo* oxidative stress dependent interaction of Mxr2 and Mge1

2.3.5 Oxidation of Mge1 at methionine 155 and its subsequent reduction by Mxr2 *in vitro*

2.3.6 Mge1 is a physiological substrate of Mxr2

2.3.7 *In vivo* oxidation of Mge1

2.3.8 Mge1 M155L protects cells from stress mediated protein aggregation

2.4 Discussion

Tables

2.1 Primers used in this chapter

2.2 Plasmids Used in this chapter

2.3 Yeast strains used in this chapter

2.4 Peptides generated from Mge1 after digestion with LysC enzyme

Chapter 3: R type Methionine Sulfoxide reductase reverses oxidized mammalian GrpE to regulate Hsp70 chaperone cycle

3.1 Introduction

3.2 Methodology

3.2.1 Plasmid construction

3.2.2 Proteins expression and purification

3.2.3 Yeast strains construction

3.2.4 Yeast media and growth assay

3.2.5 *In vitro* interaction assay

3.2.6 *In vitro* Mxr2 enzymatic assay and reduction of oxidized hGrpEL1

3.2.7 Hsp70 ATPase assay

3.2.8 Mitochondria Isolation

3.2.9 MALDI studies

3.3 Results

3.3.1 Human GrpEL1 is sensitive to H_2O_2 and methionine oxidation alters the ATPase stimulating activity on Hsp70

3.3.2 Human GrpEL1 complements the deletion of yMge1

3.3.3 Mammalian Methionine R sulfoxide complements yeast mxr2 deletion and

interacts with oxidized hGrpEL1

3.3.4 Reduction of hGrpEL1-Met SO at Met146 by R type enzymes

3.3.5 Human GrpEL1 M146L functionally complements the oxidative sensitive phenotype of *mxr2*Δ *in vivo*

3.4 Discussion

Tables

3.1 Primers used in this chapter

3.2 Plasmids used in this chapter

3.3 Yeast Strains are used in this chapter

3.4 Peptides generated from hGrpEL1 after digestion with trypsin enzyme

Bibliography

Publications

Acronyms

Acronyms used in this thesis

AAC	ATP/ADP carrier
APS	Ammonium per sulphate
ATP	Adenosine triphosphate
BSA	Bovine serum albumin
CCPO	Cytochrome C peroxidase
CoxIV	Cytochrome oxidase subunit IV
co-IP	Co-immunoprecipitation
Cys	Cysteine
SU9-DHFR	Subunit 9 – Dihydrofolate reductase
DTT	Dithiothreitol
DCF-DA	2′,7′-Dichlorodihydrofluorescein diacetate
ECL	Enhanced chemiluminescence
EDTA	Ethylene diamine tetra acetic acid
ETC	Electron transport complex
5- FOA	Flouro orotic acid
GST	Glutathione S transferase
HEPES	(N-(2-Hydroxyethyl)-piperizine-N'-(2-ethane sulfonic acid)
H_2O_2	Hydrogen peroxide
HSP	Heat shock protein
IgG	Immunoglobulin G
IMS	Inter membrane space
IMM	Inner mitochondrial membrane
IPTG	Isopropyl β-D-thiogalactopyranoside

I-TASSER	Iterative Threading ASSEmbly Refinement
LEU	Leucine
kDa	Kilo Dalton
M	Molar
MALDI	Matrix-assisted laser desorption/ionization
Met	Methionine
Met-SO	Methionine sulfoxide
$MgCl_2$	Magnesium chloride
MPP	Mitochondrial processing peptidase
mtDNA	Mitochondrial deoxyribonucleic acid
Msrs	Methionine sulfoxide reductases
NaCl	Sodium chloride
NADH	Nicotinamide adenine dinucleotide
NADPH	Nicotinamide adenine dinucleotide phosphate
NC	Nitrocellulose
NBD	Nucleotide binding domain
Ni-NTA	Nickel nitrilotriacetic acid
NEF	Nucleotide exchange factor
OD	Optical density
OXPHOS	Oxidative phosphorylation
PAGE	Polyacrylamide gel electrophoresis
PAM	Presequence translocase associated motor
PBS	Phosphate-buffered saline
PCR	Polymerase chain reaction
PDB	Protein data bank
PMSF	Phenyl methylsulfonyl fluoride
ROS	Reactive oxygen species
Rpm	Rotations per minute
SBD	Substrate-binding domain

SC	Synthetic complete
SAM	Sorting and assembly machinery
SEM	Sucrose-EDTA-MOPS
S. cerevisiae	Saccharomyces cerevisiae
SDS	Sodium dodecyl sulfate
Ssc1	Stress-seventy subfamily C
Ssq1	Stess-seventy subfamily Q
TIM	Translocase of inner mitochondrial membrane
TOM	Translocase of outer mitochondrial membrane
TOF/MS	Time of flight Mass spectrometry
Tris	Tris-(Hydroxymethyl) aminoethane
URA	Uracil
WT	Wild type
$\Delta\Psi m$	Mitochondrial inner membrane potential
YPD	Yeast Extract, Peptone, Dextrose
YPGE	Yeast Extract, Peptone, Gylcerol, Ethanol

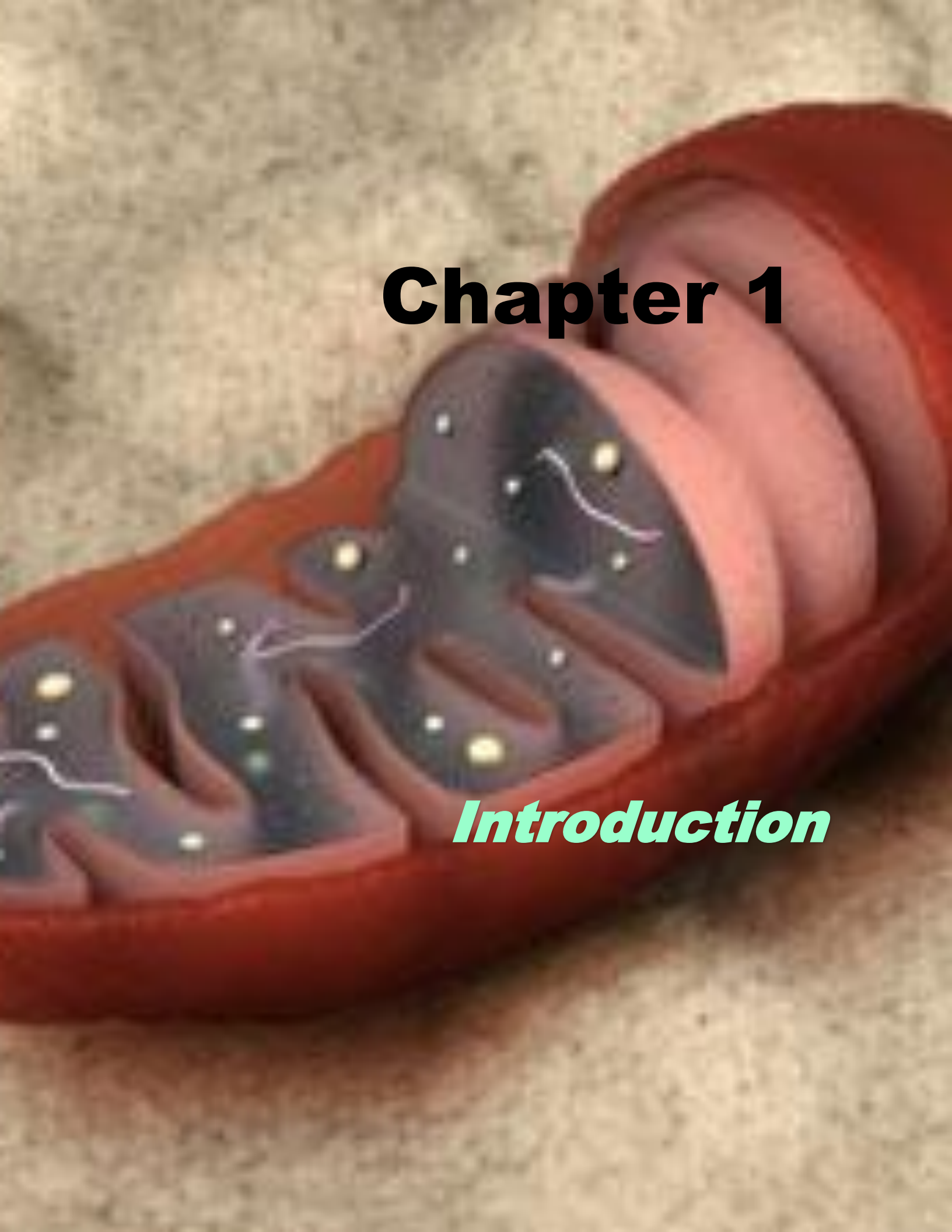

Chapter 1

Introduction

1.1 Mitochondria

Mitochondria are the power house of cell and required for performing different cellular functions ranging from cell survival to cell death [1], [2]. As indicated by endosymbiontic hypothesis, mitochondria are free living, ancient alphaproteobacteria that were occupied in the cytosol of primitive eukaryotic cell [3]. During evolutionary transition from symbiont to organized eukaryotic cell, mitochondria progressively lost independence and totally rely on nuclear encoded gene products for its biogenesis [4]. Although mitochondria lost most of the genes to nuclear genome, it contains autonomous replicating DNA and encodes proteins that play a significant role in electron transport complex (ETC) assembly. Apart from regulating various metabolic processes, mitochondria are also major site for reactive oxygen species (ROS) production [5]. Mitochondrial biogenesis requires coordination of several functions that includes nuclear encoded protein import and assembly, ETC assembly, mtDNA maintenance and mitochondrial fusion-fission [6], [7]

1.2 Mechanism of mitochondrial biogenesis

Mitochondria are double membrane organelles and consists of distinct compartments separated by outer and inner mitochondrial membranes with embedded aqueous inner mitochondrial space (IMS) and matrix [8]. Yeast mitochondria consists of nearly 1000 proteins and mammalian mitochondria contains approximately 1500 proteins [9], [10]. Most of these proteins are transcribed from nuclear genome and translated in cytosol. These pre-proteins from cytosol are imported into mitochondria through protein import machinery present on both outer and inner membranes with assistance of cytosolic and mitochondrial chaperones [11]. Assembly of precursor proteins into macromolecular complexes and mitochondrial proteostasis are mediated by a highly

conserved molecular chaperones and proteases [12], [13]. Environmental stress and external factors like nutrients,

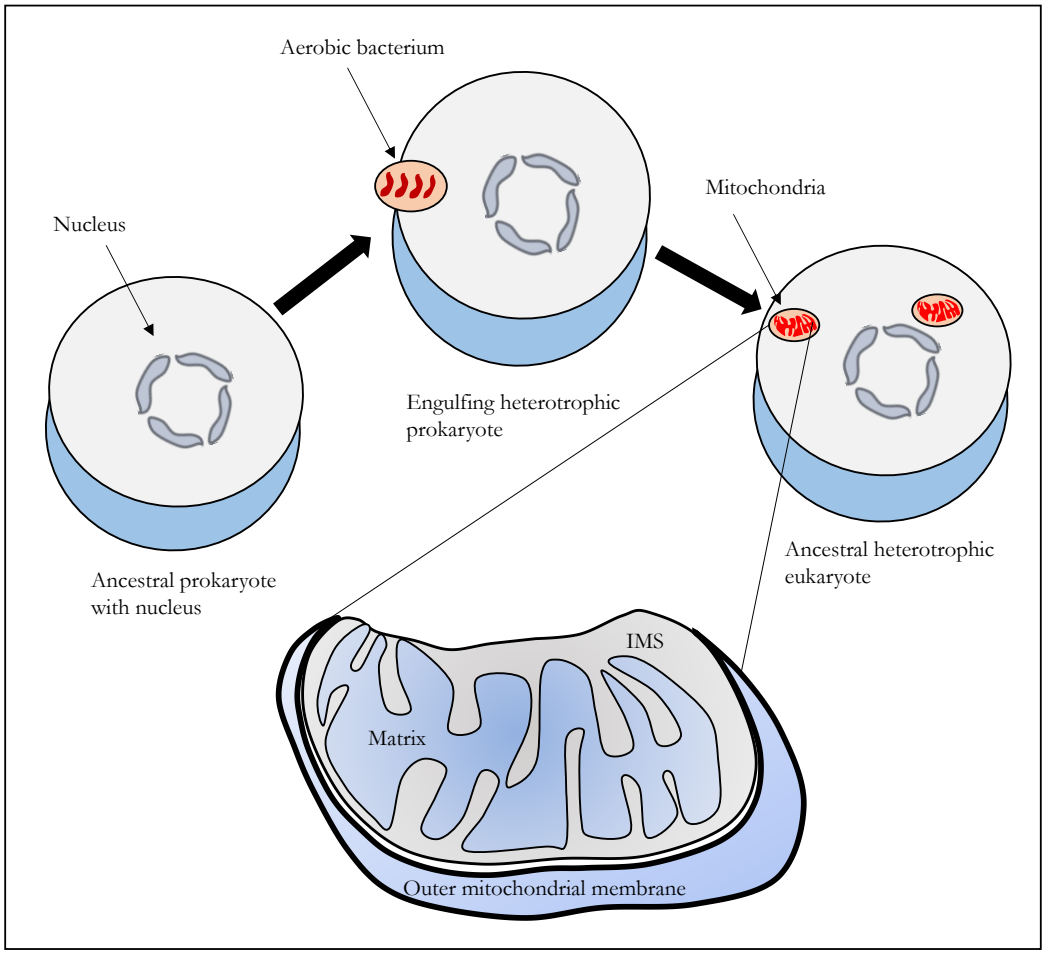

Figure 1.1 Endosymbiont theory

Alphaproteobacteria was engulfed by an ancestral prokaryote. During evolution most of genes from an ancient bacterium was transferred to a prokaryote and formed mitochondria in a eukaryotic cell. Inset image showing an ultra-structural features of mitochondria.

hormones, temperature, exercise, hypoxia and aging influence mitochondrial biogenesis and proliferation [14], [15]. Metabolic changes primarily regulate the biogenesis of mitochondria. This processes controlled by various signaling molecules and transcription factors like 5'adenosine monophosphate-activated protein kinase (AMPK), peroxisome proliferator-activated receptor γ

co-activator 1α (PGC-1alpha) and nuclear respiratory factors (NRF-1 and 2) [14]. Mitochondria are also known to contain several transcriptional factors (p53, STAT3, CREB etc.,) that are crucial for sustaining mitochondrial to nuclear communications [16], [17].

1.3 Protein import into mitochondria

Mitochondrial protein import system contains three main protein complexes that are required for translocation of nuclear encoded mitochondrial proteins. Translocase of Outer Membrane (TOM) and Translocase of Inner Membrane (TIM) complexes are outer and inner membrane components of the protein import system respectively. TOM complex acts as central entry gate for mitochondrial pre-proteins. TIM23 complex, an inner membrane TIM complex, targets most of the matrix proteins and some inner membrane proteins. TIM22 complex is also present in the inner mitochondrial membrane and helps in import and insertion of polytopic inner membrane proteins [11].

The TOM complex consists of Tom40 as a core protein and Tom5, Tom6, Tom20, Tom22 and Tom70 as associated components [18], [19]. TOM complex associated components in particular Tom20 and Tom70 not only required to stabilize the TOM complex but also has a specific role in the import of polypeptides [20]. Signals that are present in the precursor protein either at N-terminal or internal targeting sites are recognized by TOM complex machinery. Pre-proteins from TOM complex are further directed to specific locations by additional signals that are present in the protein. TIM23 complex is involved in sorting of matrix and membrane proteins and it mainly consists of Tim17, Tim23, Tim50 and translocation motor complex [20], [21, p. 50]. The driving energy for protein import into the mitochondrial matrix is mediated by translocation motor complex, which consists of Hsp70, Mge1, PAM complex (Pam16/Pam18, Pam17) and Tim44 [22],

[23] . The targeting of carrier/polytopic membrane proteins, like phosphate carrier and ADP/ATP carrier (AAC) requires TIM22 complex. It consists of Tim18, Tim22, Tim54 and small Tims (Tim8, Tim9, Tim10, Tim12, and Tim13) [24], [25]. These outer and inner membrane translocase complexes interact with each other in a dynamic manner, in coordination with molecular chaperones during protein import. Dynamic organization of translocase complex represents the key principle in protein import processes such as driving force, translocation and assembly of proteins in mitochondria [26], [27].

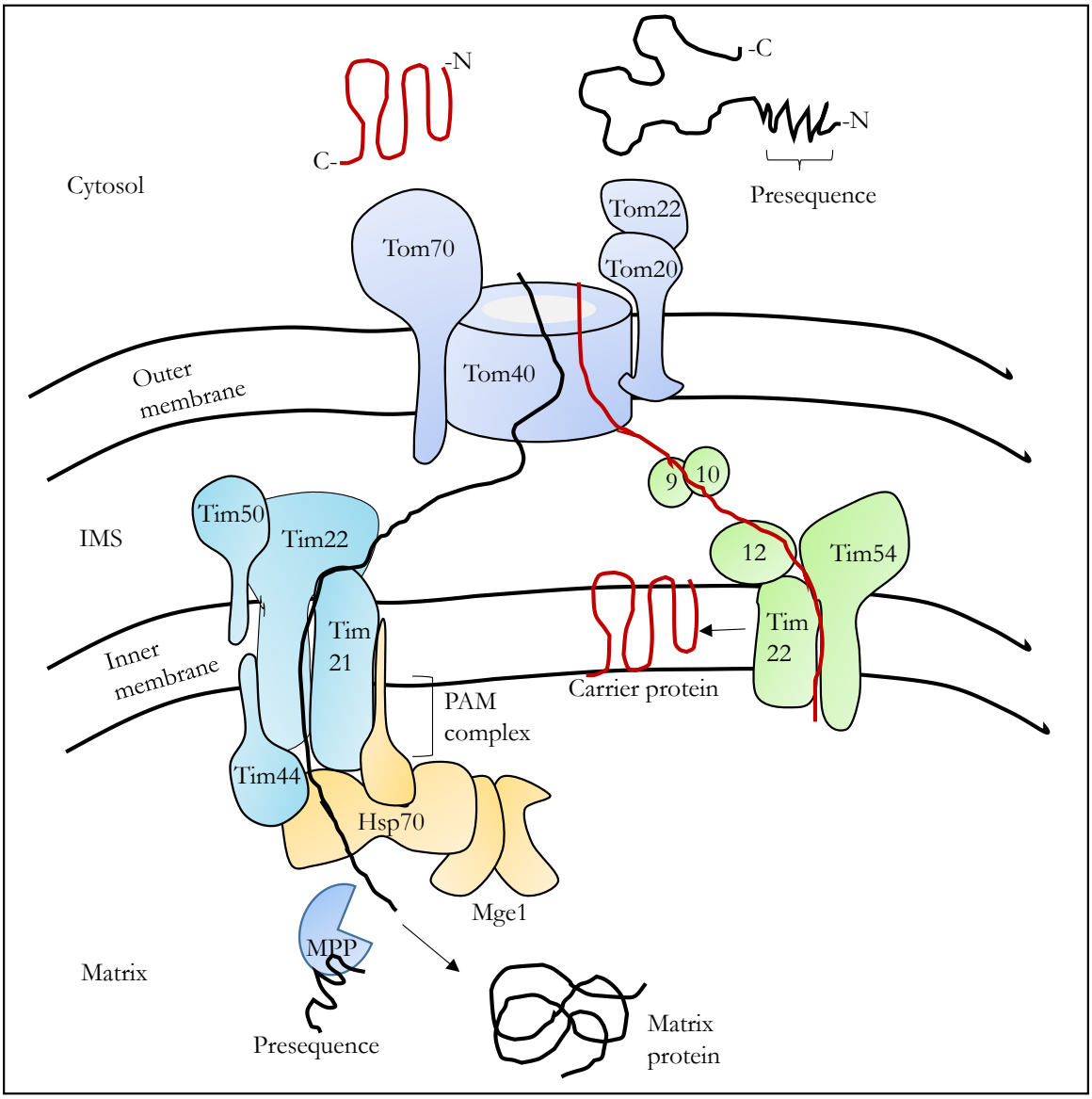

Figure 1.2 Protein import machinery in mitochondria

Nuclear encoded proteins are imported into mitochondria through translocases present on outer and inner mitochondrial membranes. Signals present on pre-proteins were identified by Translocase of outer membrane (TOM) complex. These pre-proteins are further translocated to different sub compartments of mitochondria through inner membrane translocases (TIM23 and TIM22) complexes.

Protein translocases are primary sites for mitochondrial biogenesis. Multiple investigations suggested that several kinases exert stimulatory or inhibitory effects on the protein import machinery. Mitochondrial protein import finely adjusted in response to metabolic changes, cell cycle dynamics in addition to external stress factors. For example, protein kinase A (PKA) induced phosphorylation of several components of TOM machinery, regulates the protein import at various levels. Similarly casein kinases (CKI and CKII) also regulate protein import by phosphorylation of the TOM complex, during metabolic switch from respiration to fermentation [28], [29]. Furthermore, proteomics and *in silico* approaches also predicted that phosphorylation of translocases present in IMS and TIM complex [30]–[32]. These reports intriguingly suggest that regulation of protein import in response to various external factors and metabolic changes might be crucial for mitochondrial biogenesis [33], [34].

1.4 Quality control in mitochondria

Chaperones play major role in cellular resistance to various stress conditions and participate in many constitutive cellular processes. Protein folding and intricate macromolecular assembly are indispensable mechanisms for cell survival. Molecular chaperones accomplish these tasks by recognizing either folding intermediates or non-native proteins thereby prevent the protein aggregation. Chaperones are usually called as Heat shock proteins (Hsp), owing to induce upon heat stress or other stress conditions. Most of the organisms contain five classes of chaperone families. Based on their molecular weight these chaperones are distinguished as Hsp60, Hsp70,

Hsp90, Hsp100 and small Hsps. Homologs of Hsp60, Hsp70 and Hsp100 are present in mitochondrial matrix of all eukaryotes [12], [35], [36]. Hsp70, a homolog of bacterial DnaK, is the major mitochondrial chaperone system involved in various proteostasis functions, involved in protein translocation, folding and protein aggregation [37]. Hsp60 chaperonin forms a large multimeric, cage like structure that is involved in folding of new proteins in an ATP dependent mechanism [38]. Another class of chaperone system Hsp100, mainly involved in resolubilization of protein aggregates and works in association with Hsp70 in unfolding of aggregates [39]. Mitochondrial biogenesis also requires proper functioning of cytosolic chaperones, mainly Hsp70 and Hsp90 involved in import of some specific proteins to mitochondria [40].

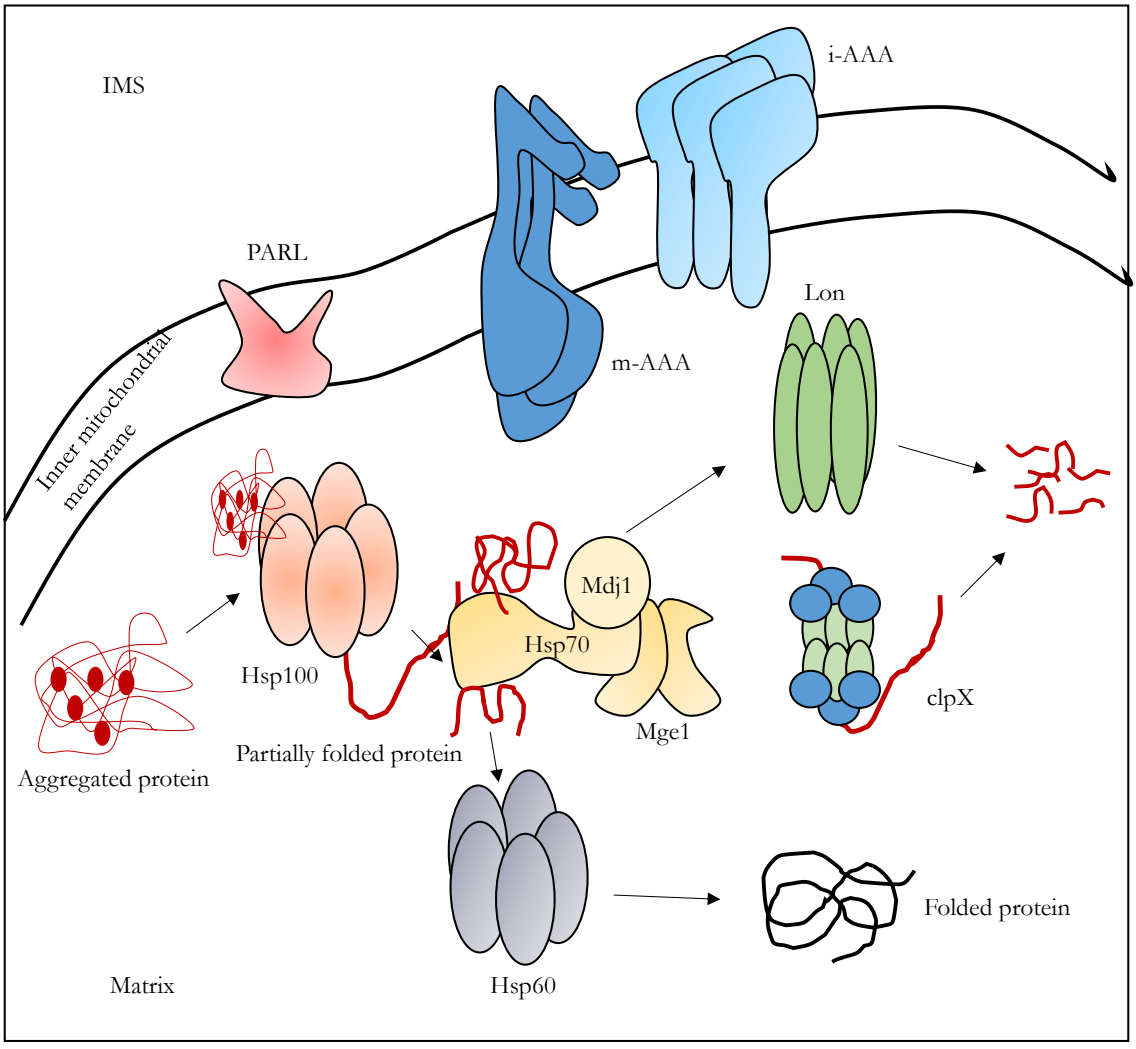

Figure 1.3 Quality control pathways in mitochondria

Mitochondrial inner membrane and matrix contain most of the proteases and chaperones. Apart from protein import and folding, Hsp70 chaperone system also involved in disaggregation and degradation of proteins. Hsp100 majorly involved in disaggregation of proteins and Hsp60 involved in protein folding. $AAA^{+,}$ PARL and Lon proteases involved in the mitochondrial protein quality control.

Proteolytic system is crucial for mitochondrial biogenesis by maintaining the mitochondrial functions through protein quality control [41]. Proteases are majorly present in matrix and inner membrane fraction of mitochondria. Two classes of proteases are present in mitochondria namely, processing peptidases and ATP dependent proteases [42]. Processing peptidases are involved in maturation of nuclear encoded proteins by removing the N-terminal targeting sequence [43], [44]. ATP dependent proteases are the main components of protein quality control system in mitochondria. Matrix proteases clpX (identified only in mammalian mitochondria) and Lon proteases are involved in the removal of unfolded or oxidized proteins in the mitochondrial matrix [45], [46]. Inner mitochondrial membrane AAA+ proteases (Yme1 and Yta10/Yta12) involved in clearance of membrane proteins and IMS proteins [47]. Prohibitins are also implicated in the proteolysis by modulating the proteolytic activities of AAA+ proteases [48]. Other proteases like HtrA2 and PARL also present in mitochondria of higher eukaryotes, involved in quality control of IMS and inner membrane proteins [49],[50]. Chaperones and proteases act sequentially during stress conditions to maintain mitochondrial protein quality control and removes aggregated or misfolded proteins [51].

1.5 Electron transport complex

Oxidative phosphorylation is the final step of aerobic metabolism and takes place at mitochondrial inner membrane. Oxidation of NADH and FADH produces electrons, these electrons are passed

through 10 redox centers to generate transmembrane proton gradient. Electron transport occurs from low to high standard redox potential mediated through redox centers present in complex I to complex IV [52]. ATP synthase complex produces ATP by translocation of protons generated during electron transport. Yeast mitochondria contain incomplete complex I and most of the ETC proteins are conserved across eukaryotes. ETC proteins are majorly nuclear encoded and few by mtDNA (Yeast 8 proteins and mammalian 10 proteins) [53].The protein products of mtDNA play major role in assembly of ETC components. Improper assembly or defective proteins of ETC complex abrogates mitochondrial functions and known to increase ROS, which eventually cause several disorders [54], [55].

1.6 Iron-Sulfur (Fe/S) cluster biogenesis

Iron-sulfur (Fe/S) clusters are essential co-factors for many biological processes, including electron transfer and redox catalysis. Although Fe/S cluster biogenesis occurs in mitochondria and cytosol, mitochondrial role is indispensable. Iron-sulfur cluster biogenesis involves several proteins and assembly factors [56]. Maturation and folding of these proteins in yeast mitochondria primarily depends on Hsp70 chaperones, like Ssq1and Ssc1 [57]. Mitochondrial matrix comprises of Iron-Sulfur Cluster assembly (ISC) machinery involved in the formation of Fe/S clusters. Assembly of cytosolic Iron-Sulfur clusters also depends on ISC machinery and mitochondrial Fe/S cluster export machinery. Fe/S clusters traverse through the inner membrane, IMS and then to outer mitochondrial membrane for the biogenesis of cytosolic Fe/S clusters. Mitochondrial outer and inner membrane contains specific proteins like mitoNEET and Abcb7 that exports iron-sulfur cluster to cytosol . Deletion of either ISC machinery proteins or export machinery components causes defective Fe/S cluster biogenesis in both cellular compartments [58], [59]. These defects

develops mitochondrial iron overload that eventually causes diseases like Frederic ataxia (FRDA) and other multiple mitochondrial dysfunctions.

1.7 MtDNA

Mitochondrial DNA is a self-replicating genome evolved from alphaproteobacteria and plays a prominent role in mitochondrial biogenesis. mtDNA encodes 11 proteins (in yeast 9 proteins) several tRNAs and some rRNAs. mtDNA encoded proteins are mainly associated with electron transport chain (ETC) and ATP synthase complex . mtDNA is highly sensitive to mutations that leads to heteroplasmy situation due to multiple copies of mtDNA, where both mutant and wild type DNA can exist in a mitochondrion [60]. Deletion of yeast mtDNA (ρ^0 cells) or mutations generate a petite phenotypes with OXPHOS dysfunctions and incapable to utilize non-fermentable carbon source [61]. To complement the mtDNA translation defects, mitochondria also known to import cytosolic tRNAs and few rRNAs. Accumulation of mtDNA mutations linked to neuromuscular diseases and also implicated more common disease like cancer, diabetes and Parkinson's disease. mtDNA mutations also a major factor for premature aging and age related pathologies [62].

1.8 Cellular sources of reactive oxygen species

ROS primarily generated as superoxide (O_2^-) by incomplete reduction of O_2 to H_2O. These further reduced to H_2O_2 by superoxide dismutase (SOD) and metal mediated conversion of O_2^-/ H_2O_2 (Fenton reaction) produces highly reactive OH·. Other free radicals generated by reacting ROS molecules with signaling molecules like NO, forming reactive nitrogen species (RNS) [63],[64]. Different intracellular process generate ROS molecule for example mitochondrial ETC, NADPH oxidase, peroxisome oxidases and endoplasmic reticulum oxidative protein folding. Mitochondria represents the major site for cellular ROS (mROS) due to inevitable electron outflow during

aerobic metabolism. There are eight prominent O_2^- generation sites in mitochondria, out of this Complex I and complex III are the primary sites for electron leakage. Mitochondrial ROS (mROS) released into matrix fraction, except Complex $IIIQ_o$, which releases into inner mitochondrial space. Theoretically ROS generated from Complex $IIIQ_o$ has easier access to cytosol. Pool of mROS in matrix fraction is more when compared to Complex $IIIQ_o$ generated IMS ROS [64],[65].

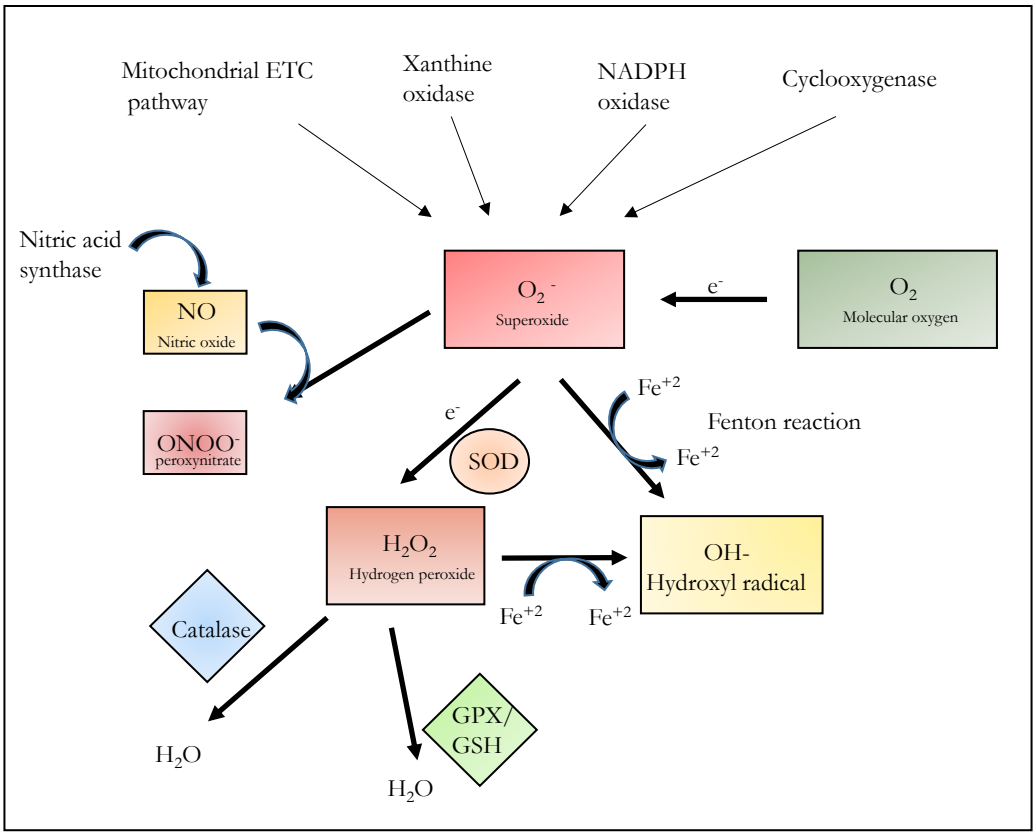

Figure 1.4 Source and mechanism of ROS production

Different sources of superoxide molecule. O_2^- molecules are neutralized by series of reductions reactions forming lower toxic ROS molecules, H_2O_2 (SOD) or H_2O (Catalase). In addition metal mediated oxidation (Fenton reaction) of H_2O_2 or O_2^- produces higher toxic OH^- radicals.

However, both mROS play major role in mitochondrial mediated signaling processes. Mitochondrial Disorders or defective mitochondrial biogenesis lead to increased production of

ROS and causes oxidative damage and cell death. Thus mitochondrial ROS is the key site for many diseases, including diabetes, neurological disorders and premature aging [66], [67].

1.9 ROS detoxification mechanisms

There are several lines of enzymatic and non-enzymatic antioxidant defense mechanisms to decrease ROS levels [68]. Enzymatic degradation of ROS is mediated by SOD, catalase, and cellular redox components (Trx, Prx and Grx systems) [69], [70]. Superoxide dismutases decreases the O_2^- levels by forming H_2O_2, through metal dependent dismutaion of superoxide molecules. Multiple isoforms of SOD proteins are present in mammals, majorly located in mitochondria and cytoplasm [71]. H_2O_2 was further neutralized to water molecule by catalase present in the sarcoplasm, nucleus, and peroxisomes. Peroxiredoxins (Prx), glutaredoxins (Grx) and thioredoxin (Trx) acts as H_2O_2 buffering agents by reducing H_2O_2 to H_2O in sequential reactions utilizing NADPH as energy equivalents. In mammals there are six Prx isoforms, including mitochondrial Prx3 and Prx5.

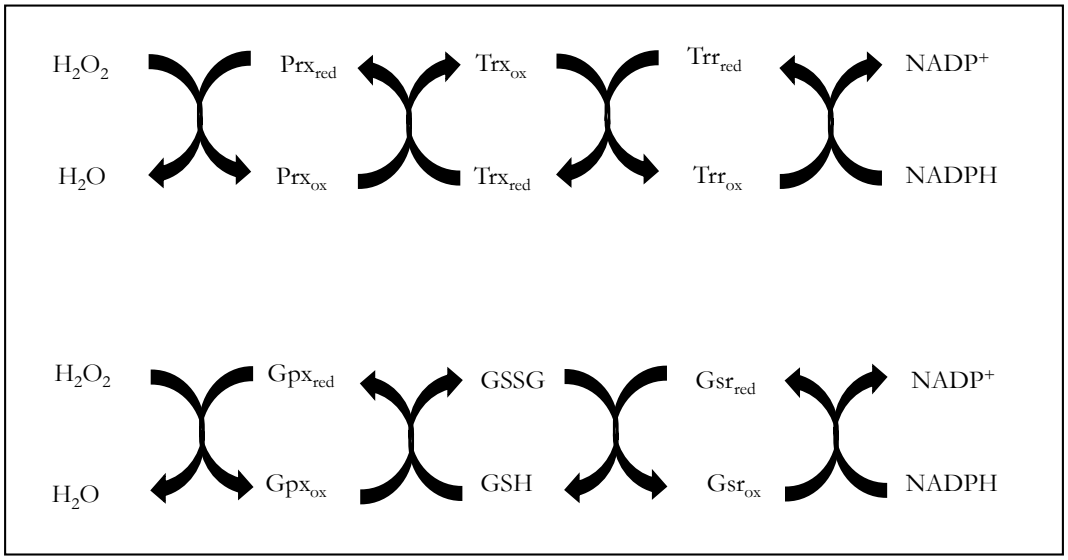

Figure 1.5 H_2O_2 clearance by antioxidant pathways

Primary antioxidant mechanism in cells is mediated by peroxiredoxin (Prx), glutaredoxin (Gpx) and thioredoxin (Trx) system. H_2O_2 primarily detoxified by Prx system. Prx protein acts on H_2O_2 and forms water and oxidized Prx (Prx_{Ox}). Prx_{Ox} was further restored by Trx system (thioredoxin, thioredoxin reductase and NADPH). Similarly H_2O_2 nullified by Glutaredoxin by forming H_2O and oxidized Gpx, which further restored back with small molecule like GSH

Prx primarily acts as H_2O_2 buffering agents because of their high abundance and high rate of reaction. Oxidized Prx was further recycled back to Prx by thioredoxin/thioredoxin reductase system [72]. Gpx also contain different isoforms in yeast and mammals, oxidized upon H_2O_2 and subsequently reduced by glutathione (GSH). Gpx also have high rates of reaction towards H_2O_2, but expressed in low levels [73]. Non-enzymatic clearance of ROS is achieved by low abundant vitamins (A, E and C), glutathione (GSH), selenium and ubiquinone. Expression levels and activity of antioxidant proteins are regulated in response to ROS levels and external or internal stress factors. Additionally signaling processes mediated by PGC1α not only induces mitochondrial biogenesis and ROS levels, but also regulates several antioxidant proteins transcriptionally [15].

1.10 Oxidative stress: real culprit for age related diseases

Oxidative stress is due to imbalance of generation of free radicals and antioxidant system. This may be due to decreased antioxidant capacity of the cell, external ROS inducing agents and age related pathologies. Oxidative stress leads to oxidation of various cellular components, primarily proteins, lipids and DNA and promotes genomic instability. Accumulation of free radicals is the major cause of several diseases, including diabetes, neurological disorders and early onset of aging. Mitochondrial damage increases ROS production and shortens lifespan in yeast and animal models. Increased ROS levels derail signaling pathways or redox sensor properties of proteins that eventually leads to disturbance of cellular homeostasis [54], [64], [67], [74], [75].

1.11 Redox - regulation of proteins

Recent evidence suggests that ROS regulates several protein functions through reversible redox mechanism. Proteins undergo reversible post translational covalent modifications in response to oxidative stress. ROS mediated modifications on proteins controls various physiological systems, including adaptation to hypoxia, regulation of several pathways comprising of autophagy, immunity, differentiation and longevity. Reversible oxidative modifications occur at cysteine and methionine residues of proteins [66], [76]. Another class of signaling molecules derived from irreversible oxidative modifications of proteins and lipids like peroxidation products and reactive electrophile species. However, the amount of ROS generated is not well defined at cellular environment and the regulation of signaling cascade predominantly is determined by levels of ROS.

1.11.1 Regulation of proteins through Cys redox mechanism

ROS/RNS molecules specifically oxidize cysteine thiol groups (-SH) forming sulfenic acid (-SOH) that may further glutathionylated by reacting with GSH or form disulfide bond (-SS-) reacting with an adjacent thiol group or even form sulfenyl amide (-SN) by reacting with amide groups. Many of these modifications cause allosteric changes in protein and alters varying downstream functions. Intra or inter disulfide bond formation is the hallmark of redox mechanisms mediated by Cys residues [77, p.], [78], [79]. Antioxidant molecules further reduce disulfide bonds formed during oxidation to retain protein native state, thereby regulating protein functions through oxidation-reduction cycles. Several reports demonstrate that the role of redox regulation of Cys residue regulates the downstream signaling processes. Majority of unicellular organisms and multicellular eukaryotes respond to oxidative stress primarily at transcription level to maintain cellular homeostasis. Several transcription factors like OxyR, c-Jun N-terminal kinase 1 (JNK1), p53, etc., acts as a redox sensor and regulate the downstream gene expression [80], [81]. For example,

cysteines in *Escherichia coli* transcription factor OxyR are sensitive to H_2O_2. Oxidation of Cys residues in OxyR results in formation of inter disulfide bonds, which causes the switch in protein function from repressor to inducer of antioxidant genes. Similarly, the eukaryotic transcription factors also undergo oxidation and mediate specific transcriptional signals. Some of the protein phosphatases (PTEN and PTBP1b) contain redox Cys at enzyme catalytic region, which undergo reversible oxidation in response to ROS and regulates dephosphorylation activity [82]. Cys redox sensor properties of many proteins control signaling pathways that arbitrate cell proliferation and survival.

1.12 Methionine oxidation and Methionine sulfoxide reductases

Recent reports suggest that reversible oxidation of methionine residues play significant role in redox regulation of proteins. Methionine oxidation in proteins causes major allosteric or tertiary structural changes that could affect protein functions or signaling pathway. Similar to Cys oxidation, methionine oxidation at the enzyme active site inhibits the catalytic activity. Oxidation of Methionine leads to the formation of either reversible methionine sulfoxide (Met-SO) or irreversible methionine sulfenic acid (Met-SO_2). Oxidation of Met to Met-SO creates two enantiomers at sulfur atom forming either Met-(S)-SO or Met-(R)-SO. Methionine sulfoxide reductases (Msrs) reduce either free Met-SO or protein bound Met-SO. Two specific Msr proteins, namely MsrA and MsrB reduce Met-(S)-SO and Met-(R)-SO respectively [75], [83], [84],[85].

All prokaryotes and eukaryotes contain both MsrA and MsrB proteins. Most of the organisms contain two MSR genes at different transcriptional origin, but few bacteria like *Neisseria* contain transcriptionally fused gene, producing both MsrA and MsrB as a single protein [86]. Some Msr genes from pathogenic bacteria exhibit stress induced expression and also play an essential role in

disease infections [87], [88]. Yeast contains three Msr proteins, namely fRMsr, Mxr1 and Mxr2. Mxr1 belongs to MsrA family, while fRMsr and Mxr2 are related to MsrB. Mxr1 contains similar catalytic efficiency towards free Met-(S)-SO and proteins bound Met-(S)-SO. Mxr2 known to act more specifically towards protein bound Met-(R)-SO, while fRMsr is active only on free Met-(R)-SO. Mxr1 and fRMsr are localized to cytosol and Mxr2 localized to mitochondria. Yeast strain with deletion of fRMsr is able to grow normally in rich medium, but sensitive when medium contains Met-(R)-SO as sole methionine source. Deletion of protein bound Met-SO reducing enzymes (MsrA and MsrB) could decrease yeast growth in presence of stress and also disrupts mitochondrial biogenesis [89]–[91]. Mammals contain multiple isoforms of MsrA and MsrB, occupied in most of the compartments of the cell. Mammalian mitochondria contain both MsrA and MsrB reducing enzymes [92].

1.12.1 Catalytic mechanism of Methionine sulfoxide reductases

Most of Msr proteins require two cysteine residues, namely catalytic cysteine and resolving cysteine for reduction of methionine sulfoxide. Catalytic cysteine attacks on Met-SO and reduces to Methionine forming an intermediate sulphenic cysteine, which then cooperates with resolving cysteine to form disulfide bond. Both MsrA and MsrB proteins require thioredoxin (Trx), thioredoxin reductase (Trr) and NADPH for recycling of disulfide bond formed during catalysis. As resolving cysteine is absent in some of the Msr proteins, catalytic Cys directly depends on Trx system for recycling. Most of MsrB proteins contain divalent metal ion and any mutation in this region decreases the enzyme activity, while MsrA Met-SO reduction activity is independent of metal ion. MsrA and MsrB proteins differ in their primary structure level and also in the mechanism of Met-SO reduction [93], [94].

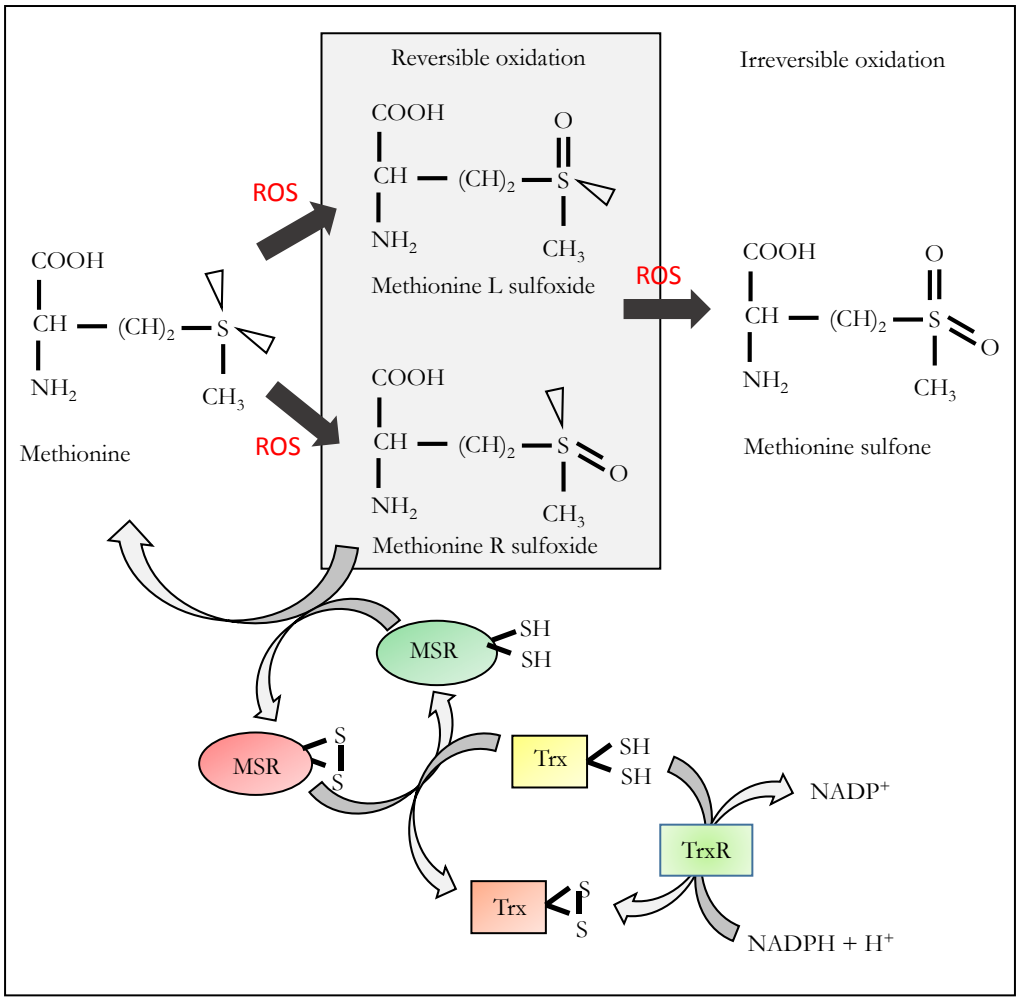

Figure 1.6 Oxidation and reduction mechanism of Methionine

Methionine oxidized by ROS molecules and forms reversible either Met-(S)-SO or Met-(R)-SO. Higher levels of ROS molecules damage Met to produce irreversible Met-SO_2. Msr proteins acts on Met-SO and reduce to methionine forming oxidized Msr proteins. Disulfide bonds or oxidized Cys residues in Msr were resolved by thioredoxin system which includes thioredoxin, thioredoxin reductase and NADPH.

1.12.2 Proteins regulated by Met oxidation

Some of the cytosolic eukaryotic proteins have been reported to be regulated by a methionine redox mechanism. For example, nuclear localization of nuclear factor-κB (NF-~~Kb~~) is controlled upon methionine oxidation in response to ROS. Oxidized NF-κB met[45] requires both MsrA and MsrB for complete reduction to native state. Special enzymes called as Micals regulate cell

morphology dynamics by oxidizing the actin at met^{46} [95]. Oxidation of Methionine causes the depolymerization of actin. MsrB enzymes specifically reduce Met-SO of actin and restores polymerization capacity [96]. In addition, potassium channels and Ca^{2+}/calmodulin-dependent protein kinase II (CaMK II) are known to be inactivated upon Met oxidation and further reactivated by Msrs enzymes [97], [98]. Cytochrome C (cytC), an electron carrier in ETC, also mediates cell death by redox induction of Cyt C to cytosol upon methionine oxidation. MsrA enzymes prevent Cyt C mediated apoptosis by reduction of Met-SO [99]. Some proteins are also activated upon methionine oxidation like *E.coli* HypT (hypochlorite-responsive transcription factor) transcription factor methionines oxidation induces the gene expression while reduction by Msr represses the gene expression [100]. Since the pool of Methionine present in a cell at any given condition is approximately 1 mM. Methionine in proteins apart from regulating the protein functions, it is also known to acts as antioxidant. Thus deletion of Msr proteins increases ROS levels and play a major role in age related diseases [92], [101].

1.13 Mitochondria - the site of redox regulation

ROS is an inevitable byproduct of mitochondrial aerobic metabolism. ROS generated by ETC complex is majorly matrix destined. This possibly suggest that most of matrix proteins are easily prone to free radical damage. Therefore, mitochondrial proteins might be regulated in response to oxidative stress to control mitochondrial protein homeostasis. ROS also play a major role in mitochondrial to nuclear communication or retrograde signaling pathways. There are few reports regarding the redox regulation of mitochondrial proteins mediated through redox sensitive cysteine or methionine residues [74], [82]. Mitochondrial biogenesis, primarily depends on protein import and metabolic capacity of mitochondria. Protein import machinery is highly regulated in response to metabolic demand and cell cycle dynamics that is primarily mediated through phosphorylation

of outer and inner mitochondrial translocase complex proteins [29]. Similarly, protein import is inhibited during oxidative environment, like treatment with ROS producing molecules antimycin A, rotenone, indicating that oxidation of specific components might halt protein import [102]. This hypothesis led us to the identification of components that are oxidatively damaged in protein import machinery. From our lab we are for the first time reported that Mge1 is an early stress response protein that was structurally destabilized and inhibited the protein import during elevated levels of ROS [103].

1.14 Hsp70 chaperone system in mitochondrial biogenesis

Hsp70 chaperones play an important role in prokaryotes and eukaryotes, majorly involved in protein translocation, folding and disaggregation of proteins. Yeast contains eight homologs of Hsp70, distributed to different compartments. Mitochondrial Hsp70 (mHsp70) homologous to bacterial DnaK and is the well characterized chaperone system [104], [35]. Three homologs of Hsp70 chaperones are present in the yeast mitochondrial matrix (Ssc1, Ssq1 and ECM10) and each mHsp70 complex consist of Hsp70 ATPase protein/J-domain protein /nucleotide exchange factor (NEF). Ssc1 is the most abundant chaperone in yeast mitochondria involved in protein import and folding, assembly, disaggregation and degradation of proteins. Ssq1 is involved in import of proteins required for Fe/S cluster biogenesis while ECM10 is involved mtDNA maintenance [57], [105]. Yeast mitochondria contain three J family co-chaperones, named as Mdj1, Jac1 and Pam16/Pam18 (PAM complex). These three J proteins interact with Hsp70 and involved in various functions. PAM complex is involved in protein import into the mitochondrial matrix. Mdj1 and Jac1 involved in protein folding of matrix proteins and Fe/S cluster biogenesis respectively [104], [106]. Mge1 is the only homolog of GrpE present in yeast mitochondria and known to act on all

Hsp70 chaperones. Although yeast mitochondria contain different Hsp70 components, the mechanism of action is conserved [107], [108].

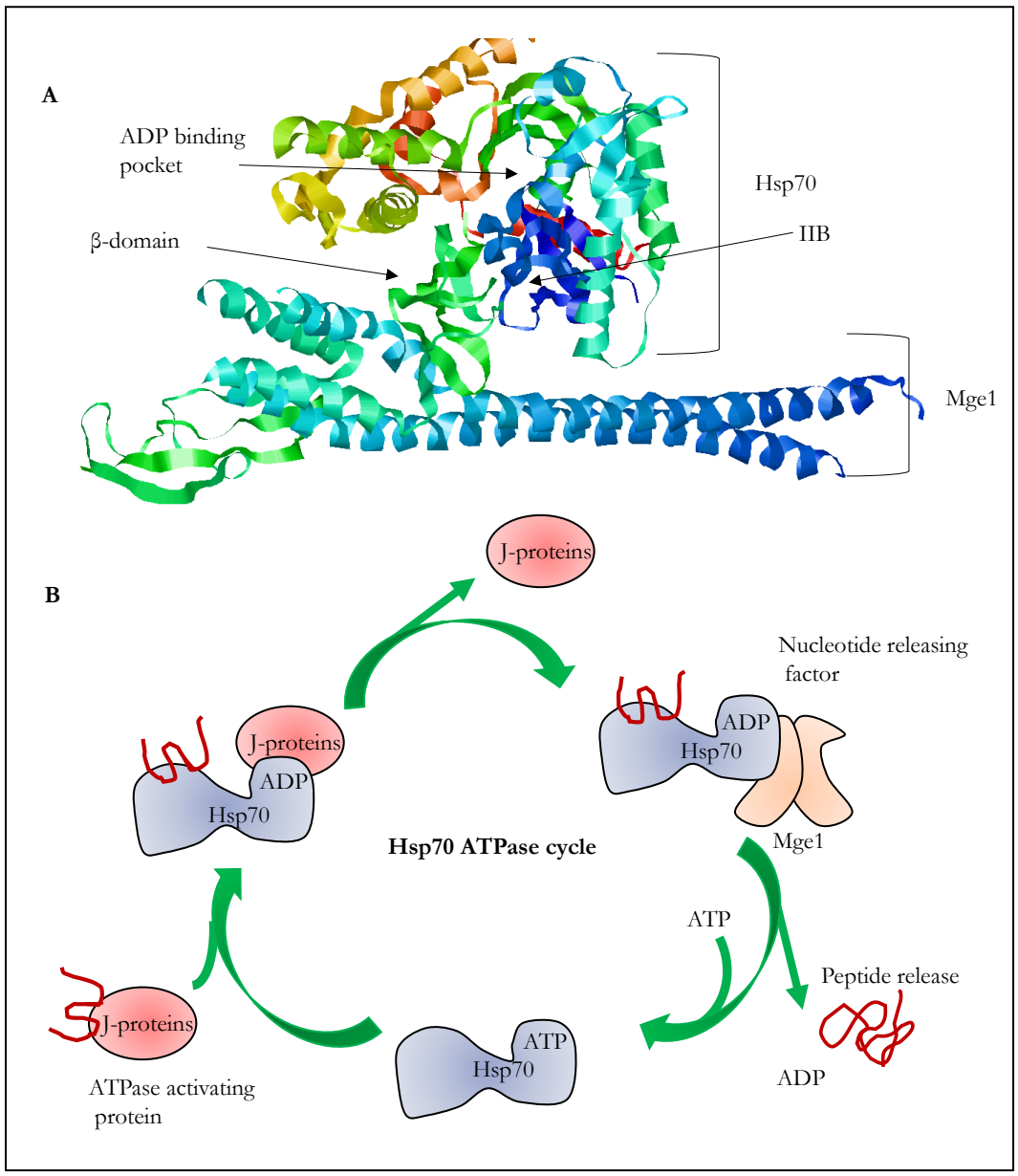

Figure 1.7 Hsp70-Mge1 structure and ATPase cycle

(A) Mge1-Hsp70 (PDB: 1DKG) structure indicating interaction sites of GrpE and DnaK. (B) Hsp70 ATPase cycle illustrating ATP hydrolysis favored by J co-chaperones and ADP release by nucleotide exchange factor (Mge1).

Hsp70 contain two domains, a highly conserved N-terminal nucleotide binding domain (NBD) and C-terminal peptide binding domain (PBD) comprising a β-sandwich and an α-helix bundle subdomains. PBD binds to short stretches of hydrophobic side chains of unfolded polypeptides, which are normally buried in the interior of protein native structures. ATP binding to the Hsp70 NBD region allosterically controls polypeptide binding to the PBD through hydrophobic interdomain linker. Hydrolysis of ATP by Hsp70 nucleotide binding domain induces conformational changes in PBD and forms Hsp70-ADP-substrate complex. J- co-chaperone family proteins enhance ATP hydrolysis and favors Hsp70-ADP-substrate complex. In the ATP-bound state, attached peptides are rapidly exchanged by Hsp70, while in the ADP-bound form peptides are firmly attached to Hsp70 [109]–[111]. The rate of dissolution of Hsp70-ADP complex is low in the absence of NEF`s and addition of NEF (Mge1) significantly accelerates the nucleotide cycling and concomitantly protein folding by Hsp70. Therefore, NEF`s enhances the rate of Hsp70 cycle approximately by 5000 fold. Thus Mge1 of mitochondria play a major role in Hsp70 dependent proteostasis. Any lethal mutations in Mge1 deliberately affect the Hsp70 activity as well as mitochondrial biogenesis, due to defect in protein homeostasis and Fe/S cluster synthesis [112], [113].

1.15 Structural topology of GrpE

Bacterial GrpE is homologous to yeast Mge1, and is the well-known NEF of Hsp70. In solution, GrpE forms homodimeric structure that interacts with single Hsp70 molecule during Hsp70-ADP complex hydrolysis. GrpE dimer composed of two long α-helical regions at N-terminus, followed by four helix bundle region and a compact β-sheet domain at the C-terminus. Four-helix bundle is formed by two short successive α-helices from each monomer arranged in anti-parallel topological fashion. Interface of four helix bundle forms square type arrangement and most of exterior amino

acids are solvent exposed [112], [114], [115]. Small β-sheet domain present at the C-terminus does not contribute to dimer interface, but this region mainly interacts with Hsp70 inserting into the central cleft of the Hsp70 NBD. This interaction results in 14° outward movement of Hsp70 IIB domain that causes nucleotide dissociation. GrpE or Mge1 mutations that destabilize DnaK interaction or Mge1 dimerization significantly inhibit Hsp70 activity [112], [116]. Mutations in the long α-helical and four helix region of Mge1 or GrpE known to exhibit thermo sensitive phenotypes and decreased Hsp70 ATPase activity.

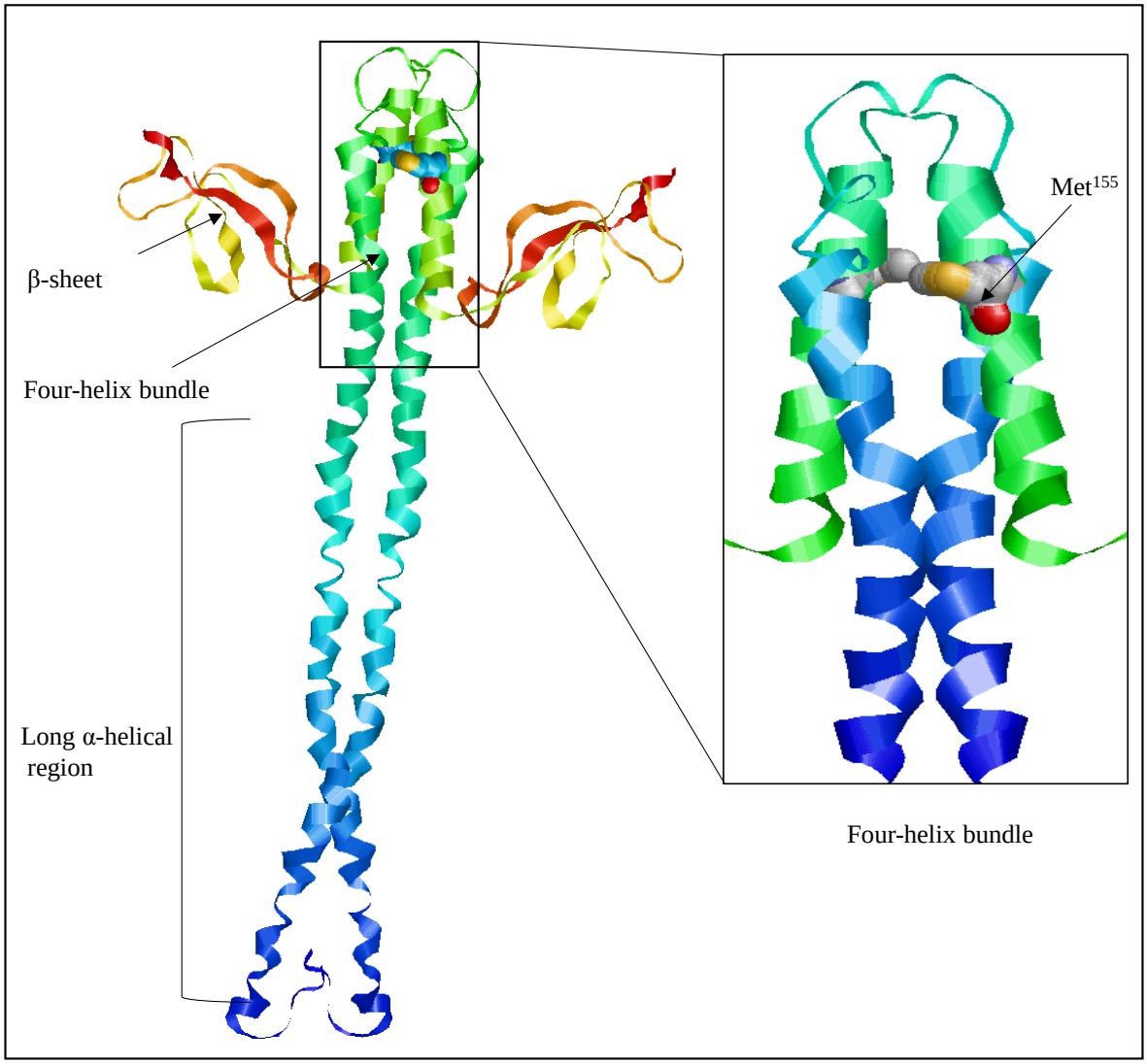

Figure 1.8 Mge1 structural and functional domains

Homodimeric structure of Mge1 contains two long α-helices, a short four helix bundle and two β-sheet domain. Long helices and β-sheet domain was formed from each monomer of GrpE and four helix bundle was formed by the interaction of two GrpE monomers. Inset image depicts four helix bundle with Met at 155 position. Structure developed by using I-TASSER and GALAXYGEMINI software's.

In yeast Mge1, thermal sensitive mutations accumulate pre-proteins in cytosol and decrease mitochondrial functions. All GrpE proteins display structural transition in response to various stress conditions and this phenomena is crucial for controlling Hsp70 functions during stress conditions [113], [103]. In response to thermal stress, most of GrpE homologs depict reversible structural transition from dimer to monomer. N-terminal α-helical region and four helix bundle structure that stabilizes homodimeric structure are primarily responsible for GrpE unfolding during stress. Dimerization capacity of Mge1 is reversible upon restoration of thermal stress and complement the Hsp70 activity. Similar to thermal stress, Mge1 is also sensitive to oxidative stress and forms monomer during oxidative stress [103].

1.16 Scope of the study

Recent investigations from our lab identified that Mge1 acts as a redox sensor and treatment of Mge1with H_2O_2 causes defective Hsp70 chaperone system. During oxidative conditions Mge1 dimer converts to monomer and incapable to from interaction with Hsp70 besides decreasing the steady state ATPase activity. Redox sensitive cysteines are absent in Mge1, however it contains one methionine at 155 position in the four-helix bundle region. Mge1 Met155 is conserved across evolution and present in all eukaryotes. Mutation of Mge1 M155L protects dimer structure and Hsp70 interaction, in response to ROS *in vitro* as well as *in vivo. In vivo* expression of Mge1 M155L in yeast strains protects the cells from oxidative damage. Met residues are well known for regulation of protein functions through reversible redox mechanism. These observations led us to an interesting hypothesis whether Mge1 Met155 residue is essential for redox regulation of Hsp70

chaperone system [103]. Therefore, we investigated whether Mge1 is structurally and functionally regulated through Msr proteins in response to oxidative stress. Since Mge1 is indispensable for protecting Hsp70 functions, analysis of this pathway, possibly address a novel mechanism of redox regulation for mitochondrial biogenesis

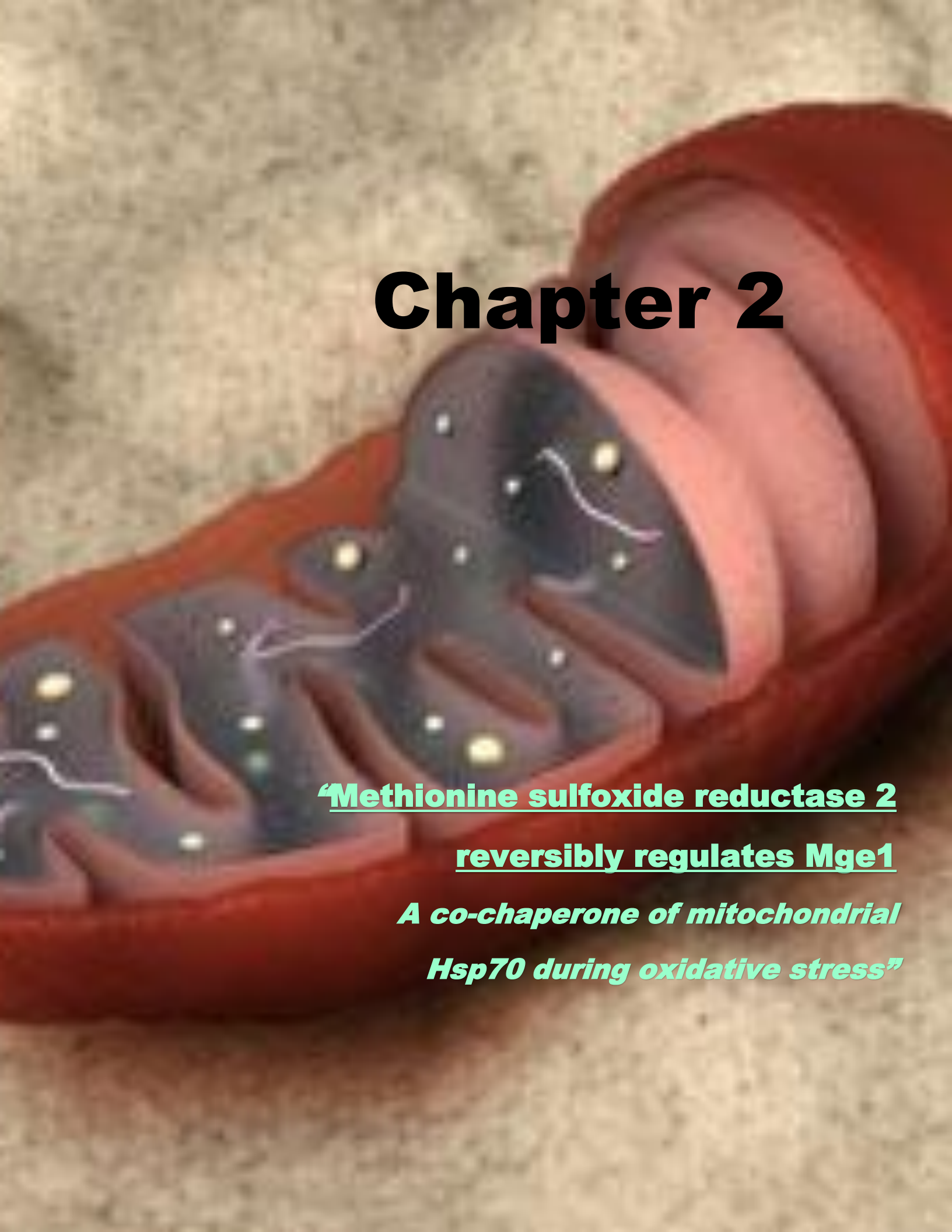

Chapter 2

"Methionine sulfoxide reductase 2 reversibly regulates Mge1

A co-chaperone of mitochondrial Hsp70 during oxidative stress"

2.1 Introduction

Persistent oxidative stress is responsible for several neurological disorders, heart failure and ageing [74], [117]. To combat oxidative stress, cellular systems have evolved several antioxidant defensive mechanisms. Methionine sulfoxide reductases (Msrs) are one of the important regulators of oxidative stress [118]. These enzymes reduce either free or protein bound oxidized methionine in a thioredoxin and thioredoxin reductase dependent mechanism to prevent the accumulation of oxidized proteins and amino acids [94], [101]. The mechanism of action of these enzymes have been well characterized *in vitro* using reconstitution assays containing purified Mxrs [93]. Homologues of Mxr proteins are present across evolution and they have been found to play an essential role in the prevention of oxidative damage to proteins mediated by ROS in bacteria, plant and animals cells [119]. These enzymes have been implicated in ageing and age related disorders such as Alzheimer's, Parkinson's, cataract development and insulin resistance [120]–[123]. Despite their clinical relevance, there is paucity of information on the identity of the physiological substrates of Mxrs and their regulation. Several reports suggest NF-kappa B, potassium channel and calmodulin as possible substrates of Mxrs [95], [97], [98]. In a recent publication, SelR, a homologue of MsrB in drosophila, has been shown to reduce the oxidized R form of methionine in actin and thereby regulate actin polymerization [96]. In yeast Mxr1 has been shown to be localized to cytosol while Mxr2 is present in the mitochondria. In yeast, deletion of MXR1 or MXR2 or both abolishes growth on non-fermentable carbon sources indicating that mitochondrial function is derailed. However, the precise role of Mxr1 or Mxr2 in mitochondria and their physiological substrates are yet to be discovered.

Mitochondrial biogenesis requires continuous translocation of nuclear encoded and cytoplasmic synthesized proteins to different compartments of mitochondria [11], [124]. Oxidative conditions

within the cell influence the import of pre-proteins into mitochondria [125]. Pre-treatment of mitochondria with antimycin A, a superoxide generating oxidizing agent reduces the import of proteins into mitochondria *in vitro*. We have recently discovered that a component of mitochondrial protein import machinery, Mge1, acts as an oxidative sensor to regulate protein import into mitochondria and that this mechanism is likely to be conserved across evolution [103], [125].

Mge1 is an essential component of the molecular protein import motor present in the mitochondrial matrix. The other components of the molecular motor are Pam18, Pam16, Hsp70 and DnaJ [115], [126]. Proteins targeted to mitochondrial matrix require TOM and TIM complexes that are present in the outer and inner membranes of mitochondria respectively. The incoming precursor protein emerging from the TIM complex interacts with Tim44 and Hsp70 in an ATP dependent manner. Hydrolysis of ATP on Hsp70 results in Hsp70-ADP complex that has a high affinity for pre-proteins [127]. Mge1, an adenine nucleotide exchange factor, in its active dimeric form exchanges ATP for ADP on Hsp70 and thereby facilitates the release of precursor protein from Hsp70 [113], [128].

In response to heat or oxidative stress, Mge1 monomerizes and fails to interact with Hsp70-ADP complex. This failure results in the halting of protein import into mitochondria. We have recently shown that the lone methionine at position 155 in Mge1 is crucial for the oxidative sensor function of Mge1. A single point mutation of methionine to leucine at position 155 (M155L) within Mge1 prolongs the time taken for the cell to respond to oxidative stress [103].

In this chapter, we present *in vivo* and *in vitro* evidence that Mge1, a conserved and an essential protein of mitochondria is a physiological substrate of Mxr2. Using genetic and biochemical methods we show that Met155 in Mge1 gets oxidized and the oxidized Mge1 interacts

with Mxr2. Mxr2 specifically reduces the oxidized Met155 in Mge1 both *in vivo* and *in vitro*. Most importantly, Mge1 M155L mutant rescues the protein aggregation and slow growth phenotype of *mxr2*Δ during oxidative stress. Our studies unravel a novel reversible mechanism that the cell employs to regulate oxidative stress in mitochondria.

2.2 Methodology

2.2.1 Plasmid construction

The primers and plasmids used in this chapter are listed in Table 2.1 and 2.2 respectively. The complete coding sequence of yeast MXR2 (Δ29 amino acids, without mitochondrial pre-sequence) was amplified using yeast genomic DNA as a template with the following primer pairs: MXR2_Fwd2 (5`-AAA ACC ATG GGC AAG AGC AAG AAA ATG AGT-3`) / MXR2_Rev2 (5'- ACCC AAGCTT ATC CTT CTT GAG GTT TAA AGA -3'). The amplified MXR2 product was cloned into *E. coli* expression vector pET28a^{+} to generate pNB483 with hexa histidine tag at the C terminus of MXR2. To create plasmid pNB485 that harbors MXR2 (Δ29 amino acids) without any tag, MXR2 was amplified using primers MXR2_Fwd2 / MXR2_Rev4 (5'- ACCC CTCGAG TTA ATC CTT CTT GAG GTT TAA -3') from yeast genomic DNA and cloned as NcoI-XhoI fragment into pet28a^{+} vector. Complete coding sequence of MXR1 was amplified from yeast genomic DNA with primers MXR1_Fwd1 (5`- AAAC GAATTC ACC ATG TCG TCG CTT ATT TCA-3`) and MXR1_Rev1 (5'- ACCC CTCGAG CTA CAT TTC TCT CAG ATA ATG -3') and cloned into pcDNA 3.1 to generate pNB467. MXR2 full length was amplified from yeast genomic DNA with primers using MXR2_Fwd4 (5`- AAAC GAA TTC ACC ATG AAT AAG TGG AGC AGG -3`) / MXR2_Rev4 and cloned into pcDNA 3.1 to generate pNB468.

To create a plasmid carrying FLAG-MXR2, full length MXR2 was initially amplified with primers MXR2_Fwd4/ MXR2_Rev5 (5'- ACCC AAGCTT ATC CTT CTT GAG GTT TAA AGA -3') and cloned into pTEF-2μ-URA to generate pNB472. pNB472 was digested with HindIII-XhoI restriction enzymes and a FLAG epitope inserted therein to generate plasmid pNB475. FLAG epitope linker was created with predigested primers FLAG_Fwd6 (5'- AG CTT GAC TAC AAG GAC GAT GAT GAC AAG GAC TAC AAG GAC GAT GAT GAC AAG CTA C -3') and FLAG_Rev6 (5'- TC GAG TAG CTT GTC ATC ATC GTC CTT GTA GTC CTT GTC ATC ATC GTC CTT GTA GTC A -3').

Plasmid pNB579 (pTEF MGE1-HIS6, 2μ, LEU) is a high copy yeast shuttle vector harboring His tag at the C terminus of MGE1. To construct pNB579, full length MGE1 was amplified with primers MGE1_Fwd7 (5` - CCCC GGATCC ACC ATG AGA GCT TTT TCA GA GCC -3`) / MGE1_Rev7 (5`-AAT T CTC GAG TTA GTG GTG GTG GTG GTG GTG CCA TGG AAT GTT CTC TTC GCC CTT AAC -3`) and cloned into pTEF 2μ, LEU vector. Plasmids containing thioredoxin (TRX) and thioredoxin reductase (TRXR) were kind gifts from Dr. Charles Williams (Medical School, University of Michigan).

2.2.2 Expression and purification of recombinant proteins

E. coli BL21 (DE3) Codon Plus (RIL) cells were transformed with pNB483 plasmid carrying HisMXR2. Recombinant protein expression was induced with 1 mM IPTG and soluble protein was purified using Talon metal affinity resin (GE Healthcare) and dialyzed in phosphate buffered saline (PBS) pH 7.2 with 5 mM β-mercaptoethanol. Wild type Mge1, mutant Mge1 M155L and Hsp70 proteins were expressed and purified with similar protocol. pNB485 plasmid was transformed into *E. coli* BL21 (DE3) Codon Plus (RIL) and un-tagged MXR2 protein was expressed by inducing bacterial cultures with 1 mM IPTG and the soluble protein fraction was

stored in PBS at -20°C. Native un-tagged Trx and TrxR proteins were expressed in *E. coli* BL21 (DE3) Codon Plus (RIL) and the soluble extracts were passed through a DEAE cellulose column. The column was washed with buffer and protein eluted with increasing concentration of NaCl. Eluted sample containing high fraction of Trx and TrxR were used for further steps. The eluted proteins were concentrated and dialyzed against PBS with 10% glycerol.

2.2.3 Yeast strains and construction

Yeast strains used in this chapter and their genotypes are shown in Table 2.3.Yeast strains used in this study were derivatives of BY4741 or BY4742. Haploid yeast strains yNB114 and yNB115 deleted for MXR1 and MXR2 respectively were purchased from Euroscarf, Germany. We used haploid yNB65 strain deleted for chromosomal MGE1 but expressing MGE1 ectopically from plasmid pNB65 (pTEF-MGE1, 2µ, URA3) for construction of diploid stain [103]. Diploid yNB118 strain heterozygous for MGE1 and MXR2 was constructed by mating haploid yNB65 strain with haploid yNB115. Standard yeast genetics methods were used to sporulate diploid yNB118 on SC-URA and the dissected haploid spores were screened for double deletion of chromosomal MGE1 and MXR2 by PCR using primers MGE1_Fwd8, MXR2_Fwd9 and KAN_REV. yNB126 strain denoted as ΔΔ, a haploid progeny contains deletion for both chromosomal genes of MGE1 and MXR2. pNB186 (pTEF-MGE1, 2µ, LEU2) and pNB187 (pTEF- MGE1 M155L, 2µ, LEU2) were transformed into yNB126 to generate yNB128 and yNB129 strains respectively. The URA3 plasmid pNB45 was evicted from yNB128 and yNB129 strains by growing them on SC plates supplemented with 5-FOA plates to generate yNB130 and yNB131 strains respectively. The strains were confirmed by the inability of these strains to grow on SC-URA plates. Strain yNB115 was transformed with plasmid pNB475 to create strain yNB124. Strain yNB115 was transformed with pNB402 (pTEF, 2µ LEU2) vector to generate

strain yNB122. The strain yNB134 expressing His-MGE1 was created by plasmid shuffling pNB579 (pTEF-MGE1-HIS6, 2µ, LEU2) into yNB126 as described above. Yeast strain yNB140 double deletion for MXR1 and MXR2 was constructed from haploid *mxr1*Δ and *mxr2*Δ strains. Briefly diploid strain obtained from mating of *mxr1*Δ and *mxr2*Δ was sporulated. Haploid strains were screened with selected markers and and PCR using primers MXR1_Fwd10, MXR2_Fwd9 and KAN_REV to confirm the double deletion of MXR1 and MXR2.

2.2.4 Yeast media - growth conditions

Yeast *Saccharomyces cerevisiae* was grown in standard YPD medium containing 1% yeast extract, 2% peptone and 2% dextrose unless otherwise stated. For retaining the plasmids, yeast strains were grown in synthetic complete (SC) medium containing yeast nitrogen base (YNB) and with all amino acids except Uracil (SC-URA) or Leucine (SC-LEU) was used. Synthetic media was prepared as follows: 2% dextrose, 0.67% SC medium and pH was adjusted to 5.5 with NaOH. Nonfermentable carbon source medium had either 2% lactic acid (YPL) or 3% glycerol and 2% Ethanol (YPGE) instead of dextrose in YPD. To evict URA3 plasmid, strains were grown on SC medium containing 5-FOA (0.67% SC-URA, 2% dextrose, 60 µg/ml uracil, 2% agar and 0.1% 5-FOA). Yeast transformation was done by LiOAc chemical method [129]. Yeast strains were grown at 30°C with shaking.

2.2.5 Spotting assay

Freshly streaked yeast cultures were grown overnight in YPD or SD medium and normalized to OD_{600} 0.5. 10 µl of each dilution was spotted on YPD or SC-LEU containing various concentrations of H_2O_2 as indicated in the legends and plates were incubated at 30°C for 2 days. Spotting assay that was carried out on YPGE plates incubated at 30°C for 4-5 days. Growth curve

experiments were performed in YPD medium with starting OD_{600} 0.02. The inoculum for the growth curve was taken from overnight cultures grown in YPD. The cultures for monitoring growth rate were grown at 30°C in the presence or absence of H_2O_2 and the optical density at 600nm was monitored at regular intervals. Growth of each strain was carried out in triplicate by taking three different colonies for culture and the average OD_{600} was calculated for each time point.

2.2.6 Isolation of mitochondria

Yeast strains were grown in YPL/YPGE medium at 30°C and cells were harvested when the cultures reached 1 or 2 OD_{600}. Cultures were centrifuged at 5000 rpm for 5 min and the cell pellets washed with autoclaved distilled water. The cells were treated with 10 mM DTT in 0.1 M Tris-SO_4, pH 9.4 buffer for 15 min and centrifuged at 5000 rpm for 5 min. Cells were converted to spheroplasts by using Zymolyase in 1.2 M Sorbitol /20 mM phosphate buffer pH 7.0. After obtaining 50% lysis of cells (lysis correlated to a decrease in OD_{600} of 100 µl cells in 900 µl water), the resulting spheroplasts were gently washed with 1.2 M Sorbitol two or three times. The spheroplasts pellets were suspended in SEM buffer (250 mM sucrose, 1 mM EDTA, 10 mM MOPS, 1 mM PMSF, 0.2% BSA pH 7.0) and homogenized using dounce homogenizer (15 times). The homogenates were centrifuged at 3500 rpm. The supernatants were collected and centrifuged at 10,000 rpm for 10 min. The resultant pellets were dissolved in SEM buffer and centrifuged at 3500 rpm for 5 min. The supernatants were once again centrifuged at 10000 rpm for 10 min and pellets washed 3 times in SEM buffer. The mitochondria were solubilized to a concentration of 1mg/ ml in SEM buffer (without BSA) and kept frozen at -80°C.

2.2.7 *In vitro* protein import

[^{35}S] radiolabelled full length proteins Mxr1, Mxr2 and Su9-DHFR were generated using a T7 or Sp6 *in vitro* coupled transcription translation system (Promega, Madison, WI). 100 µg of mitochondria was suspended in import buffer (0.2% fatty acid–free bovine serum albumin, 250 mM sucrose, 80 mM KCl, 5 mM $MgCl_2$, 5 mM MOPS pH 7.0, 5 mM ATP and 1 mM dithiothreitol) and treated with valinomycin (5 µM) for 15 min. Next, [^{35}S] proteins were added and incubated at 30°C for 20 min. After import, each import sample was divided into two equal halves. One half was treated with trypsin (50 µg/ml) for 15 min on ice while the other half was processed directly. Trypsin inhibitor was added to the import sample after the trypsin treatment. The samples were washed with SEM buffer, solubilized in 2X sample buffer, resolved on a SDS-PAGE gel and analyzed by autoradiography.

2.2.8 Preparation of mitoplasts and treatment with proteinase K

100 µg of yeast mitochondria was suspended in hypotonic buffer (20 mM KCl, 10 mM HEPES pH 7.2) and incubated for 20 min with occasional mixing on ice followed by a spin at 10000 rpm 10 min at 4°C to generate mitoplasts as pellet. Mitoplasts were collected and re-suspended in SEM buffer. Mitochondria, mitoplasts and 0.1% Triton X-100 solubilized mitochondrial extract were treated with or without proteinase K (50 µg/ml) in SEM buffer. After incubation for 10 min on ice, PMSF (1 mM) was added and the samples centrifuged at 10000 rpm for 10 min. Sample buffer was added to the pellets and the protein suspensions were resolved on a SDS-PAGE, the gel western transferred and the membrane probed with the antibodies.

2.2.9 Ni pull down assay

Soluble bacterial protein fraction enriched in recombinant Mxr2 and yeast mitochondrial fractions containing Flag-Mxr2 or Flag alone were solubilized in RIPA buffer. The fractions were pre-

cleared with Talon metal affinity resin and the supernatants collected. Purified recombinant His-Mge1 or His-Mge1 M155L proteins was treated with increasing concentrations of H_2O_2 for 2 hrs before allowing it to bind to Ni-NTA beads. The pre-cleared Mxr2 containing bacterial lysate fractions or mitochondrial fraction containing Flag-Mxr2 or Flag alone were added to the Ni-NTA beads that had been pre-bound with His-Mge1 in separate assays. The samples were kept on a rotisserie for 1 hr at 4°C, washed thrice in PBS/RIPA buffer containing 10 mM imidazole and the beads were collected by centrifuging at 2000 rpm for 5 min at 4°C. The beads were directly processed for SDS-PAGE followed by coomassie staining or western immunoblotting.

2.2.10 Co-immunoprecipitation

500 µg of mitochondria from yeast expressing Flag-Mxr2 was suspended in 100 µl of SEM buffer and centrifuged at 10000 rpm for 10 min. The mitochondrial pellet was solubilized in RIPA buffer and pre-cleared with protein A beads (GE Healthcare).The resultant supernatant was incubated with FLAG M2 (Sigma Aldrich) antibody or control IgG at 4°C on a rotisserie for 4 hrs before addition of protein A beads. The sample was centrifuged at 2000 rpm and the beads washed with RIPA buffer thrice. The beads were suspended in sample buffer without β-mercaptoethanol and loaded on a SDS-PAGE gel to resolve the bound proteins. The resolved proteins were western transferred and the membrane was probed with Flag and Mge1 antibodies.

2.2.11 Mxr2 enzymatic assay

The activity of oxidized protein (50 µM) or free Met-SO (1 mM) was assayed at 37°C in 50 mM sodium phosphate buffer pH 7.2 containing 50 mM NaCl, 0.2 mM NADPH, 10 µg thioredoxin and 20 µg of thioredoxin reductase. Recombinant His-Mge1 and GST proteins were treated with 20 mM H_2O_2 for 4 hours and dialyzed overnight prior to addition to the assay. The assay was

initiated with the addition of Mxr2 and the decrease in absorption at 340 nm was continuously monitored for 60 minutes. A small decrease in the absorption with Mxr2 control in the absence of substrate was deducted at all-time points and used to calculate the enzymatic activity of Mxr2.

2.2.12 ATPase assay of Hsp70

ATPase activity assay was performed in ATPase buffer (50 mM HEPES pH 7.2, 5 mM $MgCl_2$, and 100 mM KCl). Recombinant Mge1 was treated with 5 mM H_2O_2 for 2 hours and incubated with or without 5 µg of His-Mxr2 in presence of 10 mM DTT before using it for ATPase activity assay of Hsp70. Equivalent amount of His-Mxr2 was used in the control reactions that had Hsp70 or Hsp70 and Mge1 prior to start of the ATPase assay. The amount of radioactive inorganic phosphate (p_i) released at various time points was measured in a scintillation counter.

2.2.13 ROS measurement

Yeast strains were grown overnight in liquid medium before diluting them in 10 ml of required medium at a starting OD_{600} is 0.1. The cultures were allowed to grow at 30^{o}C until they reached OD_{600} 1.0. 20 µM of Dichlorofluorescin diacetate (DCFDA) was added to the cultures and further incubated for 1 hr at 30^{o}C. Next, the cells were washed and suspended in 100 µl of PBS. The intensity of fluorescence measured in a fluorescence spectrophotometer (Perkin Elmer) with an excitation wavelength of 480 nm and an emission wavelength of 525 nm and the emission is taken as the total ROS levels.

2.2.14 Purification of His-Mge1 from yeast cells

For purification of His-Mge1, yNB134 and yNB135 strains were grown in 4 litres of YPGE medium at 30°C until the cultures reached to 1 OD_{600}. Cells were harvested by centrifuging the cultures at 5000 rpm. Cells were washed with double distilled water and lysed with lyticase in 1.2

M sorbitol buffer. After formation 50% sphaeroplasts, lysis buffer (6 M Guanidium Chloride, 150 mM NaCl, 50 mM Tris-HCl pH 8.0, 10 mM Imidazole and 5 mM β-ME) was added. Lysates were pre-cleared by centrifuging the samples at 10000 rpm for 10 mins to remove cell debris. Ni-NTA beads were added to the lysates and incubated on a rotisserie for 4 hr at room temperature. The Ni-NTA beads were collected by spinning the samples at 2000 rpm for 5 mins. The beads were washed thrice with wash buffer (6 M Guanidinium Chloride, 150 mM NaCl, 50 mM Tris-HCl pH 8.0, 20 mM imidazole and 5 mM β-ME) followed by another wash with PBS buffer pH 7.2. His-Mge1 protein was eluted in 400 mM imidazole in PBS buffer and resolved by SDS-PAGE. The gel was coomassie stained and the His-Mge1 protein band was excised and submitted for mass spectrometry analysis.

2.2.15 *In vitro* treatment of Mge1 with H_2O_2 and Mxr2 for MALDI-TOF analysis

Mge1 protein was oxidized with 20 mM H_2O_2 in PBS for 6 hr and dialyzed in PBS pH 7.2 overnight to remove H_2O_2. 20 µg of Mge1 protein pre-treated with H_2O_2 was incubated with or without Mxr2 (2.5 µg) protein in presence of 10 mM DTT in 50 mM NaCl and 50 mM sodium phosphate buffer pH 7.2. After 4 hr incubation at room temperature, samples were processed for SDS-PAGE and the gel was coomassie stained. The Mge1 protein bands were excised and sent for mass spectrophotometric analysis at the Proteomics facilities present at University of Hyderabad and at Indian Institute of Sciences, India.

2.2.16 Mass spectrometry

For mass spectrometric analysis, all protein samples used in this study were separated by SDS-PAGE, coomassie stained and the protein band excised and subjected to mass spectrometry analysis. Proteins were reduced (10 mM DTT) and alkylated (10 mM iodoacetamide) using

standard protocols followed by in-gel Trypsin/LysC overnight digestion at 37°C**.** Peptides concentrated in a vacuum centrifuge at room temperature and suspended in 0.1% TFA / 25% acetonitrile. The peptides were analyzed by Matrix-Assisted Laser Desorption Ionization - Time of Flight Mass Spectrometry (MALDI-TOF/MS) and MALDI-TOF/TOF/MS/MS. MALDI spectra were obtained using a Bruker Daltonics mass spectrometer. PMF search was performed using MASCOT server for protein identification. Graphs plotted by taking percentage of relative intensity to the interested peptide. MS/MS fragment ions were assigned by comparing with predicted ions generated *in silico* by using a Protein Prospector (University of California, San Francisco).

2.2.17 Protein aggregation assay

For each protein aggregation assay, 50 µg of mitochondria was suspended in aggregation assay buffer (250 mM Sucrose, 10 mM MOPS, 80 mM KCl, 5 mM $MgCl_2$, 5 mM ATP and 4 mM NADH) and treated with H_2O_2 for 30 mins at room temperature. The mitochondria was centrifuged at 10000 rpm for 10 mins and the pellet was solubilized in lysis buffer (0.5% Trition X 100, 200 mM KCl, 30 mM Tris-HCl pH 7.5, 5 mM EDTA). The solubilized mitochondria were centrifuged at 25000 rpm for 1 hr. The supernatant fraction (soluble fraction) was collected and the pellet (aggregated fraction) was re-suspended in lysis buffer. 20 % of supernatant fraction and total pellet fraction were separated by SDS-PAGE and the gel was silver stained [13].

Tables

Table 2.1 Primers used in this chapter

Name	Oligonucleotide Sequence
MXR1_Fwd1	5`- AAAC GAATTC ACC ATG TCG TCG CTT ATT TCA-3`
MXR1_Rev1	5'- ACCC CTCGAG CTA CAT TTC TCT CAG ATA ATG -3'
MXR2_Fwd2	5`-AAA ACC ATG GGC AAG AGC AAG AAA ATG AGT-3`
MXR2_Rev2	5'- ACCC AAGCTT ATC CTT CTT GAG GTT TAA AGA -3'
MXR2_Fwd4	5`- AAAC GAATTC  ACC ATG AAT AAG TGG AGC AGG -3`
MXR2_Rev4	5'- ACCC CTCGAG TTA ATC CTT CTT GAG GTT TAA -3`
FLAG_Fwd6	5'- AG CTT GAC TAC AAG GAC GAT GAT GAC AAG GAC TAC AAG GAC GAT GAT GAC AAG CTA C -3'
FLAG_Rev6	5'- TC GAG TAG CTT GTC ATC ATC GTC CTT GTA GTC CTT GTC ATC ATC GTC CTT GTA GTC A -3'
MGE1_Fwd7	5` - CCCC GGATCC ACC ATG AGA GCT TTT TCA GCA GCC -3`
MGE1_Rev7	5`-AAT T CTC GAG TTA GTG GTG GTG GTG GTG GTG CCA TGG AAT GTT CTC TTC GCC CTT AAC -3`
MGE1_Fwd8	5` TCG TGA ACG GCC ATC TCC AA 3`

MXR2_Fwd9	5` CGTGGATATACACCAAGTTATCACA 3`
KAN_REV	5 ' CTG CAG CGA GGA GCC GTA AT 3 '

Table 2.2 Plasmids used in this chapter

Name	Description	Reference
NB45	pTEF-MGE1, 2µ, URA	103
NB186	pTEF-MGE1, 2µ, LEU	103
NB187	pTEF-MGE1 M155L, 2µ, LEU	103
NB467	pcDNA 3.1 MXR1	This study
NB468	pcDNA 3.1 MXR2	This study
NB475	pTEF MXR2-FLAG, 2µ, LEU	This study
NB483	pET28a^{+} MXR2 (without His tag)	This study
NB485	pET28a^{+} MXR2-His6	This study
NB579	pTEF-2µ-LEU MGE1-His6	This study

Table 2.3 Yeast strains used in this chapter

Strain	Genotype	Resource
BY4741	*MAT*a, *his3*Δ 1, *leu2*Δ 0, *met15*Δ 0, *ura3*Δ 0	In House

BY4742	*MATα* , *his3*Δ 1, *leu2*Δ 0, *lys2*Δ 0, *ura3*Δ 0	In House
yNB65	*Mat* a, *his*Δ1, *leu2*Δ0, *lys2*Δ0, *ura3*Δ0, YOR232w::KANMX4	103
yNB114	*Mat* a, *his3*Δ1, *leu2*Δ0, *lys2*Δ0, *ura3*Δ0, YER042w::KANMX4	Euroscarf
yNB115	*Mat* α, *his*3Δ, *leu2*Δ0, *lys2*Δ0, *ura3*Δ0, YCL033c::KANMX4	Euroscarf
yNB118	*Mat* a/α, *his3*Δ1, *leu2*Δ0, *lys2*Δ0, *ura3*Δ0, YCL033c::KANMX4, YOR232w::KANMX4, pTEF-MGE1, 2µ, URA.	This study
yNB122	*Mat* a, *his3*Δ1, *le*u2Δ0, *lys2*Δ0, *ura3*Δ0, YCL033c::KANMX4, pTEF-2µ-LEU	This study
yNB124	*Mat* a, *his3*Δ1, *leu2*Δ0, *lys2*Δ0, *ura3*Δ0, YCL033c::KANMX4, pTEF-2µ-URA MXR2-FLAG	This study
yNB126	*Mat* a, *his3*Δ1, *leu2*Δ0, *lys*2Δ0, *ura3*Δ0, YCL033c::KANMX4, YOR232w::KANMX4, pTEF-MGE1, 2µ, URA.	This study
yNB130	*Mat a, his3*Δ1, *leu2*Δ0, *lys2*Δ0, *ura3*Δ0, YCL033c::KANMX4, YOR232w::KANMX4, pTEF-MGE1, 2µ, LEU.	This study

yNB131	*Mat a*, *his3*Δ1, *leu2*Δ0, *lys2*Δ0, *ura3*Δ0, YCL033c::KANMX4, YOR232w::KANMX4, pTEF-M155L MGE1, 2µ, LEU.	This study
yNB132	yNB130 transformed with plasmid pTEF-2µ, URA	This study
yNB133	yNB130 transformed with plasmid pTEF- MXR2-FLAG, 2µ, URA	This study
yNB134	*Mat a*, *his3*Δ1, *leu2*Δ0, *lys2*Δ0, *ura3*Δ0, YCL033c::KANMX4, YOR232w::KANMX4; pTEF-WT MGE1-HIS6, 2µ, LEU.	This study
yNB135	yNB134 transformed with plasmid pTEF-MXR2-FLAG, 2µ, URA	This study

Table 2.4 Peptides generated from Mge1 after digestion with LysC enzyme

Peptide Mass (m/z**)**	Amino acid region in Mge1	Amino acid sequence
2722.4787	152-175	EPGTVFHVQQLGFTLNDRVI RPAK
2643.3559	101-122	EISDLYTGVRMTRDVFENTL RK
2159.2043	42-59	DRLLRSVADFRNLQQVTK

1889.9391	76-92	DLLESVDNFGHALNAFK
1677.7449	11-24	ENNEDLTEEQSEIK
1411.6852	140-151	HEATFELPQPDK
1341.6685	128-139	LDPLGEPFDPNK
875.4832	26-33	LESQLSAK
761.3675	93-98	EEDLQK
721.3879	67-72	DFALQK
676.3512	36-41	EASELK
583.3198	123-127	HGIEK
579.2620	6-10	SEESK
549.2515	1-5	SDEAK
515.3551	76-180	VGIVK
503.2824	61-64	DIQK

2.3 Results

2.3.1 Deletion of MXR2 exacerbates sensitivity to H_2O_2

Yeast Mxr1 and Mxr2 are peptide methionine sulfoxide reductases located in the cytoplasm and mitochondria respectively. Given the similar function for both the enzymes, we wished to investigate whether their functions are redundant in the oxidative stress response pathway. Oxidative stress response can be elicited in yeast cells by addition of H_2O_2. Hence, we monitored the growth of serially diluted yeast *Saccharomyces cerevisiae* cells in wild type (BY4741) or deleted for MXR1 (*mxr1*Δ) or deleted for MXR2 (*mxr2*Δ) on YPD plates with or without the addition of 1 mM H_2O_2. Both the deletion strains exhibited normal growth similar to wild type strain on control YPD plates (Fig. 2.1A, top left panel) while slow growth was observed in case of all the strains on YPD plates with 1 mM H_2O_2. Most interestingly, cells deleted for MXR2 were found to be highly sensitive to H_2O_2 when compared to wild type or *mxr1*Δ strains (Fig. 2.1A, top right panel). Similar results were obtained when we grew all the strains in liquid YPD medium with or without H_2O_2 (Fig. 2.1B). These results implicate Mxr2 rather than Mxr1 with a potential role in the oxidative stress response pathway. However, yeast having double deletion of MXR1 and MXR2 are much more sensitive to H_2O_2 than yeast harboring only MXR2 deletion (Fig. 2.1C).

Fig.2.1

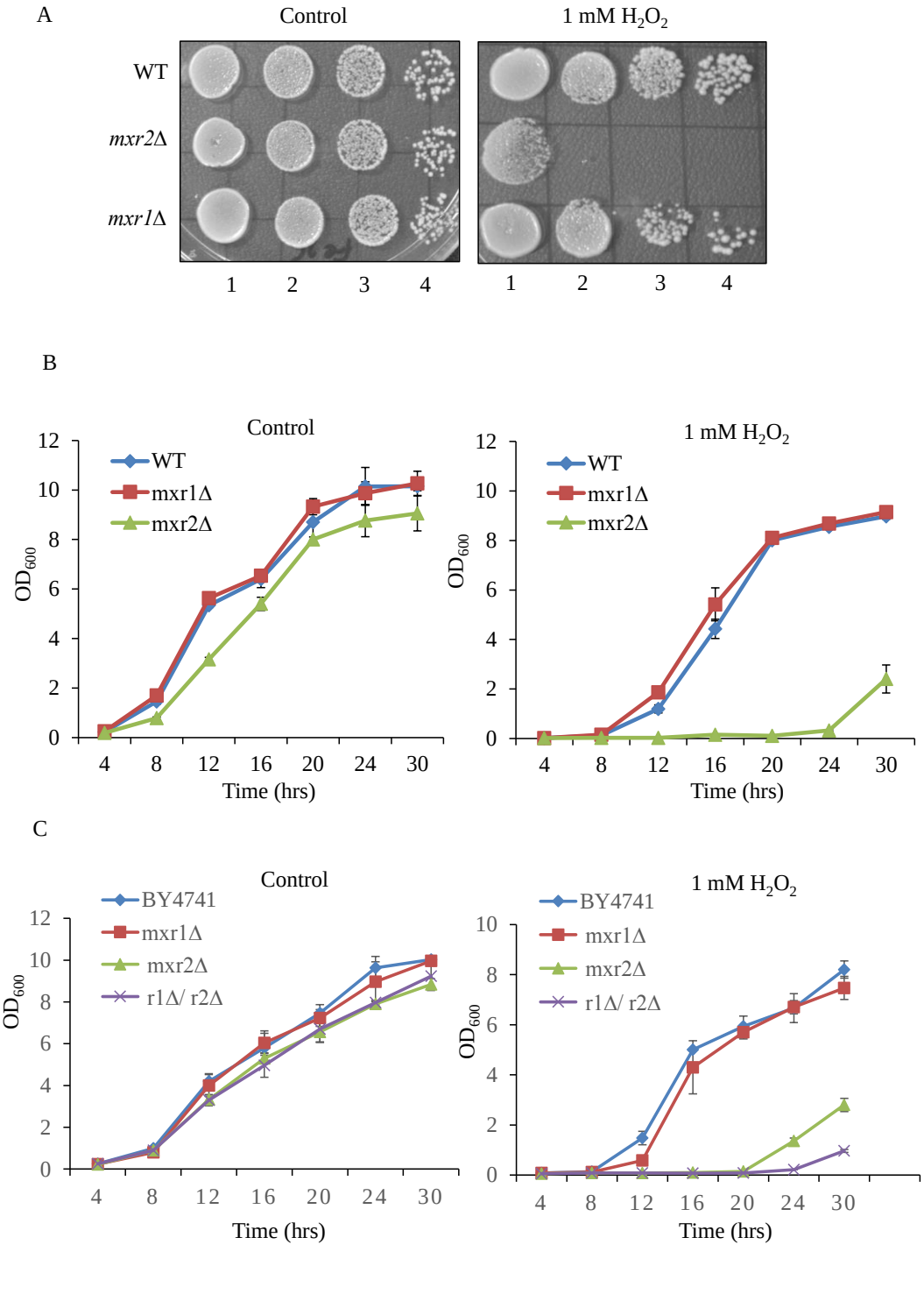
A
Control
1 mM H_2O_2
WT
mxr2Δ
mxr1Δ
1 2 3 4
1 2 3 4
B
Control
1 mM H_2O_2
WT
mxr1Δ
mxr2Δ
OD_{600}
Time (hrs)
C
Control
1 mM H_2O_2
BY4741
mxr1Δ
mxr2Δ
r1Δ/ r2Δ
OD_{600}
Time (hrs)

Figure 2.1 Mitochondrial localization and sensitivity of MXR2 deleted cells to H_2O_2

(A). Spotting assay. Yeast BY4741 (WT) strain and its derivatives *mxr1*Δ (yNB114) and *mxr2*Δ (yNB115) were tested for growth on solid and liquid medium besides monitoring for mitochondrial localization of proteins. (All the three strains were grown overnight in YPD medium. 0.5 OD of cells were serially diluted (1:10) and 10 µl of each suspension was spotted on YPD plates supplemented with or without 1 mM H_2O_2 and incubated at 30˚C for 2 days. (B) Strains were grown overnight in YPD medium prior to diluting them in fresh YPD medium +/- H_2O_2 (1 mM) and were allowed to grow at 30°C with shaking. Growth was monitored at various time points as shown by taking the OD at 600 nm. (C) Double deletion strain of MXR1 and MXR2 (indicated by r1Δ/r2Δ) studied for growth phenotype along with controls (BY474, *mxr1*Δ and *mxr2*Δ strains).Yeast strains were grown overnight in YPD medium and inoculate to fresh YPD medium +/- H_2O_2 (1 mM) and were allowed to grow at 30°C with shaking. Growth was monitored at various time points by taking the OD at 600nm.

2.3.2 Mxr2 localized to mitochondrial matrix

Epifluorescence studies have shown that GFP-Mxr2 is present in the mitochondria while GFP-Mxr1 stays in the cytoplasm [91]. However, the precise sub-compartmental localization of Mxr2 within the mitochondria is not known. To determine the localization of Mxr2 within the mitochondria, we monitored the import of *in vitro* [^{35}S] labeled Mxr2 along with cytoplasmic localized Mxr1 and a known mitochondrial matrix localized protein, Su9-DHFR into mitochondria. Our results show that Mxr1 is poorly bound to mitochondria as it is found to be sensitive to externally added protease confirming its cytosolic localization (Fig. 2.2A, Bottom panel). We find both Mxr2 and Su9-DHFR are enriched in the mitochondrial matrix fraction. Like Su9-DHFR, Mxr2 appears to be effectively processed by a mitochondrial matrix localized processing peptidase and the processed mature protein band is protected from the externally added trypsin (Fig. 2.2A). However, both the imported proteins become accessible to trypsin when the membranes get solubilized with Triton X-100 prior to protease treatment (Fig. 2.2A, lane 5) indicating the matrix localization of Mxr2 and Su9-DHFR. Valinomycin dissipates the membrane

potential and inhibits the import of matrix targeted proteins. We observe complete abolishment of the import of Mxr2 into valinomycin treated mitochondria (Fig. 2.2A, lanes 3 and 4). To further confirm the matrix localization of Mxr2, the cytoplasmic and mitochondrial fractions from the strain expressing Flag-Mxr2 were resolved on SDS-PAGE before carrying out western blot analysis using antibodies against proteins that are benchmarks for the two fractions besides Flag antibody for detecting Mxr2. Flag-Mxr2 was detected only in the mitochondrial fraction (Fig. 2.2B). Tom40, known to be enriched in the mitochondrial fraction and Fun12, a marker for cytosolic fraction were used as controls. The mitochondrial fraction was further sub-fractionated to mitoplasts or subjected to Triton X-100 treatment as described in the Methods section. The fractions containing mitochondria, mitoplasts and Triton X-100 treated mitochondria were further incubated with or without Proteinase K and subjected to western blot analysis. Proteins Tom40, CCP1 and Aconitase that are hallmarks of the outer membrane, inter membrane space and matrix fractions respectively were used as controls. Flag-Mxr2 along with Aconitase were detected in the matrix fraction as they were resistant to protease action in the mitochondria and mitoplasts fractions while Tom40, and CCP1 protein were susceptible to protease treatment (Fig. 2.2C). When the mitochondrial membranes were solubilized with Triton X-100, all proteins were susceptible to externally added protease (Fig. 2.2C, lane 6). Taken together, these results clearly show that Mxr2 is targeted to matrix region of mitochondria and functions in the oxidative stress response pathway.

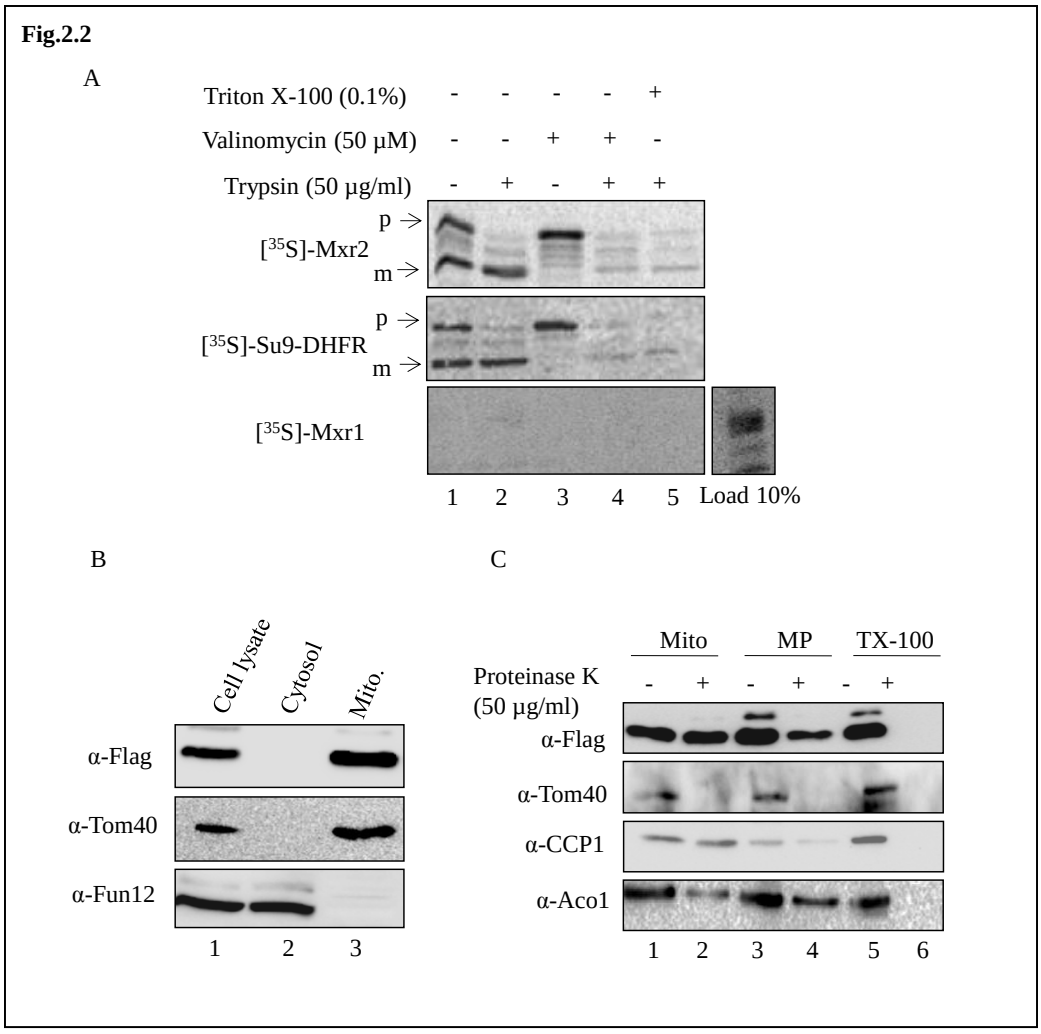

Figure 2.2 Mitochondrial localization of Mxr2

(A) Autoradiogram of a mitochondrial import assay. ^{35}S labeled Su9-DHFR, Mxr1 and Mxr2 proteins were incubated with mitochondria in the presence (lanes 3 and 4) or absence (lanes 1, 2 and 5) of 5 µM valinomycin. Import was carried out for 20 min at 30˚C in the presence or absence of 50 µg/ml trypsin and/or Triton X-100 as shown in the panel. Samples were resolved on an SDS-PAGE gel and subjected to autoradiography. The 'load' lane represents 10% of Mxr1 that was used in the import assay. The letter 'p' shown in the figure indicates precursor and 'm' indicates mature form of precursor protein. (B) Flag-Mxr2 protein localizes to mitochondria. Whole Cell Extract (WCE) of yeast strain expressing Flag-Mxr2 was subjected to differential centrifugation to fractionate mitochondrial and cytosolic fractions. The figure is a western blot probed with antibodies specific for Flag, Fun12 and Tom40. (C) Flag-Mxr2 is enriched in the mitochondrial matrix. Mitochondrial and mitoplast fractions were purified from strain that expresses Flag-Mxr2. The two fractions were incubated with or without proteinase K. The mitochondrial fractions were

additionally subjected to Triton X-100. Samples were resolved by SDS-PAGE, western transferred and probed with the following antibodies that detect proteins which are hallmarks for various mitochondrial fractions: Aconitase (mitochondria matrix), CCP1 (inter membrane space), Tom40 (outer membrane) and Flag for finding sub-mitochondrial localization of Mxr2.

2.3.3 Mxr2 interacts with Mge1 in an oxidative stress dependent manner

We have shown earlier that Mge1, a nucleotide exchange stimulating factor of Hsp70, undergoes oxidation in the presence of H_2O_2 and thereby loses its stimulating activity. Coincidentally, like Mxr2 as shown here, Mge1 is also present in the mitochondrial matrix. Site directed mutational studies suggested that Met155, the lone methionine within Mge1 could be the likely oxidation site. Given that both Mxr2 and Mge1 respond to H_2O_2 triggered oxidative stress and the complementing activity of Mxr2 for restoring the functions of methionine oxidized proteins *in vitro*, we hypothesized that Mxr2 may be interacting with Mge1. To test our hypothesis, we initially expressed mature Mxr2 protein in its native form in bacterial cells. A prominent protein band corresponding to the molecular weight of Mxr2 (~15 kDa) is observed upon induction (Fig. 2.3A, left Panel). Purified recombinant His-Mge1 used in this chapter is shown (Fig. 2.3A, right panel). Two equal amounts of recombinant purified His-Mge1 were taken and were pre-treated with or without H_2O_2 and mixed with soluble bacterial protein fraction enriched in native untagged Mxr2 and then allowed to bind to Ni-NTA beads. After washing the beads, Mge1 was eluted, resolved on SDS-PAGE and stained with coomassie blue. Mge1 was detected in the eluates from both the beads (Fig. 2.3.3B). However, a protein band corresponding to the molecular weight of Mxr2 was consistently observed only in the eluate from the beads that had H_2O_2 treated Mge1 (Fig. 2.3B, lane 2). The band was excised from the gel and subjected to MS/MS and the protein was confirmed to be Mxr2 (Fig. 2.3C). This finding suggests that Mxr2 has affinity only for Mge1 that is apparently oxidized by H_2O_2 *in vitro*. The active site of Mxr2 contains two Cys amino acids that

are known as catalytic cysteine and resolving cysteine and mutation of any of these two amino acids result in an inactive enzyme [93]. The binding of Mxr2 to Mge1 may also require these cysteine amino acids in Mxr2. To test the importance of these two cysteine amino acids in the binding of Mxr2 to Mge1, we employed the classical biochemical route of reducing the cysteine with dithiothreitol (DTT) followed by blocking it with iodoacetamide (IAA) to prevent reverse reaction. Bacterial lysate enriched for Mxr2 was initially treated either with DTT or with DTT and IAA and then was allowed to bind Ni-NTA beads that was pre-bound with H_2O_2 treated recombinant His-Mge1. The beads were washed and His-Mge1 was made to elute, resolved on SDS-PAGE and the gel was stained with coomassie (Fig. 2.3D). A protein band corresponding to the molecular weight of Mxr2 is detected only in the eluate from the beads that had DTT treated Mxr2. Recombinant H_2O_2 treated His-Mge1 is able to pull down Mxr2 from the bacterial lysate that was treated with DTT but fails to do so when DTT and IAA were added to the bacterial lysate (Fig. 2.3D). These results show that functional cysteine residues within Mxr2 are important for efficient binding to Mge1. To test the specificity, we used recombinant H_2O_2 treated methionine substitution mutant (Mge1 M155L) in the pull down assay and we could not detect any Mxr2 in

Fig.2.3

A

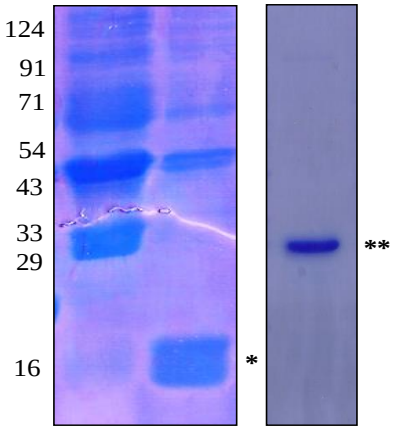

B

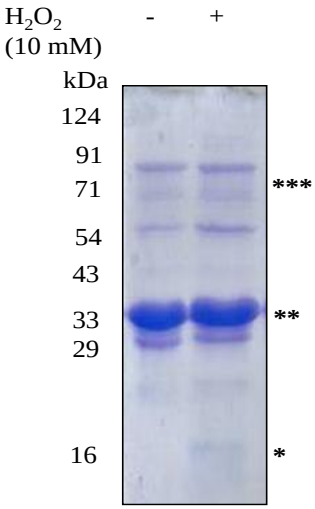

C

Protein sequence coverage: 45%
Matched peptides shown in *bold red*

MNKWSRLYVITVRR**TFPG**
RRNIVLTQYWNKSKKMS
DESNDVKWNDALTPLQL
MVLRDKATERPNTGAYL
HTNESGVYHCANCDRPLY
SSKAKFDAR**CGWPAFYE**
EVSPGAITYHRDNSLMPA
RVEICCAR**CGGHLGHVF**
EGEGWKQLLNLPKDTRH
CVNSASLNLKKD

MS/MS sequence of m/z peak 2239.5

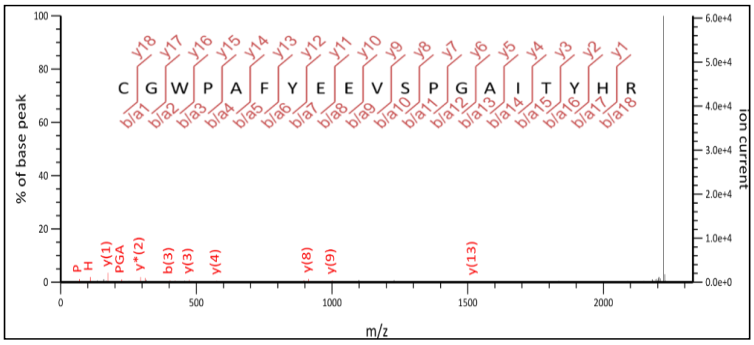

D

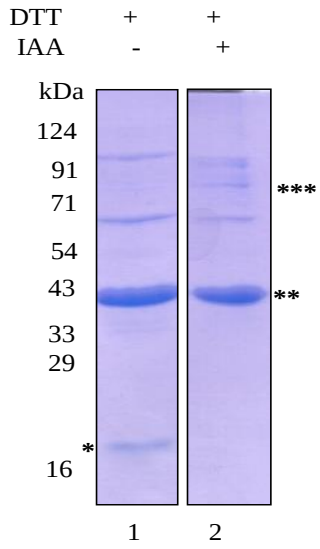

E

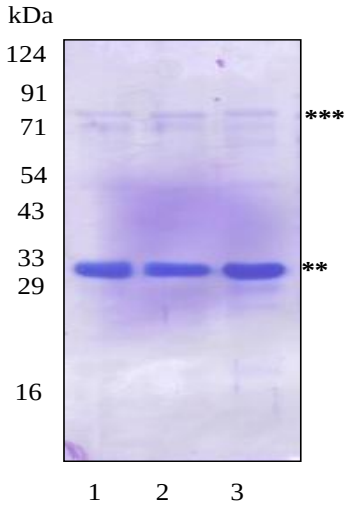

Figure 2.3 *In vitro* interaction of Mxr2 with Mge1 in the presence of H_2O_2

(A) Soluble protein fractions were prepared from bacteria transformed with vector or vector expressing recombinant Mxr2. An aliquot of the soluble protein fractions were resolved by SDS-PAGE and the gel coomassie stained (left panel). Purified recombinant His-Mge1 was resolved by SDS-PAGE and the coomassie stained gel is shown (right panel). (B) Soluble protein fraction of bacterial transformant expressing Mxr2 was incubated with purified His-Mge1 that was pre-treated with or without H_2O_2. His-Mge1 was recovered using Ni-NTA beads, resolved on SDS-PAGE and the coomassie stained gel is shown. (* Mxr2, ** Mge1-His and *** indicates the non-specific bands co-eluted with Mge1). (C) Proteins (from the soluble lysate prepared from bacteria expressing Mxr2) that interacted with His-Mge1 were resolved on a SDS-PAGE and coomassie stained. The proteins bands were excised, digested with trypsin and the peptides analyzed by MALDI-TOF/MS/MS. The peptide mass fingerprint (PMF) obtained by MALDI.-TOF/MS are shown with sequences matching Mxr2 marked in bold red. m/z 2239 Da peptide was further subjected to MALDI-TOF/MS/MS and sequence was matched to the indicated peptide of Mxr2. (D) Bacterial lysate expressing Mxr2 was treated with 10 mM DTT for 10 mins before dividing it into two equal portions and one portion was treated with 50 mM IAA. Both portions containing Mxr2 were incubated with purified His-Mge1 that was pre-treated with H_2O_2. His-Mge1 and its interacting partners were recovered using Ni-NTA beads and separated on a SDS-PAGE and the proteins resolved on the gel were stained with coomassie. (E) Purified His Mge1 M155L was pretreated with or without H_2O_2 and incubated with bacterial lysate expressing Mxr2. Interacting protein were resolved on SDS-PAGE and coomassie stained

the eluate (Fig. 2.3E). This finding suggests that Mxr2 has affinity only for Mge1 that is apparently oxidized by H_2O_2 *in vitro*.

2.3.4 *In vivo* oxidative stress dependent interaction of Mxr2 and Mge1

To extend these studies to quasi *in vivo* conditions, we repeated the above binding assay using cholate solubilized mitochondrial extract prepared from yNB124 cells expressing Flag-Mxr2 as a source for Mxr2 instead of bacterial lysate and additionally pre-treated recombinant His-Mge1 with increasing concentrations of H_2O_2. The eluates were resolved on SDS-PAGE, western transferred and probed with Mge1 and Flag antibodies. With increasing concentrations of H_2O_2, there is a concomitant increase in the binding of Flag-Mxr2 with the amount of Mge1 being almost

same (Fig. 2.4A). To demonstrate that increased pull down of Flag-Mxr2 is indeed due to oxidation as opposed to better bait recovery, we quantified the amount of Mxr2 relative to that of Mge1 from three independent experiments and found that Flag-Mxr2 preferentially binds to oxidized Mge1 (Fig. 2.4B).

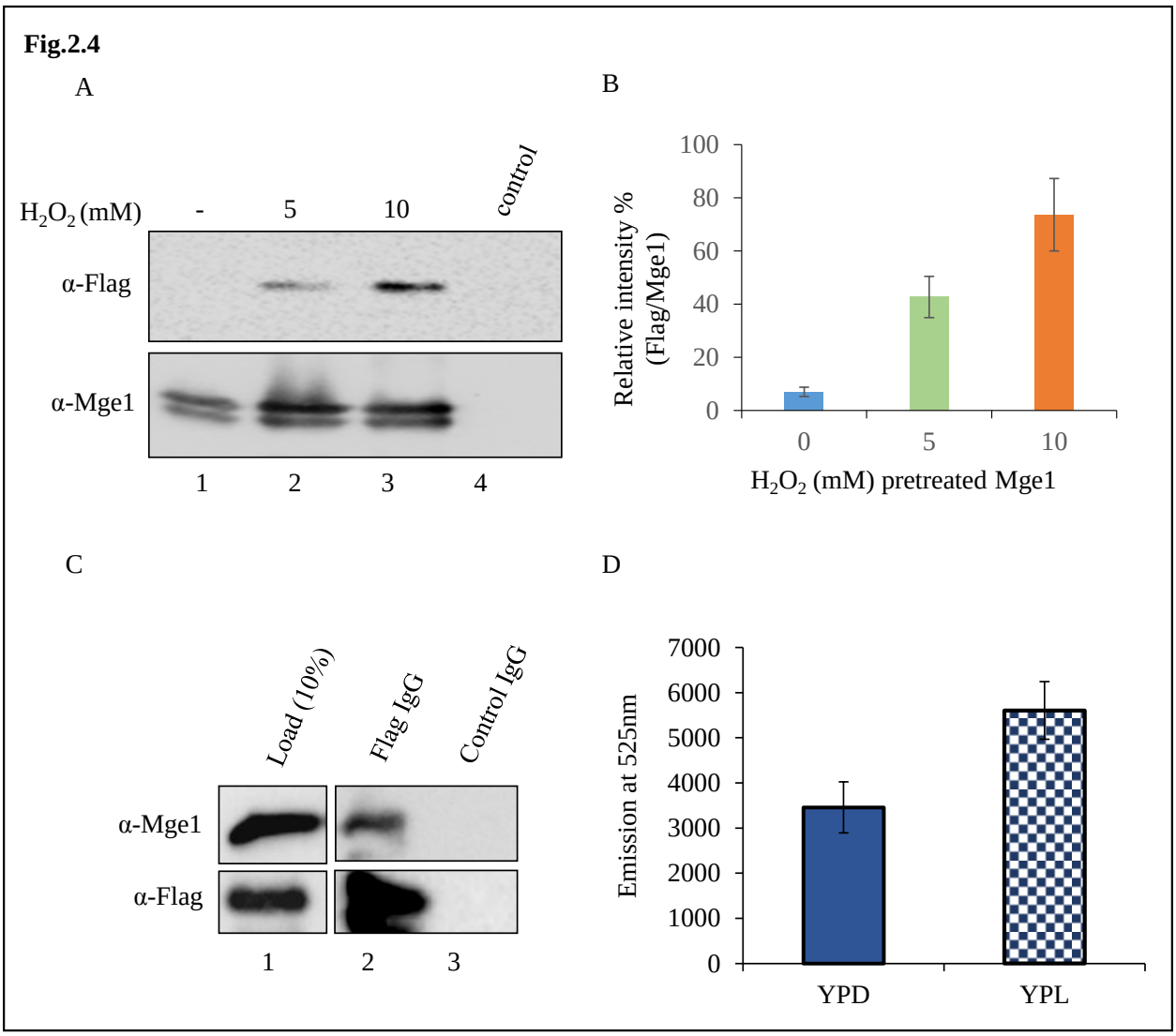

Figure 2.4 *In organello* Mxr2 interaction with Mge1 during oxidative stress

(A) Purified His-Mge1 was treated with increasing concentrations of H_2O_2 and mixed with mitochondrial extracts prepared from yeast expressing Flag-Mxr2 as described in the Methods section. His-Mge1 and bound proteins were recovered using Ni-NTA beads. As a control (lane 4), a Ni-NTA pull down was also performed using only mitochondrial extracts to exclude any non-specific binding to the beads. Samples

were resolved on SDS-PAGE and subjected to immunoblot analysis for the presence of Flag-Mxr2 and Mge1. (B) Three independent blots of Fig. 2.4A were quantified to assess the relative quantity of Mge1 to Mxr2 using ImageJ software (C) Immunoprecipitation of Flag-Mxr2. Flag-Mxr2 was immunoprecipitated from mitochondrial extracts prepared from yeast strain expressing Flag-Mxr2. A control immunoprecipitation was carried out using IgG. Samples were resolved on SDS-PAGE and subjected to immunoblot analysis using antibodies specific for Flag and Mge1. (D) Yeast stains BY4741 were grown to early log phase in different media as shown and ROS was measured as described in the Methods. The histogram represents the average emission values of DCFDA at 525 nm from three replicates.

Based on our *in vitro* and quasi *in vivo* binding assays, we conclude that Mxr2 interacts with Mge1 in an oxidative stress dependent manner and that the cysteines within Mxr2 are crucial for this interaction. We next proposed to examine if Mxr2 is indeed capable of interacting with Mge1 in the cellular context. Co-immunoprecipitation studies were carried out using mitochondria that were isolated from yeast cells expressing Flag-Mxr2. Mxr2 was immunoprecipitated with Flag antibody and probed with antibodies specific for Flag and Mge1 (Fig. 2.4C). Intriguingly, Mge1 was detected in Flag-Mxr2 immunoprecipitates without the addition of any external oxidizing agent to the yeast cells grown in YPL medium prior to isolation of mitochondria. We speculate that the internal ROS that is being produced in the mitochondrial milieu is sufficient to cause oxidation of at least a certain fraction of Mge1. To confirm our speculation, we measured the ROS levels in yeast cells grown in YPL medium and used cells grown in YPD as control. We observe relatively higher levels of ROS in yeast cells growing in YPL medium compared to cells in YPD medium (Fig. 2.4D). The cellular ROS level suggests that indeed it is possible that Mxr2 is interacting with Mge1 in an oxidation dependent manner *in vivo*, a suggestion that is consistent with our *in vitro* findings.

2.3.5 Oxidation of Mge1 at methionine 155 and its subsequent reduction by Mxr2 *in vitro*

Amino acids like Cys, Met, Trp, Tyr, Phe and His are most vulnerable to oxidation in a protein. Given that Mxr2 interacts with Mge1 in an oxidation dependent manner, we wished to investigate which amino acids within Mge1 are being targeted for oxidation. We employed MALDI-TOF/MS/MS analysis to evaluate peptide fragments generated from Mge1 as described in the Methods section. Purified recombinant His-Mge1 was pre-treated with or without H_2O_2 before resolving on a SDS-PAGE gel. Mge1 bands were in-gel, digested with endoproteinase Lys-C and extracted peptides subjected to MALDI TOF spectrum analysis. Peptides generated from Lys-C digestion (Table 2.4) were monitored for their spectrum (Fig. 2.5A and B). All the peptides had the expected MALDI-TOF m/z values except for the Met155 containing peptide (Fig. 2.5C and D). This particular peptide from the untreated Mge1 protein displayed two m/z values, a relatively higher intensity peak of m/z value 2643.3 and a lower intensity peak with m/z value of 2659.3 (Fig .2.5C). The difference in the m/z values of the two peaks obtained from the Met155 containing peptide was ~16 Da. The Met155 containing peptide from the oxidized Mge1 also displayed two peaks with ~16 Da difference in m/z values (Fig. 2.5D). However, the second sample had majority of the intensity coming from the peak that had m/z value of 2659.3 (Fig. 2.5D). The intensity peak profile for the Met155 peptide had changed after oxidation (compare Fig. 2.5C to Fig. 2.5D). We further examined the Met155 containing peptide from both the H_2O_2 untreated and treated samples by MS/MS (Fig. 2.5E and F). From C terminal sequencing we find all the amino acids were identical in both the peptides up to methionine. In case of the peptide from the oxidized sample, after Met the subsequent peptide fragments shows an apparent shift that corresponds to oxidation (Fig. 2.5F). The difference between un-oxidized and oxidized Met155 mass by 16 Da was ascertained by comparing the y11 and y12 ions that were derived from C terminal fragmentation. Addition of 16 Da indicates the formation of methionine sulfoxide in the oxidized peptide. The

formation of methionine sulfoxide was also confirmed by the presence of ions with loss of methane sulfenate (CH3SOH, -64 Da) side chain due to instability of Methionine sulfoxide immonium ion. The MALDI-TOF/MS/MS results provide evidence that Met155 in Mge1 gets oxidized in presence of H_2O_2.

Fig.2.5

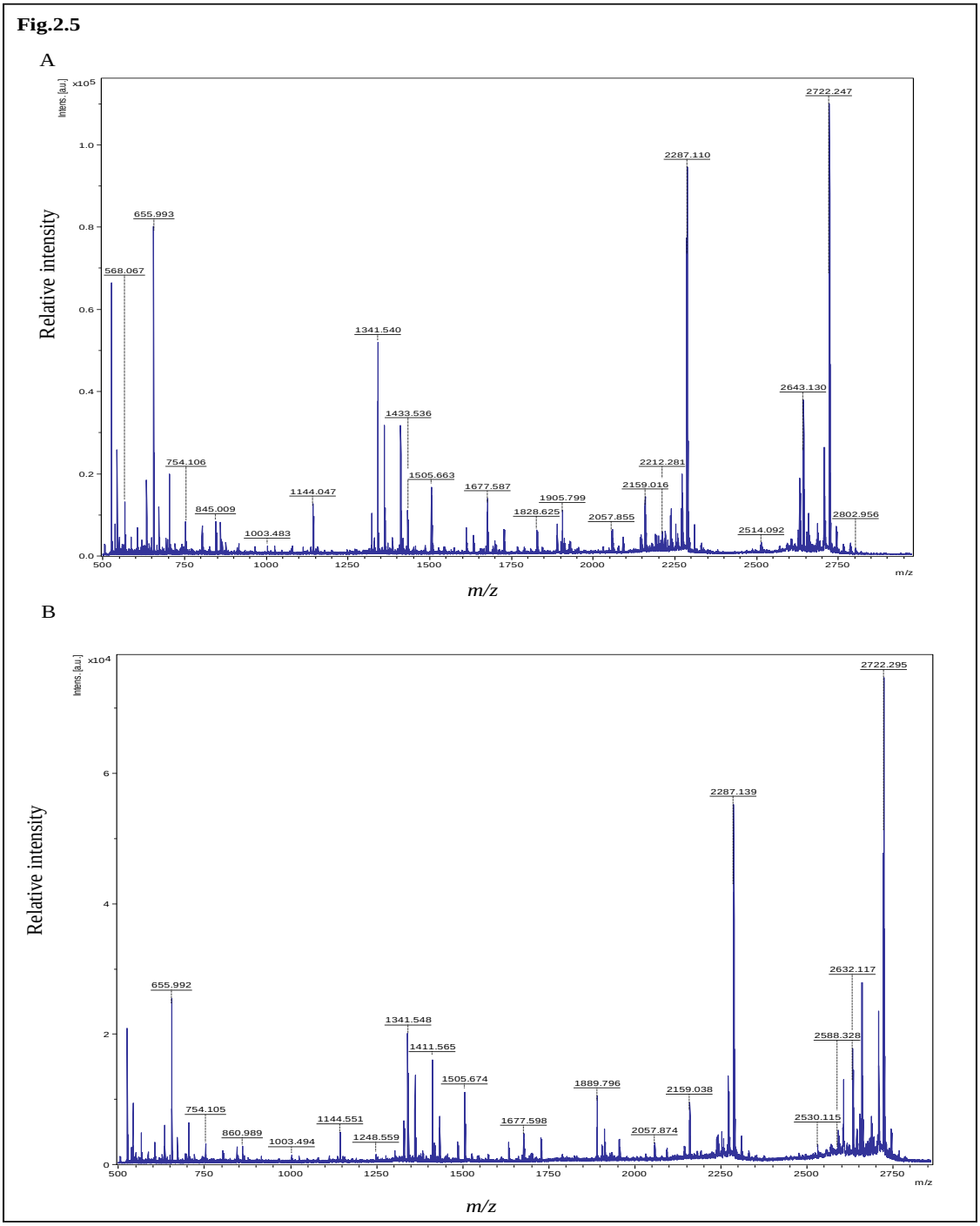

Fig.2.5

C

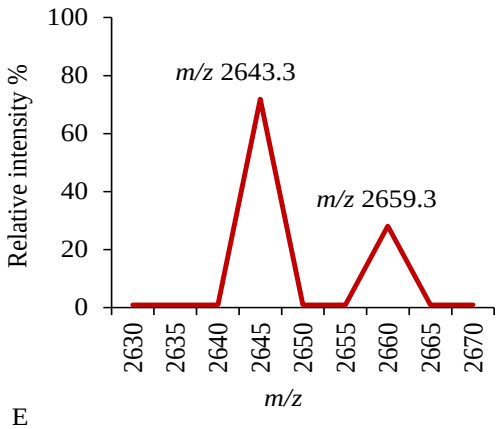
Relative intensity %
100
80
60
40
20
0
m/z 2643.3
m/z 2659.3
2630
2635
2640
2645
2650
2655
2660
2665
2670
m/z

D

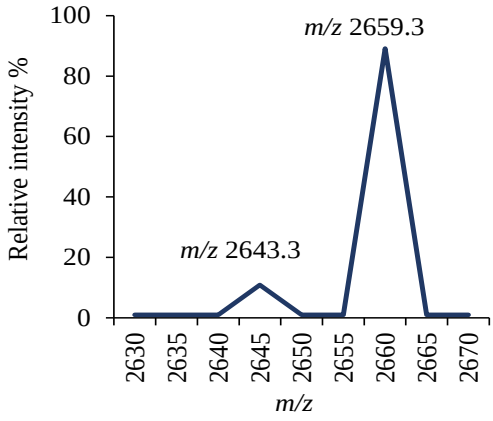
Relative intensity %
100
80
60
40
20
0
m/z 2659.3
m/z 2643.3
2630
2635
2640
2645
2650
2655
2660
2665
2670
m/z

E

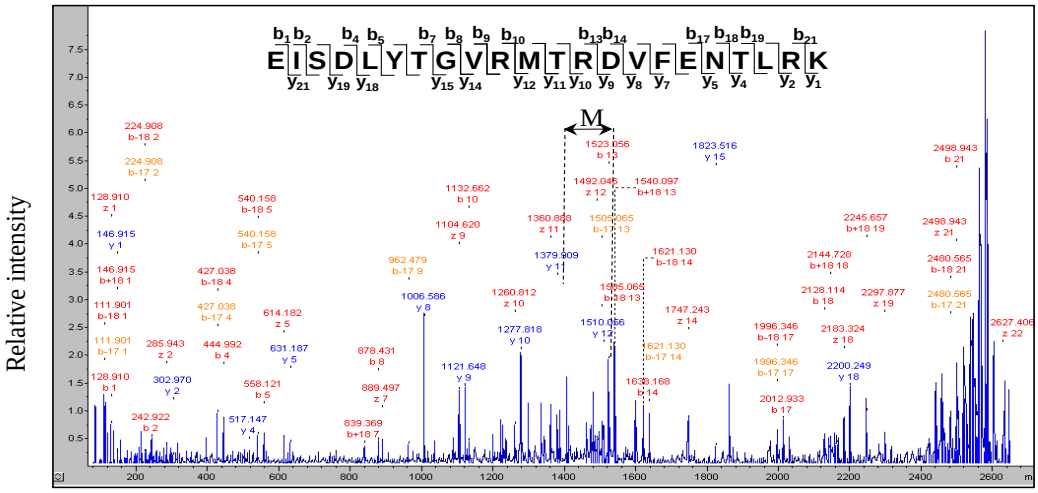
Relative intensity
EISDLYTGVRMTRDVFENTLRK
M
m/z

F

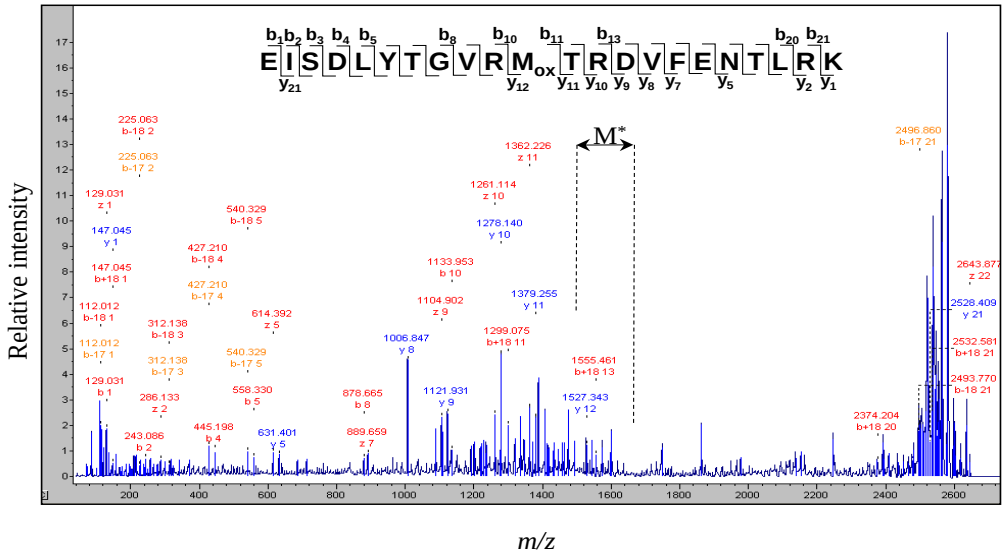
Relative intensity
EISDLYTGVRMoxTRDVFENTLRK
M*
m/z

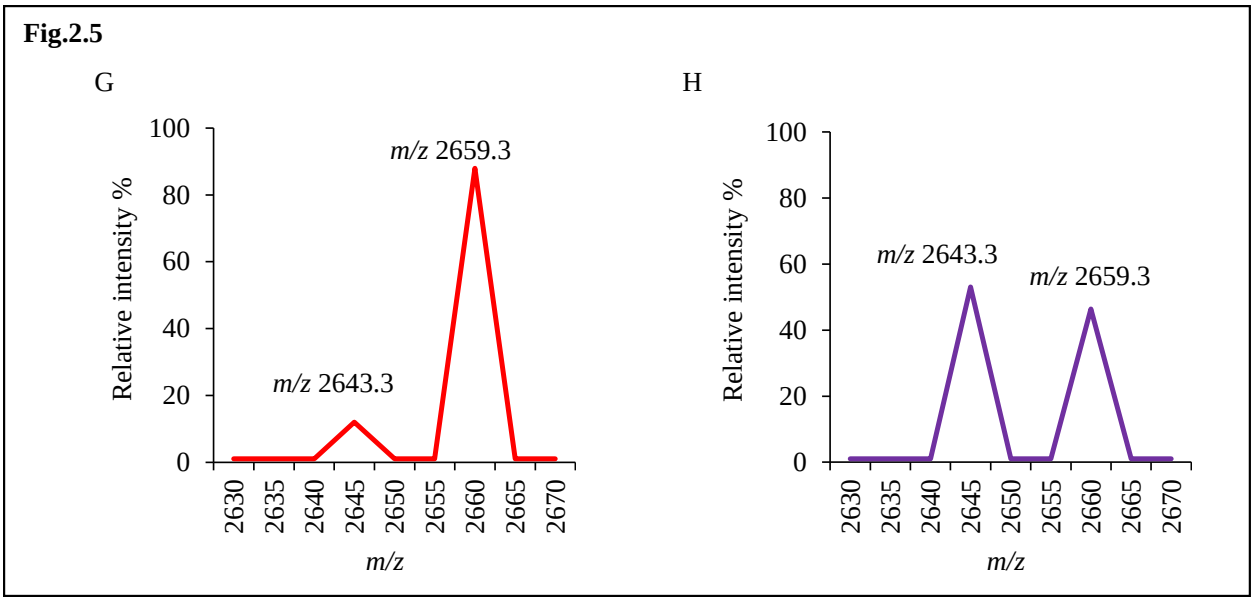

Figure 2.5 Met155 in Mge1 is oxidized by H_2O_2 and reduced by Mxr2

Untreated His-Mge1 and His-Mge1 treated with 20 mM H_2O_2 were incubated at room temperature for 4 hrs and SDS-PAGE separated and coomassie stained. Excised Mge1-His bands were processed for MALDI-TOF as described under the Methods section. The digested peptides were analyzed by MALDI TOF Spectrum of untreated (A) and H_2O_2 treated (B). (C and D) Reconstructed MALDI-TOF spectrum of Met155 peptide from His-Mge1. Relative quantification of MALDI-TOF spectrum of the Met155 containing peptides was presented (C) from Fig. 2.5A and (D) from Fig. 2.5B. (E). MS/MS spectrum of unoxidised (*m/z* 2643.3) peptide. (F). MS/MS spectrum of oxidized (*m/z* 2659.3) peptide. (G and H) Oxidized His-Mge1 was further treated with DTT (G) and DTT + Mxr2 (H) for 4 hrs prior to processing for MALDI-TOF. The MALDI-TOF spectrum of the Met155 containing peptide was presented.

Also, it shows that the apparently un-oxidized Mge1 is a mixture of small fraction of oxidized and major fraction of un-oxidized Mge1.

As the oxidized form of Mge1 alone is capable of significant interaction with Mxr2, we were interested to test if Mxr2 can reduce oxidized Mge1 and more specifically the oxidized Met at position 155 in Mge1. MALDI-TOF/MS/MS method was further employed to investigate if Mxr2 targets the oxidized Met155 for reduction. We repeated the MALDI-TOF analysis of H_2O_2 treated Mge1 protein with one modification. After H_2O_2 treatment, Mge1 was further treated with DTT in

the presence or absence of Mxr2. As shown (Fig. 2.5G), H_2O_2 treated Mge1 in the absence of Mxr2 was more than 75% enriched in the higher m/z value peak of 2659.3 indicating that H_2O_2 was able to efficiently oxidize Mge1 (Fig. 2.5G). Most importantly, Mxr2 treatment reduces the intensity of the oxidized peak of m/z value 2659.3 by nearly 50% concomitant with a corresponding increase in the intensity of the un-oxidized peak of m/z value 2643.3 (Fig. 2.5H).

To determine the specificity of Mxr2 action, we adopted a coupled NADPH dependent thioredoxin / thioredoxin reductase assay system in which wild type recombinant Mge1, free methionine sulfoxide and a known Mxr2 substrate protein, GST were used as substrates. Free methionine sulfoxide and GST were included to determine the specificity of Mxr2 activity. Equimolar amounts of purified wild type Mge1 and GST were treated with H_2O_2 for 4 hours prior to the addition of Mxr2 in the coupled assay as described in the Methods section. Mxr2 exhibits significant activity on H_2O_2 treated Mge1 and is comparable to its activity on GST (Fig. 2.6A). However, Mxr2 shows very less activity on free methionine sulfoxide indicating the specificity of Mxr2 to reduce oxidized methionine only in proteins. Our results clearly show that Mge1 is a substrate for Mxr2 and Mxr2 majorly and specifically acts on oxidized methionine at position 155 in Mge1.

As the results described above unequivocally show that Mxr2 reduces oxidized Mge1 specifically, we further wished to understand if there is any correlation to the functional activity of Mge1. In an earlier study, we have shown that dimeric Mge1 interacts with Hsp70 to form Hsp70-Mge1 complex that has a stimulatory effect on the ATPase activity of Hsp70. We have additionally shown that H_2O_2 reduces this stimulatory function of Mge1. To determine whether oxidation of methionine 155 within Mge1 is directly responsible for its loss of stimulatory activity and whether the reducing activity of Mxr2 on Mge1 will restore this function, we performed a steady state *in vitro* ATPase activity of Hsp70 as described in the Methods section.

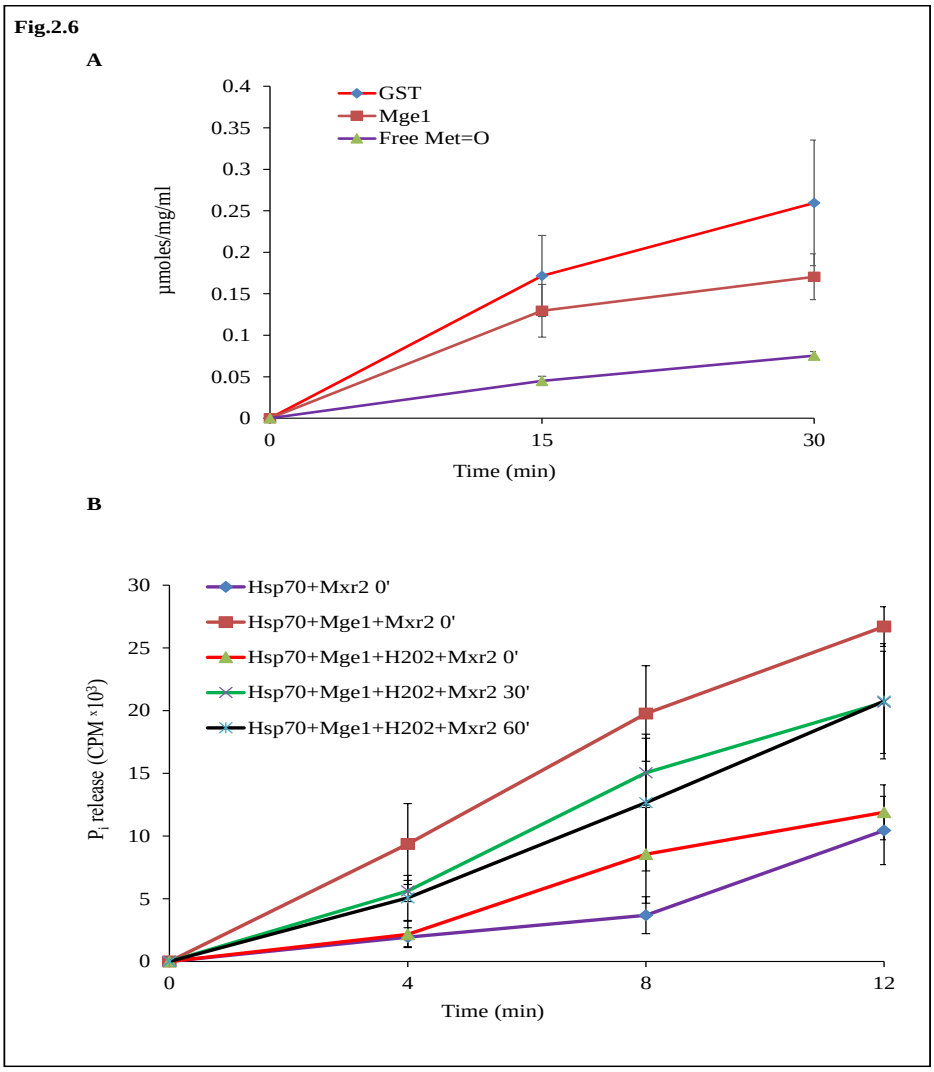

Figure 2.6 Mxr2 reduces oxidized Mge1 and restores ATPase activity of Mge1

(A) Purified recombinant His-Mge1 (50 µM) and GST (50 µM) proteins were treated with H_2O_2 prior to being used as substrates in Mxr2 enzymatic assay as described in the Methods section. Free methionine sulfoxide (Met-SO, 1 mM) was also included as a control substrate. Mxr2 activity was measured as a decrease in the absorption at OD_{340} nm. The graph represents relative activity of the enzyme and is expressed as micromoles per mg per ml. The basal activity observed in the absence of substrate was subtracted from the values obtained in the presence of substrate and enzyme. As there was no detectable enzymatic activity in the absence of Mxr2, this control is not shown. (B) Purified Mge1 was initially incubated with or without 5 mM H_2O_2 for 2 hrs in PBS pH 7.2. Later, the proteins were treated with or without Mxr2 for 0, 30 or 60 min followed by incubation with recombinant Hsp70 in an ATPase assay buffer as described previously. The release of labeled inorganic phosphate was monitored at different time

points in a scintillation counter. A control Hsp70 sample was incubated with Mxr2 to monitor non-specific ATP hydrolysis.

Mitochondrial Hsp70 has low ATPase activity in the absence of Mge1 (Fig. 2.6B). In the presence of wild type recombinant Mge1, the ATPase activity of Hsp70 is enhanced three fold. However, H_2O_2 treated Mge1 has negligible effect on the ATPase activity of Hsp70. Most importantly, prior treatment of oxidized Mge1 with Mxr2 restores the ATPase stimulatory activity of Mge1 on Hsp70 *in vitro* (Fig. 2.6B). The aforementioned results clearly show that Mge1 gets oxidized at Met155 in presence of H_2O_2 and Mxr2 specifically reduces the oxidized Met155 in Mge1 *in vitro*. We additionally provide evidence that Mge1 is a substrate for Mxr2 and that Mxr2 specifically reduces oxidized methionine at position 155 in Mge1 and modulates Hsp70 function through Mge1 in a quasi-physiological system.

2.3.6 Mge1 is a physiological substrate of Mxr2

To determine whether Mge1 is a physiological substrate of Mxr2 and if yes, to elucidate the *in vivo* functional significance of Mge1 Met-SO reduction by Mxr2, we studied the effect of deletion of MXR2 on the growth of yeast strains expressing either wild type MGE1 or MGE1 M155L mutant. Since Mge1 is an essential gene, we constructed haploid yeast strains that had chromosomal copies of both MGE1 and MXR2 deleted (indicated by ΔΔ), however, ectopically expressing either WT MGE1 (yNB130: ΔΔ/ WT MGE1) or MGE1 M155L mutant (yNB131: ΔΔ/ M155L MGE1) from high copy plasmids. The parent BY4741 strain and its derivatives yNB66 (BY4741/vector*)* and yNB122 (*mxr2*Δ, vector) were included as controls when testing for growth. We compared the growth sensitive phenotype of all the above yeast strains by spotting on YPD and SC-Leu plates that were supplemented with or without H_2O_2 (Fig. 2.7A and B). All the strains had comparable growth on YPD and SC-Leu plates. However, the growth of WT MGE1

expressing strains in *mxr2*Δ background were severely retarded in presence of H_2O_2 compared to the parent BY4741 strain which has an intact MXR2 (Fig. 2.7A and B). Most importantly, yNB131 strain expressing MGE1 M155L in the MXR2 deletion background was able to grow robustly in the presence of H_2O_2. Similar results were obtained when the above mentioned yeast strains were grown in liquid YPD in the presence or absence of H_2O_2 (Fig. 2.7C). Our results suggest that MGE1 and MXR2 have a functional genetic interaction and that MXR2 is epispastic to MGE1.

It has been shown previously that deletion of MXR2 compromises the growth of yeast on media containing non-fermentable carbon sources. To examine whether MGE1 M155L mutant can rescue this growth defect, we tested the growth of yNB66, yNB122, yNB130 and yNB131 strains on YPGE plates that contain ethanol and glycerol as non-fermentable carbon sources. As shown (Fig. 2.7D), over-expression of MGE1 M155L mutant partially rescues the growth defect of *mxr2*Δ strain when compared to *mxr2*Δ strain expressing wild type MGE1 on YPGE plates. We additionally transformed yNB130 with a high copy URA3 vector or with pNB475 to create yNB132 (ΔΔ/WT Mge1, vector) and yNB133 (ΔΔ/WT MGE1, FLAG-MXR2) strains respectively to check if ectopic expression of MXR2 can compensate the chromosomal deletion of MXR2. Ectopic expression of MXR2 is able to compensate the chromosomal deletion of MXR2 as the strain yNB133 displayed better growth compared to yNB132 in presence of H_2O_2 (Fig. 2.7E).

Fig.2.7

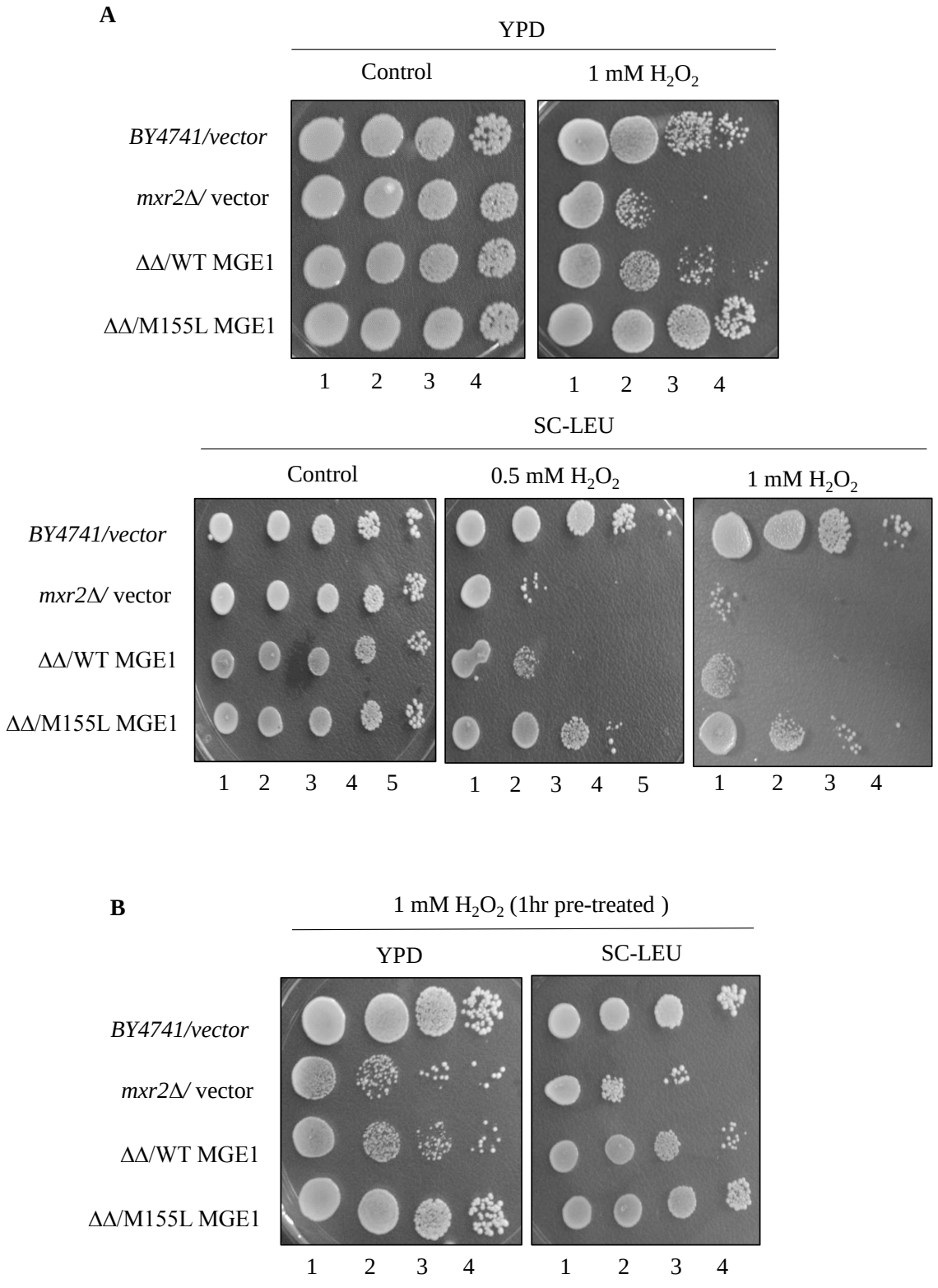
A
YPD
Control
1 mM H2O2
BY4741/vector
mxr2Δ/ vector
ΔΔ/WT MGE1
ΔΔ/M155L MGE1
1 2 3 4
1 2 3 4
SC-LEU
Control
0.5 mM H2O2
1 mM H2O2
BY4741/vector
mxr2Δ/ vector
ΔΔ/WT MGE1
ΔΔ/M155L MGE1
1 2 3 4 5
1 2 3 4 5
1 2 3 4
B
1 mM H2O2 (1hr pre-treated)
YPD
SC-LEU
BY4741/vector
mxr2Δ/ vector
ΔΔ/WT MGE1
ΔΔ/M155L MGE1
1 2 3 4
1 2 3 4

Fig.2.7

C

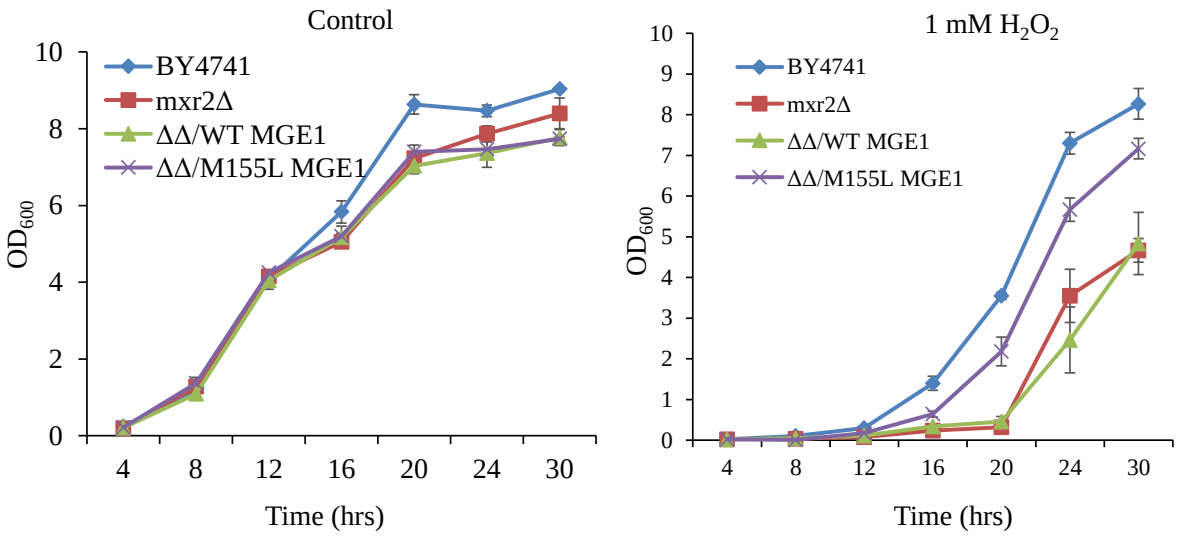
Control
BY4741
mxr2Δ
ΔΔ/WT MGE1
ΔΔ/M155L MGE1
OD600
Time (hrs)
1 mM H2O2
BY4741
mxr2Δ
ΔΔ/WT MGE1
ΔΔ/M155L MGE1
OD600
Time (hrs)

D

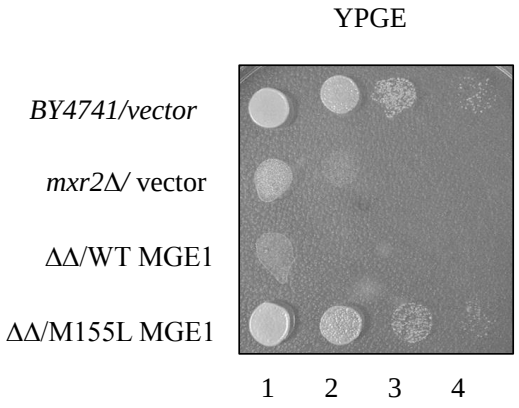
YPGE
BY4741/vector
mxr2Δ/ vector
ΔΔ/WT MGE1
ΔΔ/M155L MGE1
1 2 3 4

E

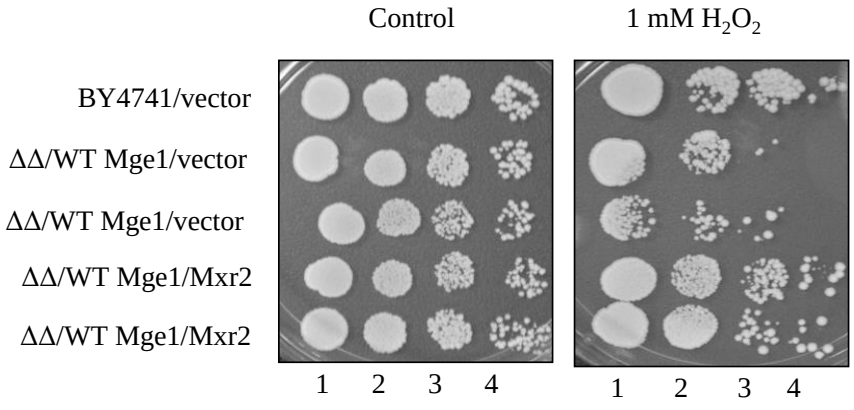
Control
1 mM H2O2
BY4741/vector
ΔΔ/WT Mge1/vector
ΔΔ/WT Mge1/vector
ΔΔ/WT Mge1/Mxr2
ΔΔ/WT Mge1/Mxr2
1 2 3 4
1 2 3 4

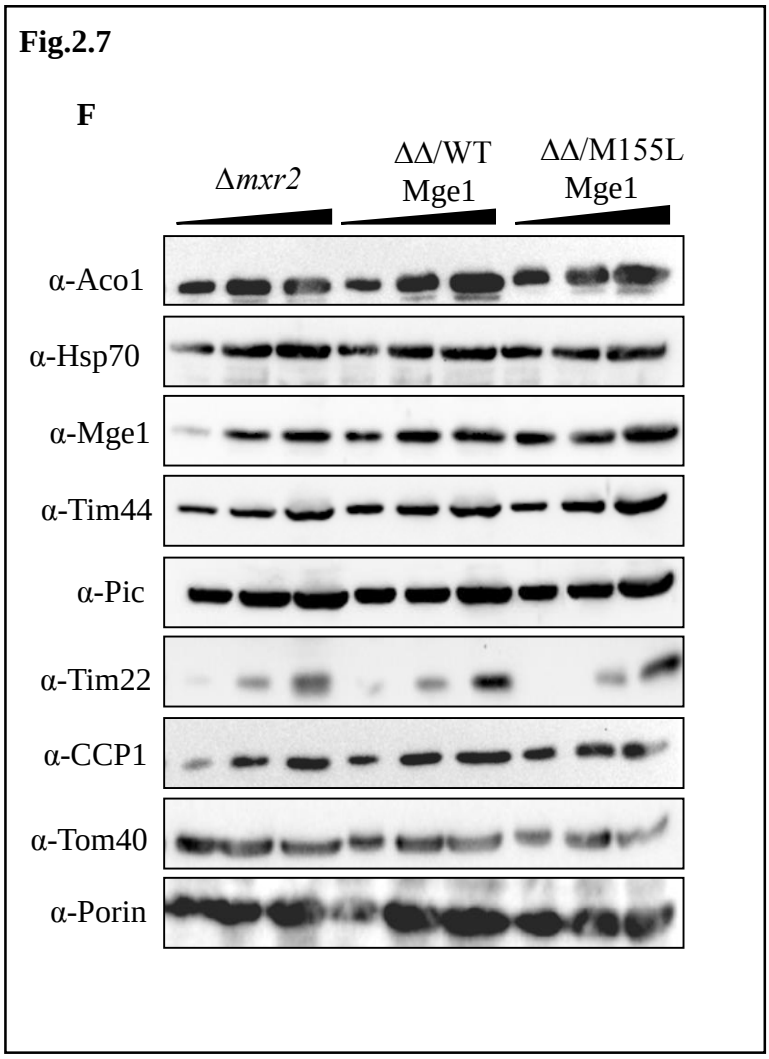

Figure 2.7 Mge1 is a physiological mitochondrial substrate of Mxr2

Yeast strains yNB62 (BY4741/vector), yNB115 (*mxr2Δ*), yNB130 (ΔΔ/WT MGE1), yNB131 (ΔΔ/M155L MGE1), yNB122 (*mxr2*ΔΔ/vector*)*, yNB132 (ΔΔ/WT MGE1/vector) and yNB133 (ΔΔ/WT MGE1/Flag-Mxr2) were studied for growth on solid and liquid medium during stress conditions. (A, C, and D) Spotting Assay. All strains were grown overnight in YPD medium before being serially diluted the cells from strains yNB62, yNB115, yNB130 and yNB131 and spotted on a YPD +/- 1 mM H_2O_2 (A), SC-LEU +/- 0.5 mM / 1 mM H_2O_2 (A, Middle Panel) and on YPG Ethanol (YPGE) (C) plates. (B) Growth curve. Yeast strains were grown overnight in YPD medium and used to inoculate fresh YPD media supplemented with or without H_2O_2. Growth was monitored by taking OD_{600} nm every 4 hr over a 30 hr time period. (D) Overnight grown yeast cells from the strains yNB62, yNB130 and yNB131 were spotted on an YPD plate with or without 1 mM H_2O_2. (E) Mitochondria were isolated from indicated strains and increasing concentrations of the mitochondrial fraction (10, 25 and 50 μg) were resolved on SDS-PAGE and subjected

to immunoblot analysis using antibodies against mitochondrial proteins. (ΔΔ indicates the chromosomal deletion of both MXR2 and MGE1).

To rule out the possibility that altered protein expression may be responsible for the resistance offered by MGE1 M155L expression in the absence of MXR2, we evaluated the steady state level of mitochondrial proteins in yNB122, (*mxr2*Δ), yNB130 (ΔΔ/WT MGE1) and yNB131 (ΔΔ/MGE1 M155L) strains. Isolated mitochondrial samples were resolved on SDS-PAGE, western transferred and probed with antibodies specific for Porin, Tim44, Hsp70, Tim22, CCPO, Aconitase, Tim23 and Tom40 (Fig. 2.7F). We did not observe any significant change in the expression of the tested proteins. Taken together, the above results show that MGE1 M155L is not susceptible to oxidation and thereby overcomes the requirement of MXR2 by the yeast cell to grow in presence of oxidative stress.

2.3.7 *In vivo* oxidation of Mge1

To ascertain if Mge1 is indeed getting oxidized at methionine 155 *in vivo* and subsequently gets reduced by Mxr2, we constructed two yeast strains, yNB134 (ΔΔ/ His-MGE1) and yNB135 (ΔΔ/ His-MGE1, Flag-MXR2) as described in the Methods. Yeast strains yNB134 and yNB135 were spotted on YPGE plates. As expected, yeast strain yNB134 has very poor growth on YPGE plate. However, yNB135 exhibits better growth as Flag-MXR2 is apparently able to compensate for the MXR2 deletion (Fig. 2.8A). Further, we have observed that the internal ROS is much higher when cells are grown in non-fermentable carbon medium (YPGE) compared to YPL/YPD medium (Fig. 2.8B). Yeast strains yNB134 and yNB135 were grown in liquid YPGE medium and His-Mge1 was affinity purified by passing the yeast cells extract through a Ni-NTA column as described in the Methods section. Purified His-Mge1 was resolved on SDS-PAGE, stained with coomassie and the His-Mge1 protein band was extracted from the gel for MALDI-TOF/MS-MS analysis as

described above. The relative mass spectrum of His-Mge1 from strains yNB134 and yNB135 are similar (Fig. 2.8 C and D). MALDI-TOF analysis revealed that in the absence of MXR2, the Met155 containing peptide of Mge1 exists in both oxidized (m/z 2659.3) and un-oxidized (m/z 2643.3) forms (Fig. 2.8B). However, the relative intensity of the oxidized peak is much higher than the un-oxidized peak in case of the Met155 peptide from yNB134 that lacks MXR2. In contrast, the reverse is true in case of yNB135 that ectopically expresses Flag-MXR2. Interestingly, this result shows that the internal ROS generated during growth in YPGE medium is sufficient to trigger oxidation of Mge1. Nevertheless, the MALDI-TOF results are consistent with the slow growth

Fig.2.8

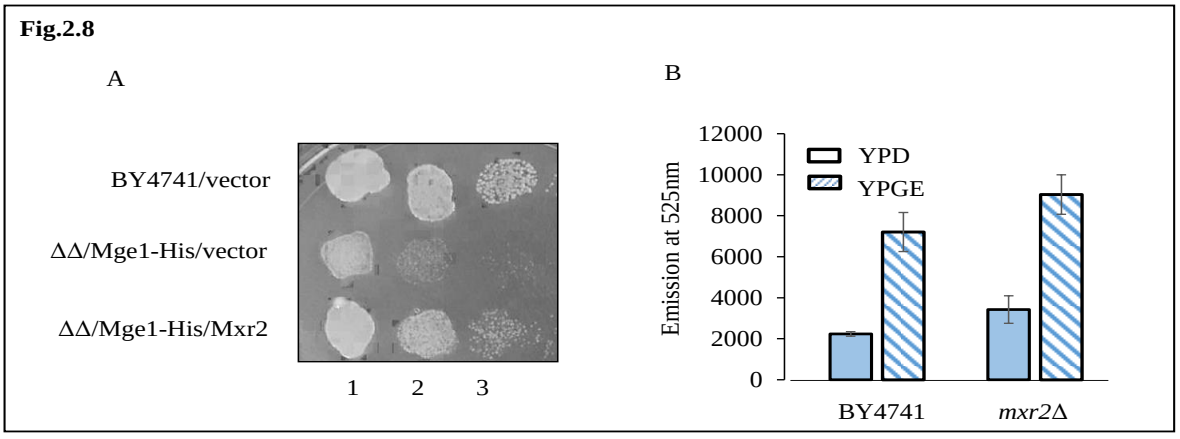

Fig.2.8

C

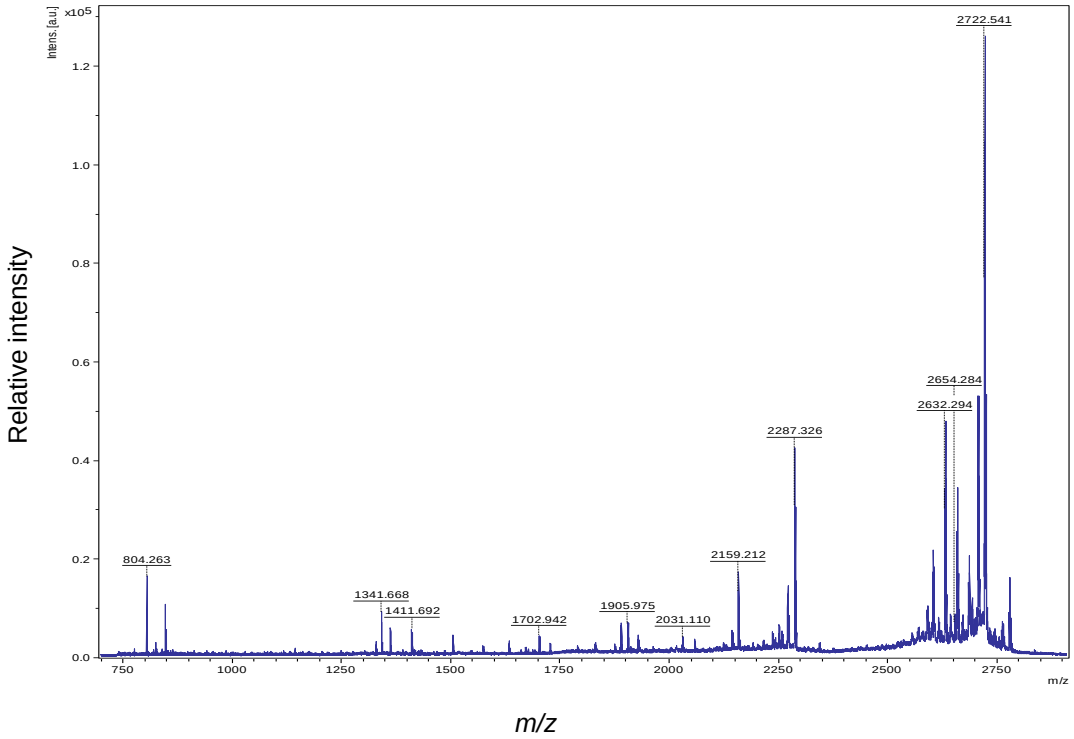

Relative intensity

m/z

D

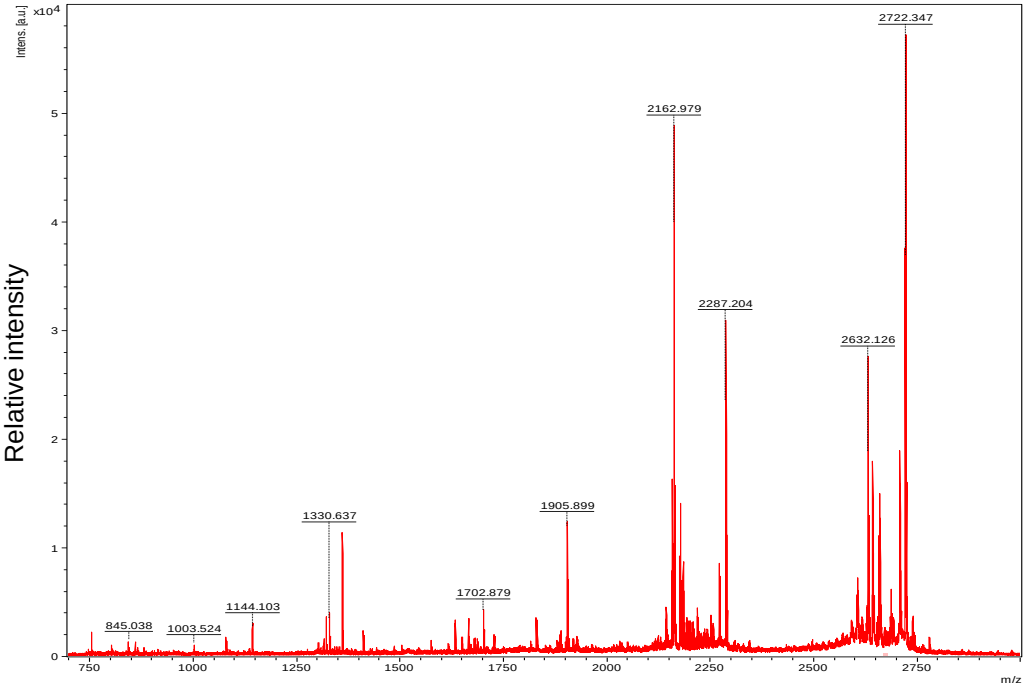

Relative intensity

m/z

Fig.2.8

E

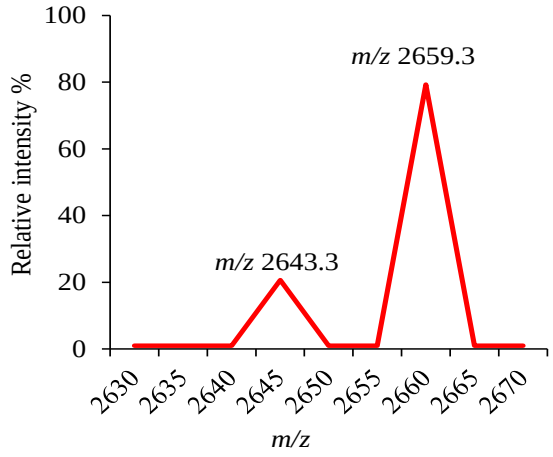

F

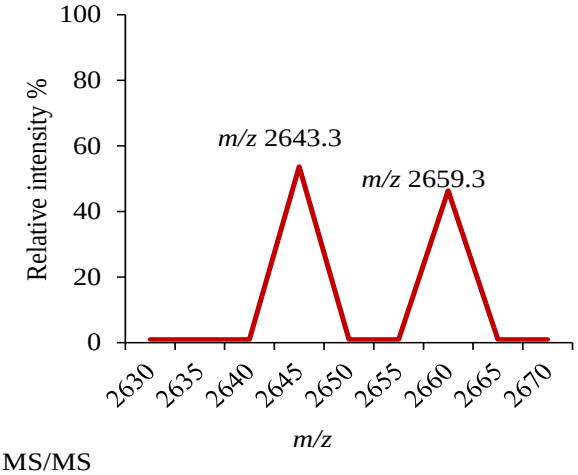

G

m/z 2643 MS/MS

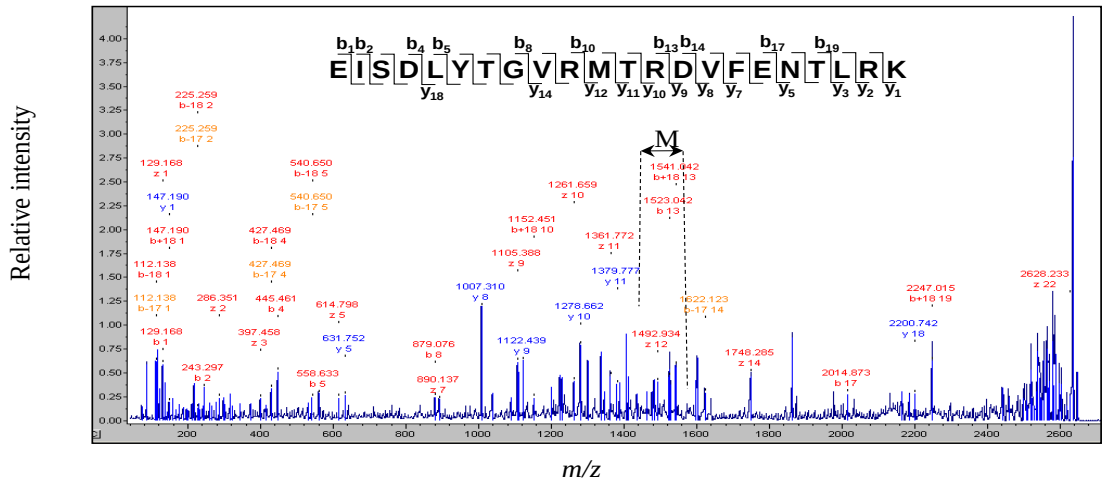

H

m/z 2659 MS/MS

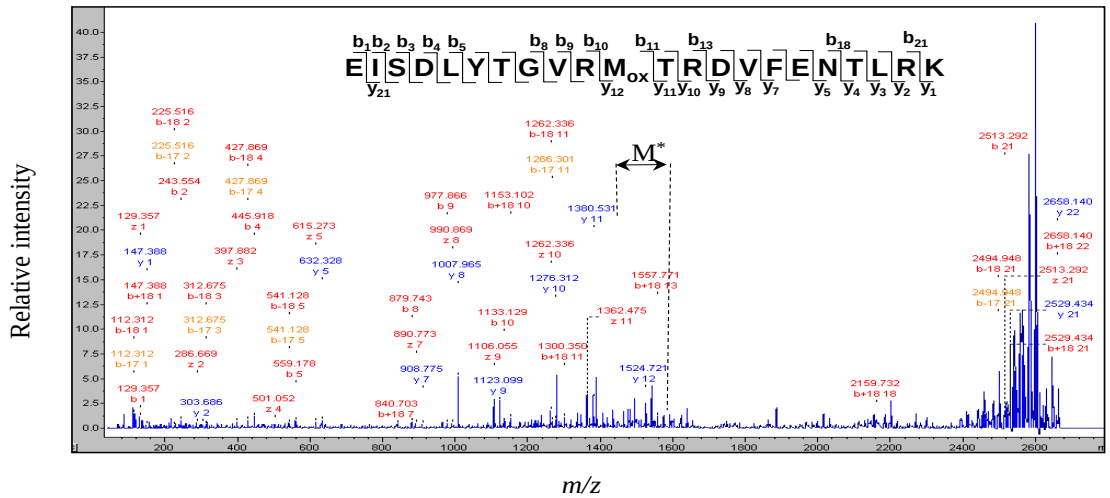

Figure 2.8 MALDI-TOF spectrum of Met155 peptide of intracellular His-Mge1

(A).Yeast strains BY4741, yNB134 (ΔΔ/His-MGE1*)* and yNB135 (ΔΔ/His-MGE1/Flag-MXR2) were grown overnight in YPD medium and serial diluted the cells and spotted on YPGE plates. (B) Yeast strains BY4741 and yNB115 were grown to early log phase either in YPD or YPGE and equal amount of cells were used to measure the ROS as mentioned in Methods. The histogram represents the average emission values of DCFDA at 525 nm from three replicates. (C and D) As mentioned in methods Mge1 His protein purified from yeast cells containing with or without MXR2 gene and SDS-PAGE separated. The excised Mge1 protein was extracted from gel and digested with LysC. The complete MALDI TOF Spectrum of digested peptides from *mxr2Δ* background (C) and MXR2 expressing strain (D). (E and F). Reconstructed MALDI-TOF spectrum of His-Mge1 *in vivo*. MALDI-TOF spectrum of the Met155 containing peptide of His-Mge1 from yNB134 (E) and yNB135 (F) is shown. The peak with m/z value 2643.3 represents the unoxidized Met155 peptide while the peak with m/z value of 2659.3 represents the oxidized Met155 peptide as deduced from the MS/MS spectrum (Fig 2.8 C and D respectively). Met155 containing peptides of oxidized and un-oxidized His-Mge1 were further subjected to MS/MS analysis. The appearance of oxidized methionine of ~16 atomic mass units in y_{11} and y_{12} ions is indicated. (G) MS/MS spectrum of un-oxidized (*m/z* 2643.3 Da) peptide. (H) MS/MS spectrum of oxidized (*m/z* 2659.3 Da) peptide.

phenotype of yNB134 strain (ΔΔ/His MGE1) on YPGE plates and our co-immunoprecipitation results which showed that Mge1 interacts with Mxr2 *in vivo* (Fig. 2.4C). Most importantly, ectopic expression of MXR2 is able to reduce the oxidized form of His-Mge1 as there is an increase in the intensity of the un-oxidized Met155 peptide (m/z value 2643.3) concomitant with a decrease in the Met155 oxidized peptide (m/z value 2659.3) (Fig. 2.8C). We further confirmed the oxidation status of the Met155 peptide by MS/MS analysis using protein isolated from above strains (Fig. 2.8 G and H). Consistent with our *in vitro* findings, we find that Mge1 indeed is capable of getting oxidized at Met155 *in vivo*. Most notably, we show through genetic complementation experiments and by MALDI-TOF/MS/MS that expression of MXR2 is essential for restoring growth during oxidative stress and for reducing oxidized Mge1 at Met155.

2.3.8 Mge1 M155L protects cells from stress mediated protein aggregation

In order to understand the functional consequence of Mge1 Met155 oxidation in the absence of MXR2, we monitored protein aggregation in strains that express wild type MGE1 or MGE1 M155L mutant in a MXR2 deletion background. Most of the proteins have a finite tendency to misfold or unfold during stress conditions and form protein aggregates. Oxidative stress in the form of H_2O_2 can induce aggregation of proteins in mitochondria. So far, the evidence has implicated Mge1 with a role of an oxidative sensor, a modulator of Hsp70 and a regulator of mitochondrial protein import in the oxidative stress response pathway. We wished to examine the role of Mge1 M155L mutant in prevention of aggregation of proteins during oxidative stress. Towards this end, we employed two strains, a BY4741 as control and a second strain, yNB115 that is deleted for MXR2. Strains BY4741 and yNB115 were grown in YPL medium for 24 hrs before harvesting the cells. Mitochondria were isolated from both the strains and were treated with increasing concentration of H_2O_2 (0, 5, 10 mM) for 30 minutes in presence of energy before centrifuging the samples. ATP dependent Hsp70 activity is inhibited when energy is not present and it is likely that any differences in protein aggregation will be masked by this low activity. Hence, energy in the form of ATP was included. The supernatant and pellet fractions were resolved on SDS-PAGE, silver stained and the protein profile examined (Fig 2.9) for protein aggregation. Absence of MXR2 triggers increased protein aggregation compared to control sample in the pellet fraction even at low concentration of H_2O_2 (Fig 2.9B). We repeated the above experiment in strains ectopically expressing either MGE1 M155L mutant (yNB131) or MGE1 (yNB130) wild type in MXR2 deletion background (Fig 2.9C & D). We find that the mitochondria isolated from the strain harboring MGE1 M155L mutant is partially protected from protein aggregation (Fig 2.9C). In case of mitochondria from the strain carrying wild type MGE1, protein aggregation is observed even at 5 mM H_2O_2. These results lend support to our hypothesis that protein aggregation is prevented

because of an efficient Hsp70-Mge1 M155L mutant complex. In case of wild type Mge1, Met155 gets oxidized and destabilizes the Hsp70-Mge1 complex leading to protein aggregation.

Fig.2.9

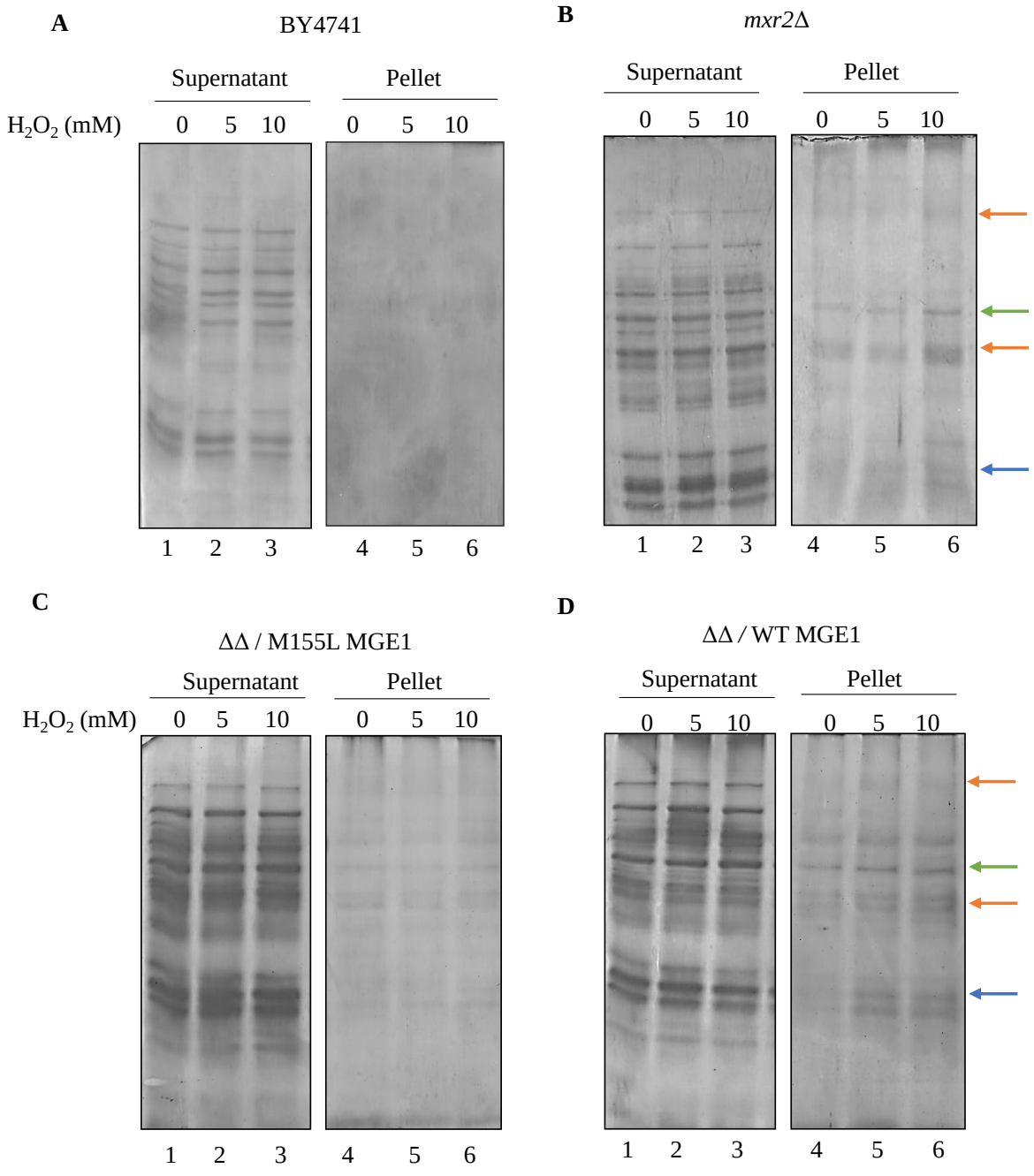

Figure 2.9 Oxidative modification of WT Mge1 causes loss of function

(A, B, C, D) Mitochondria (50 µg) were isolated from strains BY4741, yNB115 (*mxr2*Δ), yNB130 (ΔΔ/M155L Mge1), and yNB131 (ΔΔ/WT Mge1) and treated with increasing concentrations of H_2O_2 in the presence of energy as indicated in the Figure and processed as described under 'Protein Aggregation' in the Methods section. The figures are pictures of silver stained SDS-PAGE gels of supernatant and pellet fractions of mitochondria.

Our findings provide compelling evidence that Mge1 and Mxr2 are components of the oxidative response pathway and that Mxr2 is epistatic to Mge1. We have presented genetic and biochemical evidence to show that Mge1 is a physiological substrate of Mxr2. MGE1 M155L mutant can effectively compensate for the absence of MXR2 as it relieves the growth defect associated with MXR2 deletion in presence of H_2O_2 and on non-fermentable carbon sources. Most importantly, we have shown that Met155 in Mge1 gets oxidized *in vitro* and *in vivo* and that Mxr2 very specifically can reduce oxidized Met155 within Mge1. We conclude that oxidized Mge1 is a substrate of Mxr2 and that methionine 155 is crucial for the reversible regulation of Mge1 thereby adding a new paradigm in the regulation to the oxidative stress response pathway.

2.4 Discussion

Oxidative stress causes an imbalance in the redox potential that may lead to the development of several neurological disorders and ageing [85]. Several antioxidative defensive mechanisms have evolved to neutralize the oxidative stress and thereby protect cells from oxidative damage [130], [131]. More than 90% of cellular oxygen is consumed within mitochondria, making mitochondria the main contributor of ROS and mitochondrial proteins as major and immediate targets of ROS [64], [66], [117]. ROS generated in mitochondria has been implicated in multiple signaling pathways ranging from apoptosis, tumor survival to turnover of mitochondria also known as autophagy. Increasing evidence suggests that ROS is also essential for several biological processes such as growth and development [74], [76]. Sulfur containing amino acids methionine and cysteine

are easily susceptible to oxidation thereby placing the cell on alert. This mechanism plays an important role in regulating protein function and redox signaling. Like cysteine, hydrophobic methionine is also capable of getting oxidized to create a hydrophilic environment within its proximity with an increased affinity for hydrogen bonding. Hydrogen bonding causes a conformational change in the proteins. The reversibility of the oxidation status of Cys and Met amino acids in a protein transforms these amino acids into powerful regulators of the proteins function in which they reside and also regulate the interaction of the protein with its partners [118]. Interestingly, yeast Mge1 harbors only one methionine and this is present in the helical region of the protein. Substitution of methionine to leucine renders the Mge1 protein resistant to oxidation and is also sufficient to stabilize the dimer formation and interaction with Hsp70 *both in vitro* and *in vivo* from oxidative stress.

Mge1 mediated ADP release is the rate limiting step in the exchange of ADP for ATP by Hsp70. Presence of Mge1 increases this nucleotide exchange activity of Hsp70 by 5000 fold [132]. The Mge1 dimer has two long α-helices, a four-helix bundle and six β-strands. The α-helical bundles are essential for dimer formation besides providing a surface for Mge1-Hsp70 interaction [133]. The amino acids present on the exterior surface of the four α-helical bundles are uniquely exposed to high solvent content [114]. Impaired Mge1 dimer formation and failure to interact with Hps70 contributes to the lowered efficiency of Hsp70 [134]. Intriguingly, the Met155 resides in this four α-helical bundle motif. Our *in vitro* results have shown that oxidation of Met155 decreases interaction of Mge1 with Hsp70 and decreases Hsp70 ATPase activity (Fig. 2.6B). Hence, we think that four α-helical region is crucial for oxidation sensor activities of Mge1 for regulating Hsp70 function.

Methionine sulfoxide reductases are important regulators of oxidative stress. Oxidation of methionines in proteins alerts these reductases to reduce the oxidized proteins and thereby protect the function of proteins and the cell from oxidative damage. Although mitochondrial proteins have been known to be major targets of ROS, yet there have been no reports on the functional regulation of these proteins by methionine oxidation. The current study underscores the importance of the mitochondrial localized MXR2 as yeast cells devoid of MXR2 are sensitive to H_2O_2 stress. In yeast, deletion of cytosolic localized MXR1 also causes the dysfunctional mitochondria [91]. Yeast deleted for MXR1 is only sensitive to H_2O_2 at higher concentrations whereas deletion of MXR2 results in increased sensitivity even at low concentration (Fig. 2.1A). Intriguingly, yeast having double deletion of MXR1 and MXR2 are much more sensitive to H_2O_2 than yeast harboring only MXR2 deletion (Fig. 2.1C). We suspect that Mxr1 might be having a role in regulating the cytosolic redox balance and thereby indirectly affects mitochondrial function. The isoforms of reductases have increased with evolution underlining their increased requirement. In higher eukaryotes, both Mxr1 and Mxr2 isoforms are present in the mitochondria indicating the presence of multiple substrates and increased complexity in regulation of redox homeostasis. HGrpEL1, the human homologue of Mge1 is similarly sensitive to H_2O_2. To our knowledge, Mge1 will be the first *in vivo* substrate of mitochondrial Mxrs. We have also shown that the function of Mge1 is reversibly regulated by oxidation / reduction status of its methionine residue present in the four α-helical bundle motif (Fig 2.4 and 2.5).

Hsp70 complex (DnaK70-DnaJ-GrpE, prokaryotic homologs) laterally with GroEl/GroEs chaperonins increases the efficiency of protein folding and prevents misfolded proteins which leads to aggregation [104], [113]. Whereas Prokaryotic chaperone ClpB in association with DnaK, the prokaryotic homologue of Hsp70 binds large aggregated proteins and dissociates them into

smaller aggregates or individual proteins. The small aggregates are further dissolved by former system. In addition to protein folding, dissociation of the aggregated protein requires energy in the form of ATP as Hsp70 system and the other components of the chaperone system are otherwise in the switch off mode [12], [135]–[137]. In the absence of Mxr2, the oxidative resistant mutant of Mge1 (M155L) stalls protein aggregation to a certain extent in presence of energy (Fig. 2.9). These results lend further support to our conclusion that oxidation of Met155 in Mge1 causes loss of function of the Mge1-Hsp70 complex and this is manifested as an oxidative sensitive phenotype in the *mxr2*Δ strain that has wild type Mge1 in presence of H_2O_2. The substitution of methionine to leucine at position 155 in Mge1 is a gain of function mutation as it is able to protect yeast cells deleted for *mxr2*Δ from oxidative stress to a certain level.

As Mge1 has multi-functional roles, it is important that small perturbation in ROS levels should not alter the functions of Mge1. Most likely, the cell employs Mxr2 to reduce any oxidized Mge1 so that Mge1 dependent pathways operate smoothly and continuously. The cell may be utilizing the reversible modification of the methionine residues in such proteins to revert to normalcy rapidly once the duress is released. It is possible that such a mechanism operates during heat, cold and other stresses besides oxidative stress that has been described here. Thus, the oxidative stress response pathway mediated by Mge1 and Mxr2 will eventually help in identifying additional components involved in redox biology and in developing therapeutics for oxidative stress mediated diseases.

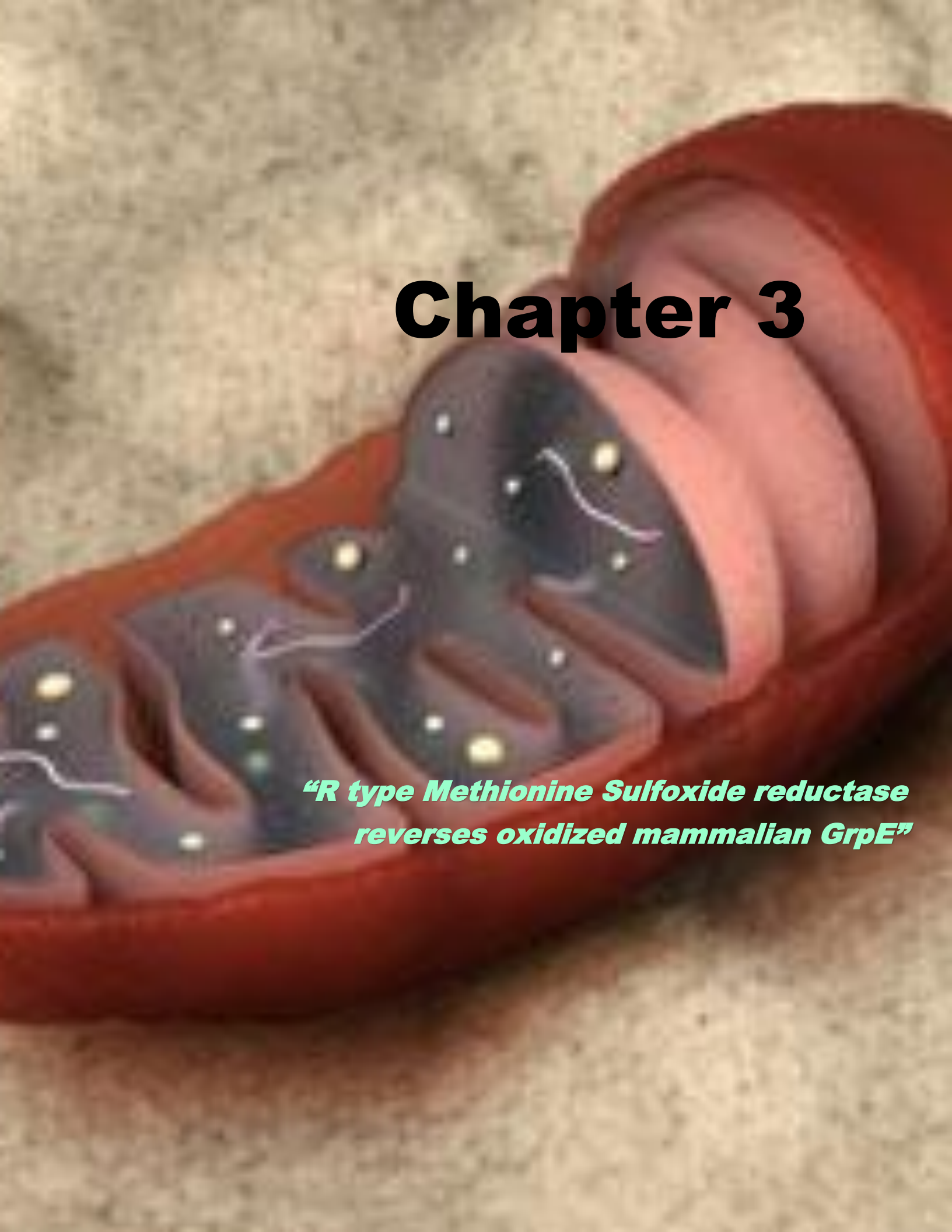

Chapter 3

"R type Methionine Sulfoxide reductase reverses oxidized mammalian GrpE"

3.1 Introduction

ROS is an important signaling molecule for various cellular functions such as redox regulation of several transcription factors, kinases and enzymes [138], [139]. However, enhanced levels of ROS can damage most of biomolecules and hence cell employs several detoxification mechanisms to maintain optimal levels of ROS [75]. ROS imbalance is a factor for myriad of several diseases including metabolic and neurodegenerative disorders. Biomolecular aging was possibly due to buildup of both reversible and irreversibly oxidatively damaged macromolecule aggregates. Destabilization of redox mechanism is the hallmark of various diseases due to change in either cellular signaling or loss of protein activity [140], [141]. Protein reversible oxidative modification can occur only at cysteine and methionine amino acids. Oxidation of cysteine forms reversible cystine (disulfide bonds) in proteins and these oxidized forms are further reduced by antioxidant enzymes like glutaredoxins, thioredoxin and peroxiredoxins [142]. Methionine upon oxidation forms reversible diastreomeric methionine sulfoxide (Met-S-SO or Met-R-SO) and these oxidized methionines are specifically reduced by methionine sulfoxide reductase MsrA or MsrB respectively in a thioredoxin dependent mechanism. Methionine in proteins not only acts as antioxidants but also regulates several proteins that undergo Met-SO dependent structural destabilization. Recent studies predict that methionine could act like a protein phosphorylation in cellular signaling and thereby controls several protein functions. Deletion of Msrs known to increase the ROS levels and that has been implicated in several diseases including diabetes, neurodegeneration, and aging [143], [144].

Chaperons play an important role in mitochondrial biogenesis through efficient protein translocation, assembly, iron-sulfur cluster formation and protein homeostasis. Indispensable Hsp70 chaperone system consists of highly conserved components (DnaK/DnaJ or J-

complex/GrpE proteins) involved in mitochondrial proteostasis like protein import and folding, disaggregation or degradation of proteins, Fe/S cluster biogenesis, and mtDNA maintenance. Mge1, a homologue of E.coli GrpE, in its dimeric form interacts with Hsp70-ADP complex and facilitate the release of ADP and binding of ATP to initiate another round of Hsp70 cycle. Consequently, Mge1 enhances the Hsp70 ATPase cycle by 5000 fold [111], [145]. Mge1/GrpE has been identified till date as the only component of Hsp70 system that can undergo early stress dependent structural transition and regulates Hsp70 chaperone efficacy [126]. Oxidative stress is known to change the ratio between active dimeric Mge1 to inactive monomer. We have shown earlier that lone conserved methionine at 155th position in Mge1 responds to oxidative stress. Further, we have shown that mitochondrial localized methionine sulfoxide reductase 2 reversibly regulates Mge1 by selectively reducing the Met155-SO and restores the activity of Mge1 and thereby regulate the Hsp70 ATPase cycle through redox switch [103], [146]. GrpEL1 a mammalian homolog of yeast Mge1, also known to display structural destabilization in response to oxidative stress *in vitro*. However, it is difficult to assess whether the Mge1 mediated redox regulation of Hsp70 function is evolutionarily conserved in mammals as mammalian mitochondria contain two isoforms of GrpE (GrpEL1 and GrpEL2). GrpEL1 is the major isoform and expressed across all tissues [147], [148]. However, GrpEL1 contains cysteines and two methionine residues while it counterpart yeast Mge1 lacks cysteines and contain only one methionine. Further, mammalian mitochondria contains three Msrs that can reduce both R (MsrB2 and MsrB3) and S type sulfoxide epimer (MsrA) while yeast mitochondria contain only R type Msr [92], [149], [150]. Although, MsrB specifically reduces the Met-SO of yeast Mge1, our study does not preclude the formation of only R type sulfoxide upon oxidation.

In this chapter we show that the methionine residues in GrpEL1 are oxidized upon exposure to H_2O_2. However, the conserved oxidized methionine at 146 is specifically reduced by R type of methionine sulfoxide reductase *in vitro*. Using yeast heterologous system we show that human GrpEL1 (hGrpEL1) and human R type Msr complements deletion yeast Mge1 or Mxr2 respectively. Yeast cells expressing human GrpEL1-M146L mutant conferred better growth kinetics than yeast strain expressing wild type hGrpEL1 under oxidative stress. This chapter reinforces the role of Mge1 and R type Msrs in redox regulation and evolutionarily conserved role of Mge1/GrpE in mitochondrial oxidative stress response pathway.

3.2 Methodology

3.2.1 Plasmid construction

Plasmids and primers used in this chapter were listed in Table 3.1 and 3.2 respectively. Plasmids MSRA, MSRB2, MSRB3 were purchased from DNASU plasmid repository. MSRA gene amplified with primers MSRA_Fwd1 (5`-CCCA GAATTC ACC ATG GCT GTA TTT GGA ATG -3`) and MSRA_Rev1 (5'- CCCC CTC GAG TTT TTT AAT ACC CAC TGG GCA -3') and cloned in pET28a$^+$ vector to generate pNB638, MSRB2 and MSRB3 amplified with following primers MSRB2_Fwd2 (5`- AAAA CCATG GCG CGG CTC CTC TGG -3`), MSRB2_Rev2 (5`- AAAA GGATCC ACC ATG GCG CGG CTC CTC TGG -3`), and MSRB3_Fwd3 (`5- AAAA CCATG GGC TCT GCA TTC AAC CTG CTG -3`), MSRB3_Rev3 (5'- CCCC AAG CTT CTC CGC TTT GTC TGC CTG -3') to generate pET28a$^+$ clones pNB640 and pNB648 containing genes MSRB2 and MSRB3 respectively. For *in vivo* expression in yeast, mammalian Msr genes were subcloned into pTEF-URA vector to the downstream of SU9 MTS and with C-terminal FLAG epitope. SU9 MTS was cloned into pTEF-URA vector using primers Su9-Fwd4 (5` AACC

ACTAGT ACC ATG GCC TCC ACT CGT GTC3`) and Su9-Rev4 (5` AAAA GGATCC GGA AGA GTA GGC GCG CTT 3`) with restriction sites SpeI-BamHI to create pNB543. MSRA and MSRB3 are amplified with primers MSRA-Fwd5 (5`-CCCA GGATCC ATG GCT GTA TTT GGA ATG -3`) and MSRA-Rev (5'- CCCC AAG CTT TTT TTT AAT ACC CAC TGG -3') and MSRB3-Fwd7 (5'-AAAA GGATCC ACC ATG TCT GCA TTC AAC CTG -3) and MSRB3-Rev3 with restriction sites BamHI-HindIII to generate pNB639 and pNB643 containing MSRA and MSRB3 respectively. Since MSRB2 contain internal BamHI site we amplified full length gene with primers MSRB2-Fwd2 and MSRB2-Rev2. Amplified gene was digested with NcoI-HindIII and cloned into SpeI-HindIII predigested plasmid pNB475 to express MSRB2 full length protein with FLAG epitope. Similarly GRPEL1 wt and GRPEL1 M146L were subcloned from pET28a$^+$ into pTEF LEU plasmid with Su9 MTS for yeast expression. Pet28a$^+$ plasmid pNB555 harboring GRPEL1-M146L was created by site-directed mutagenesis of GRPEL1 in pNB243 using primers GRPEL1_Fwd (5` GGG CTG GTC CTG ACT GAA GTC 3`) and GRPEL1 _Rev (5'- GAC TTC AGT CAG GAC CAG CCC -3').

3.2.2 Protein expression and purification

Plasmids containing His-MSRA, His-MSRB2, His-MSRB3 and His-MRP6 genes were transformed into *E. coli* BL21 (DE3) Codon Plus (RIL) cells. Protein expression was induced with 1 mM IPTG and soluble proteins were further purified by using Ni-NTA talon affinity resin (GE Healthcare). Purified proteins were dialyzed in phosphate buffered saline (PBS) pH 7.2 with 5 mM β-ME. Similarly hGrpEL1 wild type protein was expressed, purified and dialyzed in PBS. MXR1 gene without His tag in pET28a$^+$ vector was induced with 1 mM IPTG and supernatant fractions containing protein was collected and dialyzed against PBS.

3.2.3 Yeast strain construction

Yeast strains used in this chapter were listed in table 3.3. Yeast strain yNB65 [103] with MGE1 chromosomal copy deleted and expressing MGE1 from plasmid pTEF URA 2µ was used to generate haploid hGRPEL1 expressing yeast strain. Briefly yNB65 transformed with hGRPEL1 pTEF Leu (pNB598) and transformants were treated with 5-FOA. Yeast colonies survived upon 5-FOA treatment were screened for MGE1 deletion by plating on SC-URA plates. These strains were further confirmed the deletion of MGE1 by immunoblot analysis. To construct hGRPEL1 WT and mutant hGRPEL1-M146L in *mxr2*Δ background strain, we used yNB126 which has deletion of MXR2 and MGE1 chromosomal copy. However the deletion of essential MGE1 gene was complemented with exogenous plasmid pTEF URA 2µ MGE1. Plasmids pNB598 and pNB605 were transformed into yNB126 and treated with 5-FOA. Colonies selected and screened as mentioned above to generate yNB140 and yNB141 respectively expressing hGrpEl1 wt and mutant. To construct yeast strains expressing human mitochondrial Msr genes, we used MXR2 deletion strain yNB117. Msr genes containing plasmids pNB639, pNB641 and pNB643 were transformed into yNB117 and selected on SC-URA plates to generate yNB144, yNB145 and yNB146. Expression of respective genes was confirmed by immunoblot with FLAG antibody.

3.2.4 Yeast media and growth assay

Standard conditions were used for culturing and maintaining of yeast strains. To remove URA3 plasmid, yeast strains were plated on SC medium (0.67% SC-URA, 2% dextrose, 50 µg/ml uracil, 2% agar and 0.1% 5-FOA) containing 5-FOA. For performing growth assay, yeast strains were freshly streaked on YPD plates and the resultant colonies were grown in YPD medium overnight. These cultures were normalized to OD_{600} 1.0 and 10 fold serial diluted cultures were spotted 5 µl on YPD plates with or without 1 mM H_2O_2. Images were taken after 2 days incubation of these plates at 30°C. Spotting assay was performed on nonfermentable carbon source YPGE (1% yeast

extract. 2% peptone, 3% glycerol and 2% ethanol) plates and incubated for 3-4 days at 30°C. Growth curve experiments were performed in liquid YPD/YPGE medium treated with or without 1 mM H_2O_2.

3.2.5 *In vitro* interaction assay

Mxr1 bacterial lysate, Flag-MsrA, Flag-MsrB2, Flag-MsrB3, Flag-Mxr2 mitochondrial lysate and Flag-Mxr1 cytosol lysate were used for *in vitro* interaction studies. His-hGrpEL1 or His-Mrp6 proteins were treated with H_2O_2 and incubated with NI-NTA pre-cleared lysate expressing different Msr proteins. His tag affinity pull-down was performed and Ni-NTA beads were washed 3X times with 10 mM imidazole buffer. The beads were collected and separated by SDS-PAGE followed by coomassie stain or immunoblot analysis.

3.2.6 *In vitro* Mxr2 enzymatic assay and reduction of oxidized hGrpEL1

All Active methionine sulfoxide reductase proteins were used for reducing oxidized hGrpEL1. Msr enzyme activity was determined by the protein mobility shift assay of methionine rich proteins (MRP6) on SDS-PAGE. H_2O_2 treated MRP6 runs slower that reduced MRP6 due to oxidation of methionine's [151]. To determine the MSR activity, 20 µg of oxidized MRP6 protein was incubated with 10 µg of different Msr proteins in a reaction buffer (50 mM sodium phosphate, 50 mM sodium chloride, 10 mM DTT) [93]. The reaction was incubated at 30°C for 1 hr and proteins separated by SDS-PAGE followed by coomassie stain. Oxidized hGrpEL1 was incubated with different Msrs proteins in reaction buffer and separated by SDS-PAGE followed by mass spectrometry analysis.

3.2.7 Hsp70 ATPase assay

ATPase activity assay was performed as described in previous chapter with minor modifications. For hGrpEL1 complementation on yHsp70 ATPase activity, equivalent amounts of either Mge1 or hGrpEL1 proteins that were treated with or without H_2O_2 were added to the buffer (50 mM HEPES/ KOH, pH 7.2, 5 mM MgCl2, and 100 mM KCl) containing 2 µg of yHsp70 and 0.05 mM [γ- ^{32}P] ATP (3000 Ci/mmol). The amount of radioactive inorganic phosphate (pi) released after 5 mins was measured in a scintillation counter. The histogram was plotted from three independent experiments. Reduction of oxidized hGrpEL1 by Msr proteins was performed with His-hGrpEL1 treated with 5 mM H_2O_2 for 2 hours and incubated with or without 5 µg of different Msr proteins in presence of 10 mM DTT for 30 min before using it for Hsp70 ATPase activity assay.

3.2.8 Mitochondria isolation

Mitochondria isolation was performed as described chapter 2. Briefly yeast strains expressing Flag-MsrB2, Flag-MsrB3 and Flag-MsrA were grown overnight in 2% Lactate medium. Cells were centrifuged at 5000 rpm and washed with 100 mM Tris-SO_4 pH 9.4 followed by lysis with lyticase (Sigma- L2524) in 1.2 M sorbitol and 20 mM phosphate buffer pH 7.0. After 50 % lysis, cell were homogenized in SEM buffer (250 mM Sucrose, 1 mM EDTA, 10 mM MOPS) and centrifuged at 3500 rpm. The resultant supernatant was collected and centrifuged at 10000 rpm. The resultant mitochondrial pellet was suspended in SEM and stored at -80°C. Preparation of cytosol fraction from Flag-Mxr1 yeast strains was performed by the similar procedure and collected the post-mitochondrial fraction and stored at -20°C.

3.2.9 MALDI studies

H_2O_2 treated hGrpEL1 was incubated with the individual Msr proteins in a reaction buffer. The sample was incubated for 2 hrs followed by separation of proteins on SDS-PAGE. The proteins

excised from gel and digested with trypsin followed by mass spectrometric analysis. Relative levels of peptides of interest (listed in table 3.4) were quantified and plotted.

Tables

Table 3.1 Primers used in this chapter

Name	Oligonucleotide Sequence
MSRA_Fwd1	5`-CCCA GAATTC ACC ATG GCT GTA TTT GGA ATG -3`
MSRA_Rev1	5'- CCCC CTC GAG TTT TTT AAT ACC CAC TGG GCA -3'
MSRB2_Fwd2	5`- AAAA CCATG GCG CGG CTC CTC TGG -3`
MSRB2_Rev2	5`- AAAA GGATCC ACC ATG GCG CGG CTC CTC TGG -3`
MSRB3_Fwd3	5`- AAAA CCATG GGC TCT GCA TTC AAC CTG CTG -3`
MSRB3_Rev3	5'- CCCC AAG CTT CTC CGC TTT GTC TGC CTG -3'
Su9-Fwd4	5` AACC ACTAGT ACC ATG GCC TCC ACT CGT GTC3`
Su9-Rev4	5` AAAA GGATCC GGA AGA GTA GGC GCG CTT 3`
MSRA-Fwd5	5`-CCCA GGATCC ATG GCT GTA TTT GGA ATG -3`
MSRA-Rev6	5'- CCCC AAG CTT TTT TTT AAT ACC CAC TGG -3'
MSRB3-Fwd7	5'-AAAA GGATCC ACC ATG TCT GCA TTC AAC CTG -3
GrpEL1_Fwd	5` GGG CTG GTC CTG ACT GAA GTC 3`
GrpEL1 _Rev	5'- GAC TTC AGT CAG GAC CAG CCC -3'

Table 3.2 Plasmids used in this chapter

Name	Description	Reference
NB45	pTEF-MGE1, 2µ, URA	103
NB243	pET28a^{+} GRPEL1	103
NB555	pET28a^{+} GRPEL1 M146L	This study
NB638	pET28a^{+} MSRA	This study

NB640	pET28a^{+} MSRB2	This study
NB648	pET28a^{+} MSRB3	This study
NB598	pTEF- SU9-GRPEL1, 2µ, LEU	This study
NB605	pTEF- SU9-GRPEL1 M146L, 2µ, LEU	This study
NB639	pTEF-SU9-MSRA-FLAG, 2µ, URA	This study
NB645	pTEF- MSRB2-FLAG, 2µ, URA	This study
NB641	pTEF- SU9-MSRB3-FLAG, 2µ, URA	This study
NB478	pTEF- MXR1-FLAG, 2µ, URA	This study
NB483	pET28a^{+} MXR1 (without His tag)	This study

Table 3.3 Yeast strains used in this chapter

Strain	Genotype	Resource
BY4741	*MAT*a, *his3*Δ 1, *leu2*Δ 0, *met15*Δ 0, *ura3*Δ 0	In House
yNB65	*Mat* a, *his*Δ1, *leu2*Δ0, *lys2*Δ0, *ura3*Δ0, YOR232w::KANMX4, pTEF-2µ-URA MGE1	103
yNB117	*Mat* α, *his*3Δ, *leu2*Δ0, *lys2*Δ0, *ura3*Δ0, YCL033c::KANMX4	Euroscarf
yNB124	*Mat* Δ, *his3*Δ1, *leu2*Δ0, *lys2*Δ0, *ura3*Δ0, YCL033c::KANMX4, pTEF-2µ-URA MXR2-FLAG	146
yNB138	*Mat* a, *his*Δ1, *leu2*Δ0, *lys2*Δ0, *ura3*Δ0, YOR232w::KANMX4, pTEF-2µ-LEU SU9-hGRPEL1	This study
yNB140	*Mat a*, *his3*Δ1, *leu2*Δ0, *lys2*Δ0, *ura3*Δ0, YCL033c::KANMX4, YOR232w::KANMX4, pTEF- hGRPEL1, 2µ, LEU	This study
yNB141	*Mat a*, *his3*Δ1, *leu2*Δ0, *lys2*Δ0, *ura3*Δ0, YCL033c::KANMX4, YOR232w::KANMX4, pTEF- M146L hGRPEL1, 2µ, LEU	This study
yNB145	*Mat* Δ, *his3*Δ1, *leu2*Δ0, *lys2*Δ0, *ura3*Δ0, YCL033c::KANMX4, pTEF-2µ-URA SU9-MSRA-FLAG	This study
yNB146	*Mat* Δ, *his3*Δ1, *leu2*Δ0, *lys2*Δ0, *ura3*Δ0, YCL033c::KANMX4, pTEF-2µ-URA SU9-MSRB3-FLAG	This study
yNB147	*Mat* Δ, *his3*Δ1, *leu2*Δ0, *lys2*Δ0, *ura3*Δ0, YCL033c::KANMX4, pTEF-2µ-URA SU9-MSRB2-FLAG	This study

Table 3.4 Peptides generated from GrpEL1 after digestion with trypsin enzyme

Peptide Mass (m/z)	hGRPEL1 (Amino acid position)	Amino acid sequence
2015.9497	148-164	FDPYEHEALFHTPVEGK
1793.7606	**13-28**	**NSGQNLEEDMGQSEQK**
1764.200	**117-131**	**NLYEGLVMTEVQIQK**
1243.6780	88-98	DLLEVADVLEK
1152.7463	183-193	TLRPALVGVVK
1042.5390	79-87	LYGIQAFCK
1002.5214	59-67	ALADTENLR
1000.5673	165-174	EPGTVALVSK
838.4053	110-116	DDNPHLK
828.4097	29-36	ADPPATEK
759.4247	45-50	LEEQLK
749.4226	4-10	LLCTATK
746.3865	99-105	ATQCVPK
732.4138	37-42	TLLEEK
698.4195	141-147	LNPVGAK
688.3875	73-78	LVEEAK
605.3141	51-55	ETVEK
567.3613	136-140	HGLLK
518.2820	106-109	EEIK

3.3 Results

3.3.1 Human GrpEL1 is sensitive to H_2O_2 and methionine oxidation alters the ATPase stimulating activity on Hsp70

Mge1 is known to be oxidized at conserved Met155 amino acid both *in vitro* and *in vivo* upon exposure to oxidative stress. Human GrpEL1 contains methionine residue at 44th and 146th position and the later one is analogous to Mge1 Met155. To test whether hGrpEL1 is oxidized like Mge1, purified recombinant hGrpEL1 was treated without or with H_2O_2 as described in the methods and separated on SDS-PAGE, coomassie stained and trypsin digested followed by MALDI-TOF-MS/MS analysis (Fig. 3.1A and B, Table 3.4). In the absence of H_2O_2 treatment, we observed a peptide mass 1764 Da that represents the Met146 containing peptide (Fig.3.1C). However, an increase in 16 Da in Met146 peptide (1780 Da) was observed from the MALDI spectrum obtained from H_2O_2 treated hGrpEL1 (Fig. 3.1D). We further analyzed these peptides by MS/MS and confirmed that Met is getting modified to Met SO attaining a mass by 16 Da with H_2O_2 treatment (Fig. 3.1E and F). The other Met44 present at N terminus is also getting modified in presence of H_2O_2 (Fig. 3.1G and H). We hypothesize that modification of Met44 may not destabilize the structure as this domain present in the unstructured region (Fig. 3.1I). We have shown earlier that hGrpEL1 responds to H_2O_2 treatment by dissociation of dimeric form to monomer. Next, we investigated whether Met-SO formation in hGrpEL1 could alter ATPase activity of Hsp70. We performed a steady state ATPase activity of purified His-Ssc1 (His-

Fig. 3.1

A

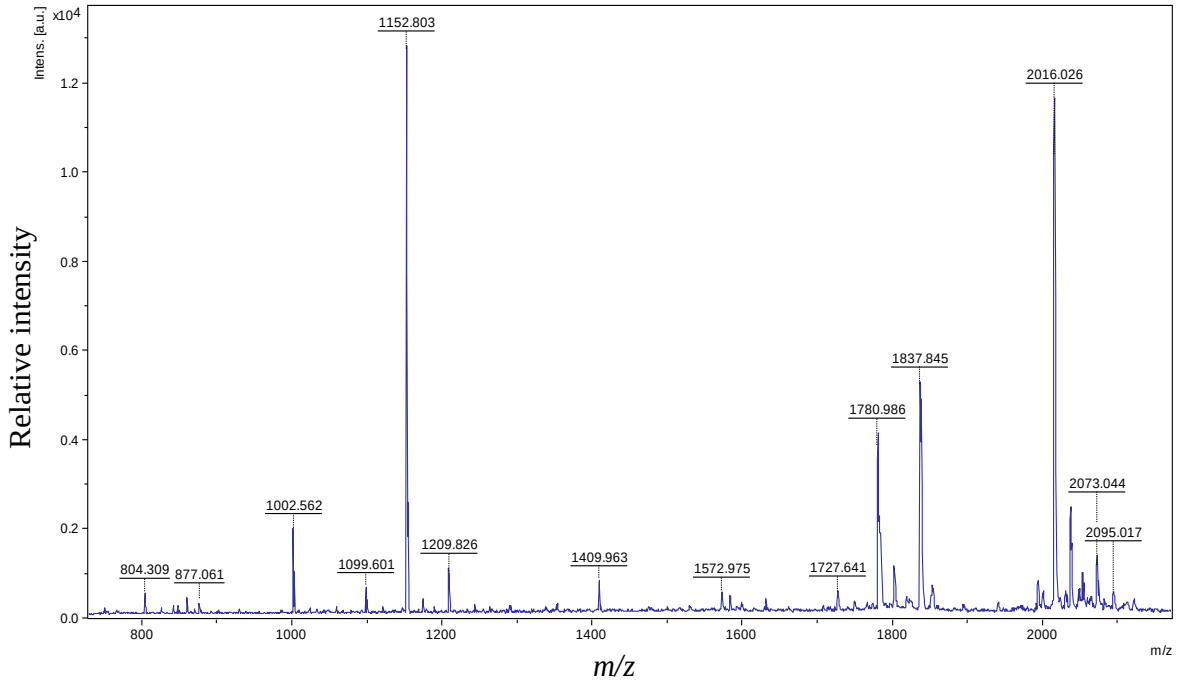
Intens. [a.u.]
x10^4
Relative intensity
1152.803
2016.026
1837.845
1780.986
2073.044
2095.017
1002.562
1209.826
1099.601
1409.963
1572.975
1727.641
804.309
877.061
m/z

B

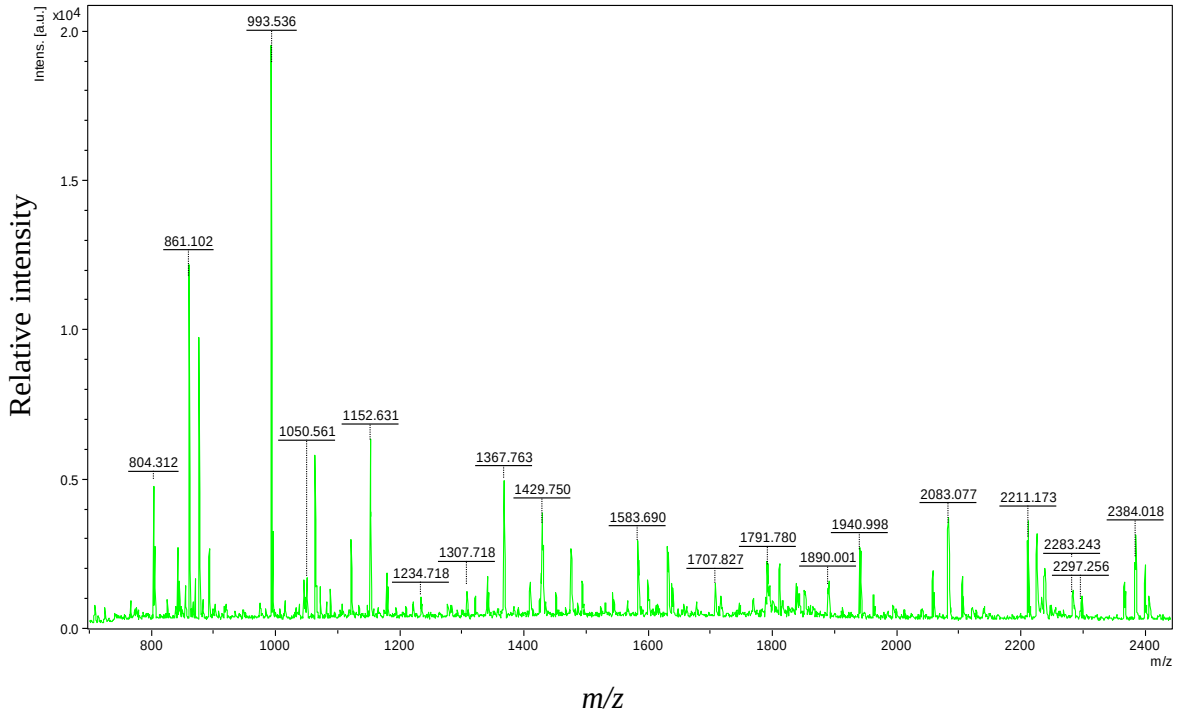
Intens. [a.u.]
x10^4
Relative intensity
993.536
861.102
1152.631
1050.561
804.312
1367.763
1429.750
1583.690
2083.077
2211.173
2384.018
1940.998
1791.780
2283.243
2297.256
1707.827
1890.001
1307.718
1234.718
m/z

Fig. 3.1

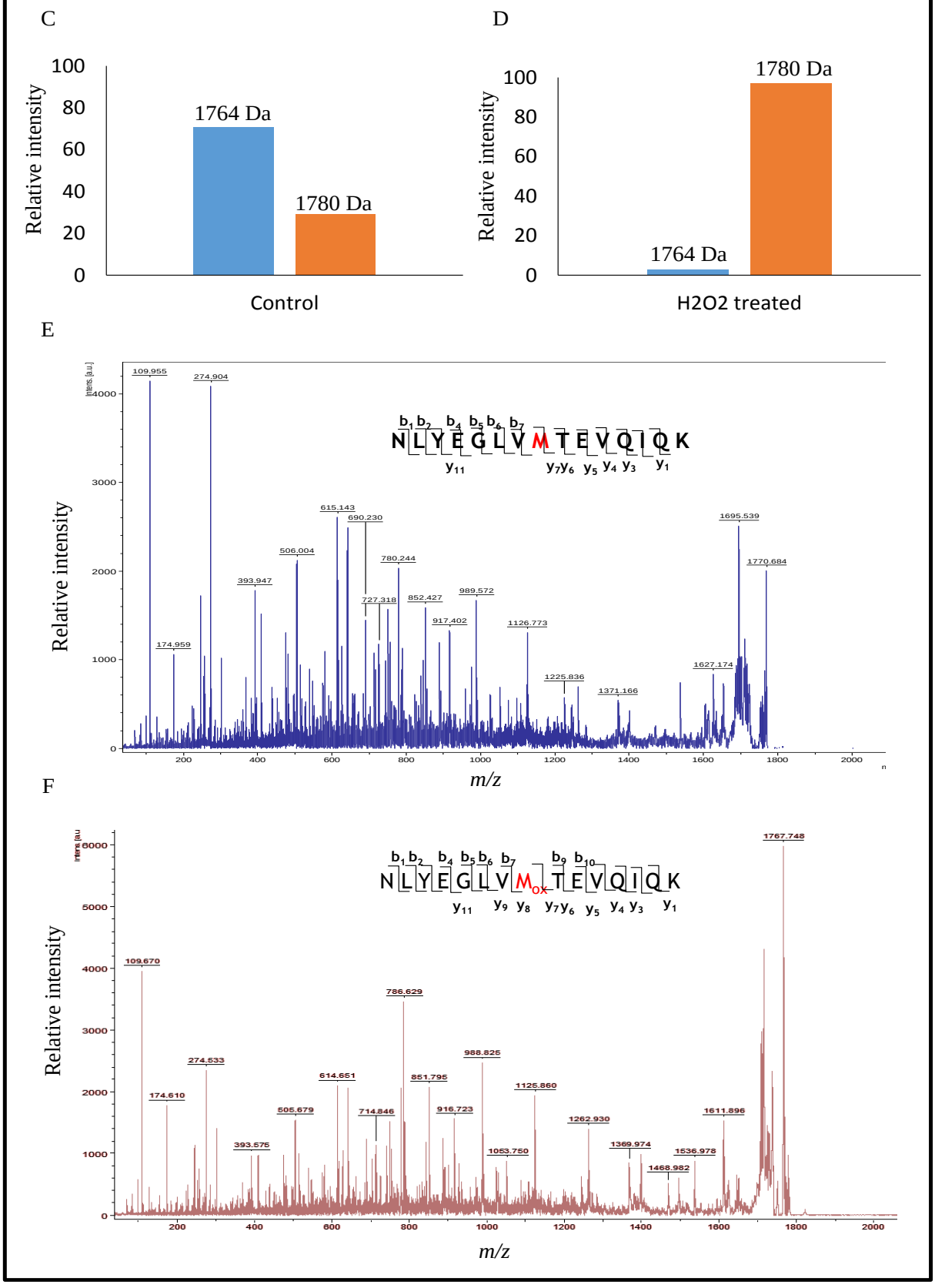
C
Relative intensity
100
80
60
40
20
0
1764 Da
1780 Da
Control
D
Relative intensity
100
80
60
40
20
0
1780 Da
1764 Da
H2O2 treated
E
Relative intensity
m/z
N L Y E G L V M T E V Q I Q K
F
Relative intensity
m/z
N L Y E G L V Mox T E V Q I Q K

Fig. 3.1

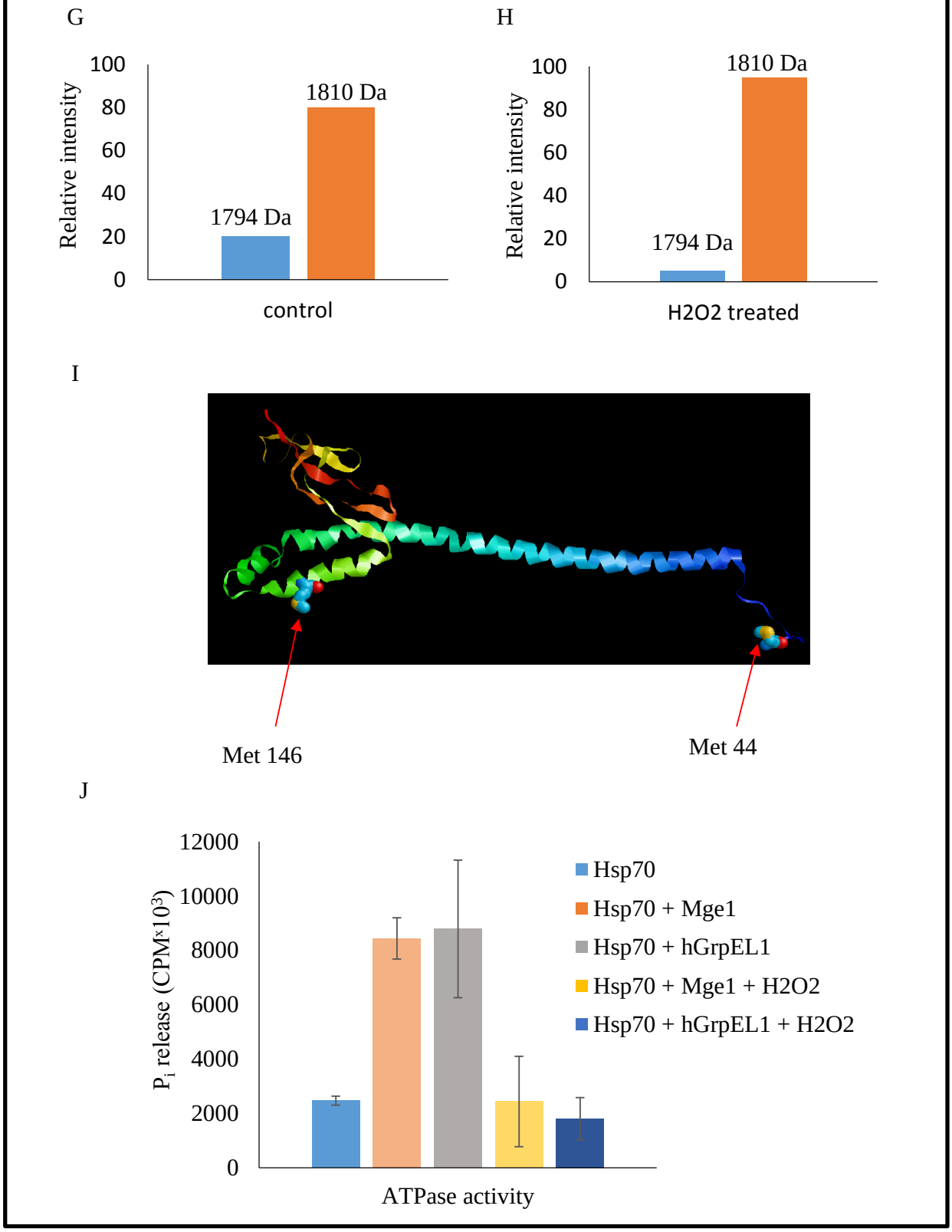
G
100
80
60
40
20
0
Relative intensity
1794 Da
1810 Da
control
H
100
80
60
40
20
0
Relative intensity
1794 Da
1810 Da
H2O2 treated
I
Met 146
Met 44
J
12000
10000
8000
6000
4000
2000
0
Pi release (CPM×10³)
Hsp70
Hsp70 + Mge1
Hsp70 + hGrpEL1
Hsp70 + Mge1 + H2O2
Hsp70 + hGrpEL1 + H2O2
ATPase activity

Figure 3.1 Met146 in hGrpEL1 is susceptible for oxidation and oxidized hGrpEL1 is inactive

Recombinant purified human His-GrpEL1 protein was treated with or without H_2O_2 and separated on SDS-PAGE followed by coomassie staining. The protein band was excised from the gel and trypsin digested peptides were analyzed by MALDI-TOF/MS/MS. Complete MALDI-TOF spectrum of untreated (A) and H_2O_2 treated (B) hGrpEL1 protein. From the MALDI spectra percentage of interested ion was calculated against highest ion species of the spectrum. (C) Met146 oxidation status from untreated hGrpEL1 (D) Met146 oxidation status from H_2O_2 treated hGrpEL1. (E) Peptide 1764 Da from Spectrum A was further sequenced and analyzed by MS/MS. (F) peptide 1780 Da from Spectrum B was sequence and analyzed the oxidation of Met by MS/MS. Met44 oxidation status was analyzed by MALDI spectrum (G) untreated hGrpEL1 (H) H_2O_2 treated hGrpEL1. (I) I-TASSER hGrpEL1 structure and space fill molecules represents methionines region. (J) ATPase activity was performed as indicated in the material and methods. Bar graphs show means of three independent experiments SD± 0.001 of radioactive ^{32}P counts measured using scintillation counter.

mtHsp70) in the presence of Mge1 or hGrpEL1 with or without H_2O_2 treatment as described in the methods. In the absence of GrpE proteins the rate of Hsp70 mediated ATP hydrolysis is low as expected. In the presence of Mge1 or hGrpEL1 the ATPase activity of Hsp70 is enhanced by several folds. However, the ATPase activity of Hsp70 is completely reduced when Mge1 or hGrpEL1 were treated with H_2O_2 prior to the assay (Fig. 3.1J). These results support the notion that Mge1/hGrpEL1 protein in eukaryotes probably regulates the Hsp70 chaperone system through oxidative modification.

3.3.2 Human GrpEL1 complements the deletion of yeast Mge1

To test whether oxidation of hGrpEL1 regulates the Hsp70 chaperone system *in vivo*, we used yeast *Saccharomyces cerevisiae* as a model system. Mge1 is an essential protein and yeast Mge1 was shown to be complements the deletion of *E. coli* GrpE [152], [153]. However, there are no reports about the human GrpE or other higher eukaryotic homologues can complement the deletion of yeast Mge1. We generated the yeast strain that exclusively carrying the hGrpEL1 plasmid by

plasmid shuffling in *mge1*Δ background as described in the methods. Further, western analysis show that the expression of hGrpE while the absence of yeast Mge1 in cell lysates obtained from the yeast strain carrying the hGrpEL1 plasmid (Fig 3.2A). These results suggest that hGrpEL1 able to complement the deletion of essential yeast Mge1. We further analyzed the growth phenotypes of cells expressing hGrpEL1 and compared with cells expressing yeast Mge1 in presence or absence of H_2O_2. Yeast strain expressing hGrpEL1 able to grow normally on YPD and YPGE plates like that of wt Mge1 at 30° C in absence of H_2O_2 (Fig. 3.2B &D). However, both the wt Mge1 and Wt hGrpEL1 expressing strains show similar slow growth phenotype on H_2O_2 supplemented YPD plates (Fig.3.2C). These results suggests that the conserved role for hGrpEL1 under oxidative conditions.

Fig. 3.2

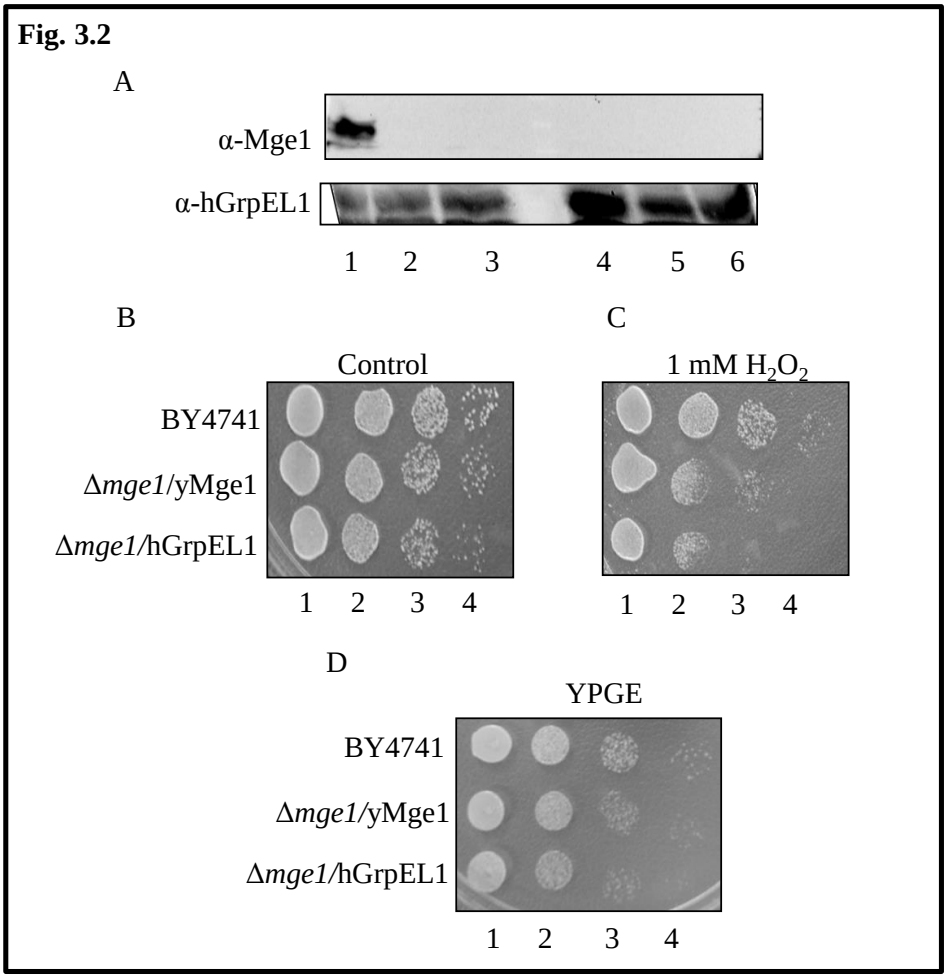

Figure 3.2 HGrpEL1 complements deletion of essential yeast MGE1 function

HGrpEL1 expressing yeast strain in the background of yeast MGE1 deletion was carried out as described in the Methods. (A) After 5-FOA treatment, yeast cells selected on SC-URA and the interested colonies were further performed immunoblot with Mge1 and hGrpEL1. (B-D) Growth phenotype of yeast strain expressing hGrpEL1 was compared with strain over-expressing WT Mge1 and parent BY4741 strain. Overnight grown cultures in YPD were normalized to OD_{600} 0.5 and 10 µl of each dilution was spotted on different plates. Plates incubated at respective temperatures for 2 days (YPD) or 4 days (YPGE). (B) YPD plates at 30°C, (C) YPD plates with 1 mM H_2O_2 and (D) YPGE at 30°C.

3.3.3 Mammalian Methionine R sulfoxide complements yeast mxr2 deletion and interacts with oxidized hGrpEL1

Since hGrpEL1 is sensitive to oxidative stress both *in vitro* and *in vivo*, we intend to test whether it is undergoing reversible Met-SO modifications as Mge1. Mammalian mitochondria contain three methionine sulfoxide reductases that include both R type (MsrB2 and MsrB3) and S (MsrA) type of sulfoxide reductase. Oxidation of Methionine known to form two enantiomers (Met-R-SO or Met-S-SO) and, some of the protein bound Met-SO are known to be specifically reduced by either of Msr enzymes [96], [154]. Previous reports shown that yeast mitochondria contain only R type Msr and it can only reduce Met-R-SO [90], [91].

Initially, we intend to analyze the role of multiple mammalian Msr genes in oxidative stress using yeast system. We constructed the yeast strains that expressing human Flag-MsrA, Flag-MsrB2 and Flag-MsrB3 in *mxr2*Δ background as described in the methods. We analyzed the growth phenotypes of Flag-Msr expressing strains with WT carrying vector alone (By4741/vc) and *mxr2*Δ strain that ectopically expressing Flag-Mxr2 on YPD plates in the presence or absence of H_2O_2. All the strains grow normally on YPD plates in the absence of H_2O_2. However, in the presence of

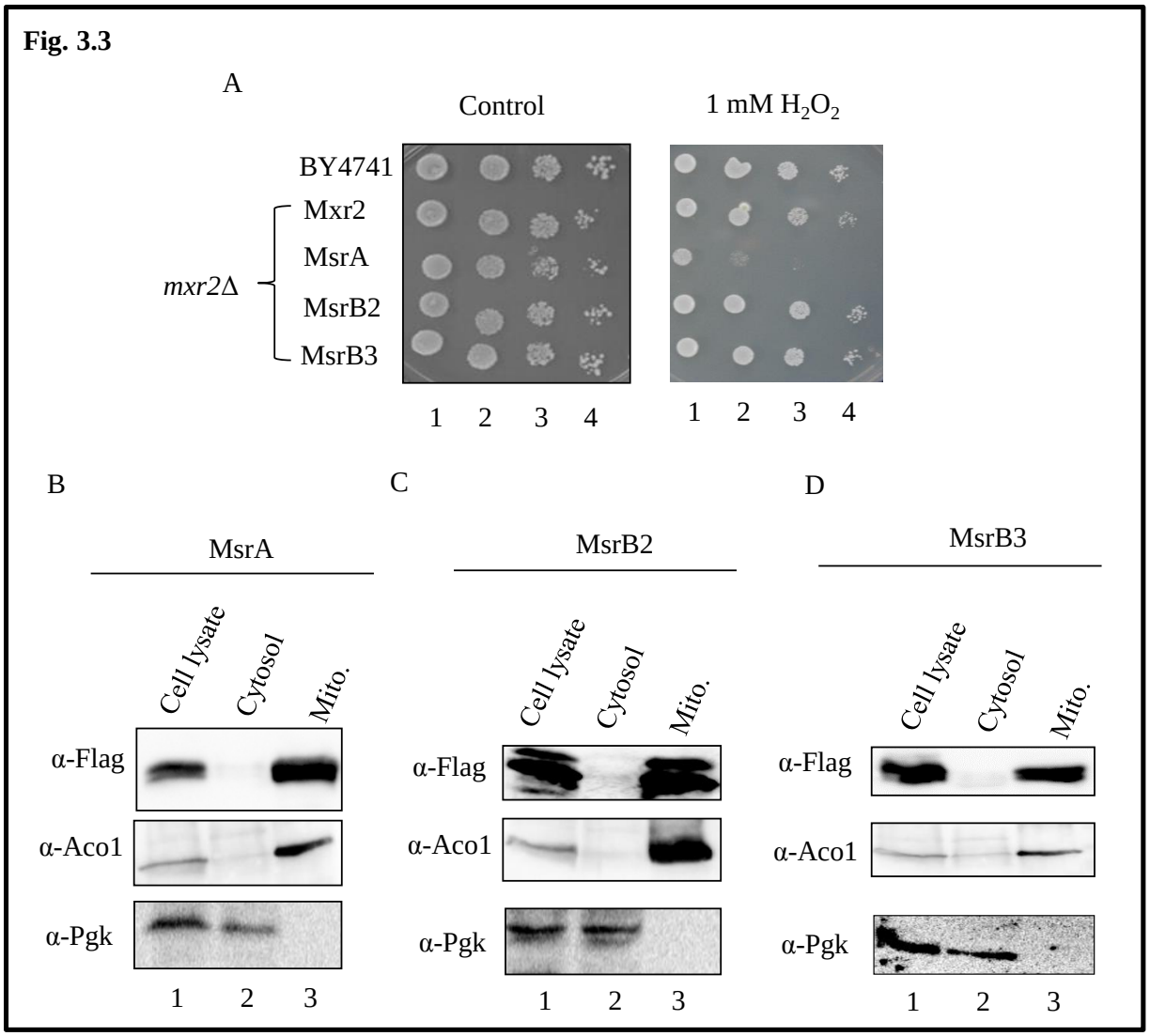

Figure 3.3 Mammalian MsrB complements yeast *mxr2*Δ

(A) Generation of mammalian MSR genes in the background in *mxr2*Δ and yeast 2μ MXR2 in *mxr2*Δ was carried out as described in the Methods. These strains were grown overnight in SC-URA medium and performed serial dilution assay as described in material and methods on SC-URA plates with or without H_2O_2. (B-D) Yeast strains expressing different human MSR genes were subjected to subcellular fractionation. Total cell lysate, cytosol and mitochondrial fractions were separated on SDS-PAGE and probed with antibodies specific to cytosolic (Pgk1) and mitochondria (AcoI) (B) MsrA, (C) MsrB2 and (D) MsrB3.

H_2O_2, the growth of the strains expressing mammalian Met-R-SO reducing enzymes MsrB2, MsrB3 and yeast Mxr2 able to grow similar to the WT strain (Fig.3.3A). But the strain expressing

mammalian MsrA is unable to complement H_2O_2 sensitive phenotype of *mxr2*Δ. These results suggest that only mammalian Met-R-SO reducing enzymes efficiently complement the mxr2 deletion. To further confirm the mitochondrial localization of these Msrs, subcellular fractionation of yeast strains expressing different Flag-Msr was carried out and the fractions were probed with antibodies specific to the mitochondria fraction (Tom40) and cytosolic faction (Glycerol kinase) along with Flag. As shown in the Figure 3, Flag-Msr proteins are enriched in the mitochondrial fraction like Tom40 (Fig. 3.3B, C &D). These results suggest that MsrB proteins are efficiently targeted to the mitochondria and able to complement yeast Mxr2.

Since oxidation of methionine can form R or S type of enantiomers or both enantiomers in proteins [150], we intend to analyze the type of Met-SO formation upon oxidation of hGrpEL1 by examining the interaction of Flag-Msr proteins towards hGrpEL1 Met-SO. We performed an *in vitro* Ni-NTA pull down assay to show the specificity of Msr interaction with oxidized hGrpEL1. The cell lysates expressing Flag-Msrs proteins were passed through the Ni-NTA bound oxidized or unoxidized recombinant purified hGrpEL1 and bound proteins were eluted and analyzed by western immunoblot as described in the methods. No Msr protein is present in the eluate when unoxidized hGrpEL1was used as bait. However, Flag-MsrB2 and Flag-MsrB3 but not Flag-MsrA proteins are present in the eluates when oxidized hGrpEL1 was used as bait (Fig. 3.4A, B &C). We further analyzed the specificity of Met-R-SO reducing enzymes interaction with oxidized hGrpEL1. We used yeast cells expressing either Flag-Mxr2 or Flag Mxr1 as prey. Unoxidized hGrpEL1 is incompetent to interact with yeast Mxr2 while oxidized hGrpEL1 specifically interacts with yMxr2 (Fig. 3.4D). However, yeast Mxr1 fails to interact with either oxidized or unoxidized hGrpEL1 (Fig.3.4E). However, when we performed pull down assay with MRP6 a known MsrA substrate, we find a specific interaction of MsrA protein with oxidized MRP6 (Fig. 3.4F). These

results suggest that R epimer reducing Msrs able to interact with oxidized hGrpEL1 and GrpE protein might be forming Met-R-SO upon oxidation at conserved Met146 region.

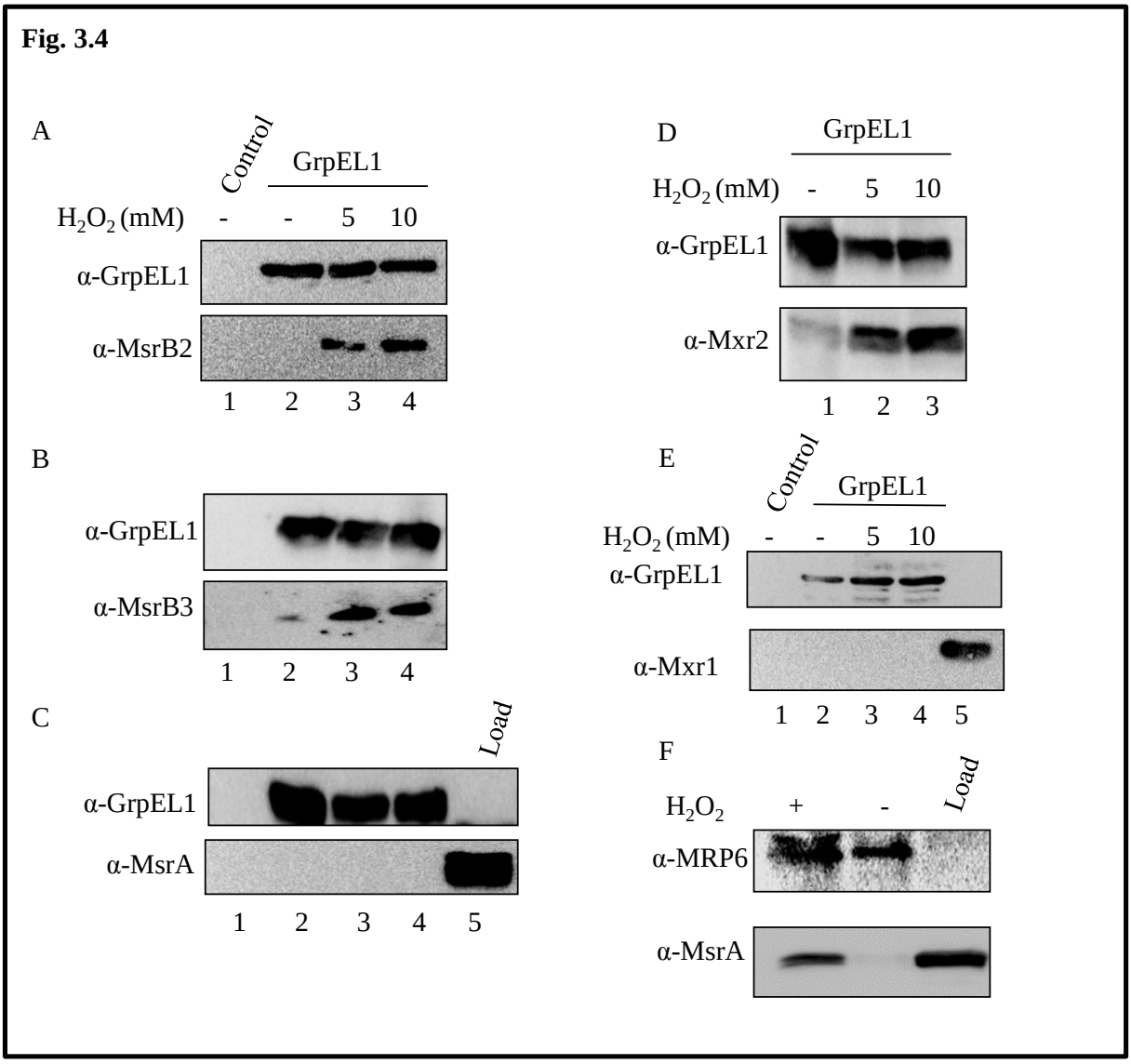

Figure 3.4 Oxidation dependent interaction of HGrpEL1 with methionine sulfoxide reductases

Purified hGrpEL1 protein was pretreated with H_2O_2 for 2 hr and used for studying *in vitro* interaction with different Msr`s. Mitochondrial lysate isolated from the strains expressing Flag-Mxr2, Flag-MsrA and Flag-MsrB and cytosolic extract isolated from the strain expression Flag-Mxr1 were mixed and incubated with oxidized or unoxidized hGrpEL1 protein for 1 hr and pass it through the Ni-NTA column. Bound proteins to the beads were eluted and separated on SDS-PAGE followed by probing with antibodies specific to FLAG and hGrpEL1 antibodies. Interaction assay was performed with (A) Flag-MsrB2, (B) Flag-MsrB3,

(C) Flag-MsrA, (D) Flag-Mxr2 and (E) Flag-Mxr1. (F) MsrA specificity was assayed by treating His-Mrp6 protein with or without H_2O_2 followed by Ni-NTA pull-down with extract containing Flag-MsrA as described in material and methods.

3.3.4 Reduction of hGrpEL1-Met SO at Met146 by R type enzymes

So far our result suggests that methionine sulfoxide R reductases are predominantly interacts with oxidized hGrpEL1/Mge1 while Met-S-SO reducing enzymes failed to interact. To further support our assumption, the recombinant hGrpEL1 protein was treated with H_2O_2 and subjected to MALDI/TOF/MS/MS analysis as described in the methods. In another case the oxidized hGrpEL1 protein was incubated with Msr enzymes prior to MALDI/TOF/MS/MS analysis. All active enzymes were used for reduction of oxidized GrpEL1. Msrs enzyme activity was tested using MRP6 based reduction assay as described in material and methods (Fig 3.5 A, B & C). Most of recombinant hGrpEL1 protein is oxidized with H_2O_2 treatment as we observed a peptide peak 1780 Da that corresponds to oxidized Met146 peptide (Fig. 3.5D). Strikingly, when the oxidized hGrpEL1 was incubated with R type of reductases (MsrB2 or MsrB3) we have observed a prominent Met1764 Da peptide indicating that reduction of oxidized peptide (Fig. 3.5E &F). However, when the oxidized hGrpEL1 was incubated with MsrA, the reduction reaction was not observed and MALDI spectrum contains majorly 1780 Da peptide (Fig.3.5G). Since yeast Mxr2 is also specifically interacted with hGrpEL1, we checked whether Mxr2 protein is able to reduce oxidized hGrpEL1. From MALDI analysis, we find that even Mxr2 specifically reduces the hGrpEL1 Met SO probably at Met146 (Fig. 3.5H). MALDI analysis further shows the oxidation of methionine 44 in hGrpEL1 with H_2O_2 treatment. However, either Met R or Met S sulfoxide reducing enzymes failed to reduce the oxidize methionine 44 in hGrpEL1 significantly (Fig. 3.5I &J). From these studies we propose that the oxidation of Met146 probably forming Met-R-SO enantiomer and conserved oxidative regulation by MsrB enzymes.

Fig. 3.5

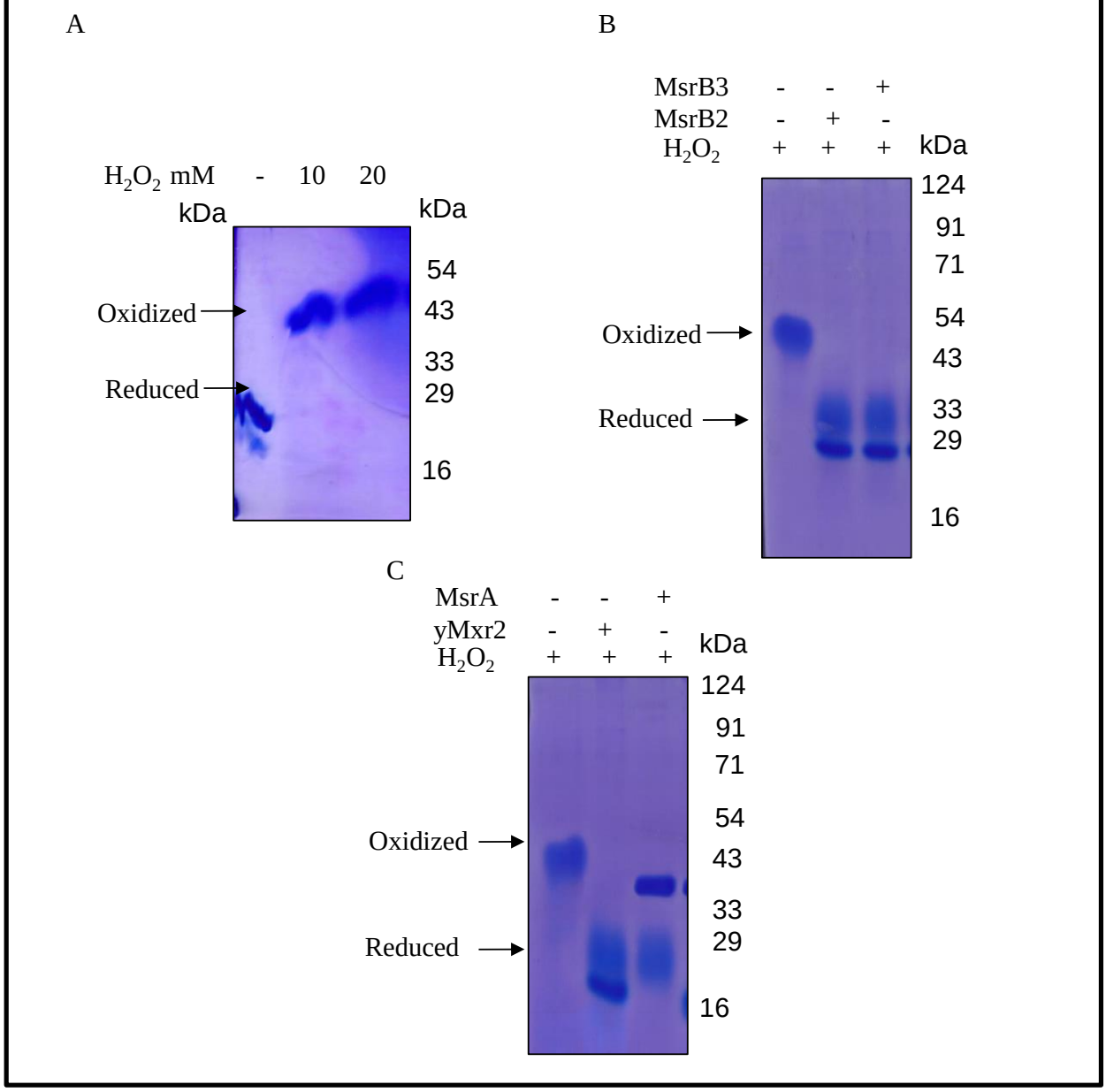

Figure 3.5 Enzyme activities of MSRs proteins

MRP6 untreated and treated can be distinguished in SDS-PAGE by their migration (A) further reduction with Msr proteins show different pattern of migration lower than treated Mrp6 (B). This observation was used to distinguish the enzyme activity of different Msr proteins. MRP6 was oxidized with 10 mM H_2O_2 and dialyzed overnight. These oxidized proteins was incubated with different Msr proteins and SDS-PAGE followed by coomassie staining (B & C).

Fig. 3.5

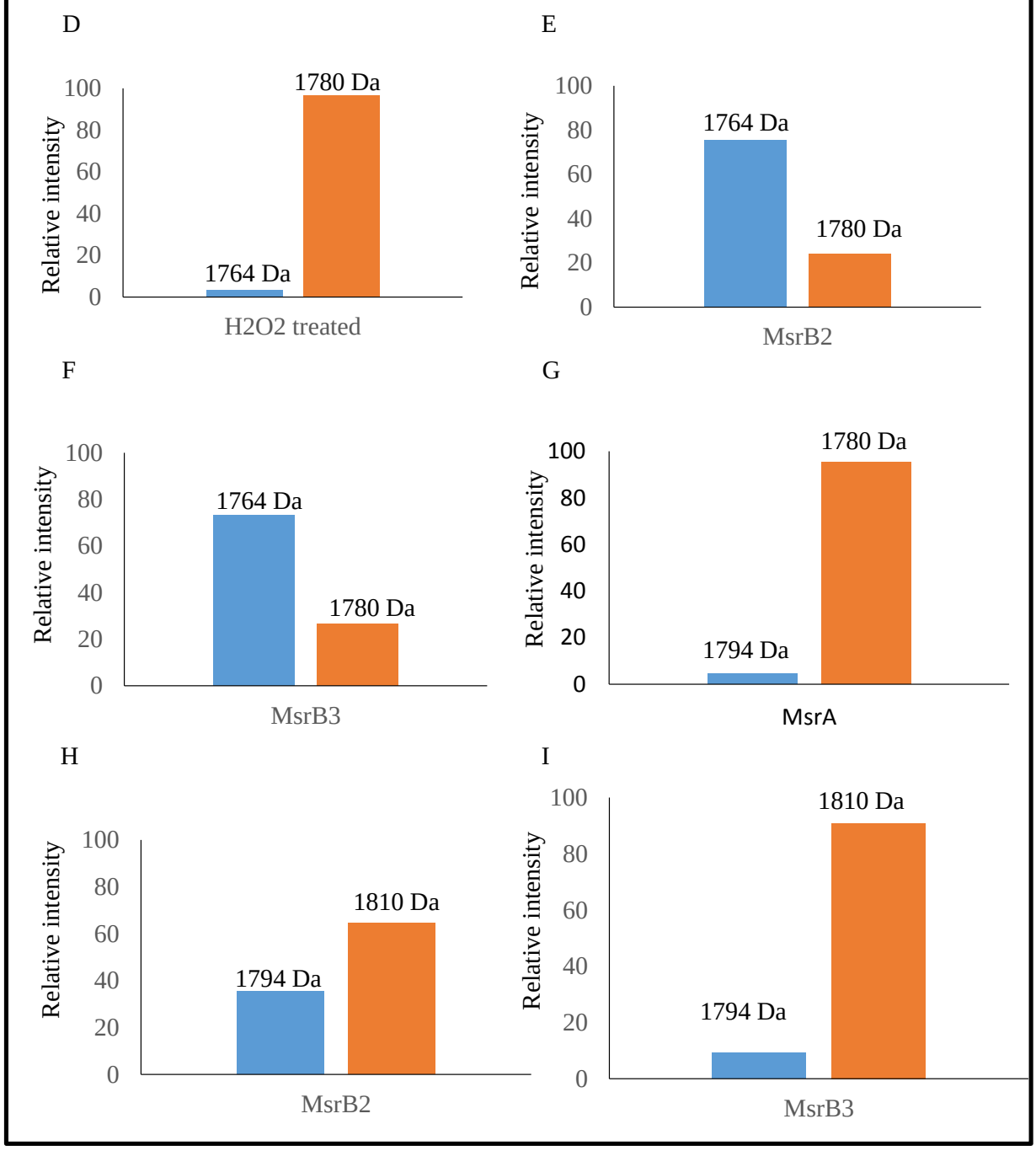
D
Relative intensity
100
80
60
40
20
0
1780 Da
1764 Da
H2O2 treated
E
Relative intensity
1764 Da
1780 Da
MsrB2
F
Relative intensity
1764 Da
1780 Da
MsrB3
G
Relative intensity
1780 Da
1794 Da
MsrA
H
Relative intensity
1810 Da
1794 Da
MsrB2
I
Relative intensity
1810 Da
1794 Da
MsrB3

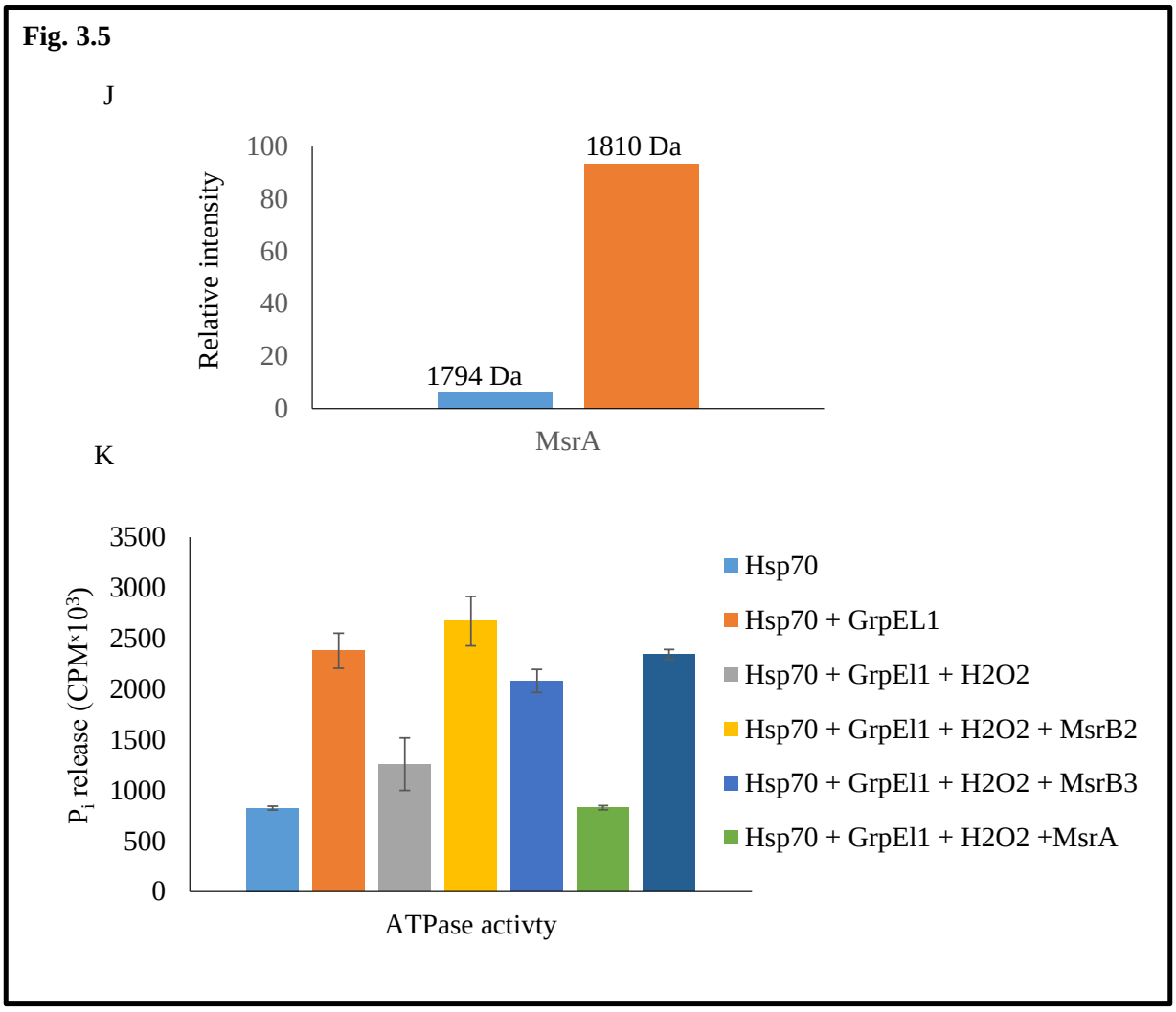

Figure 3.5 Specific reduction of oxidized hGrpEL1 protein by R type Msrs enzymes

Oxidized hGrpEl1 (20 µg) protein was incubated with each Msrs proteins (MsrA, MsrB1, MsrB, yMxr2) in a reaction buffer for 2 hours followed by separation of proteins on SDS-PAGE and coomassie stained. hGrpEL1 proteins was excised and trypsin digested and the resulting peptides were analyzed by MALDI-TOF/MS/MS. (D) hGrpEL1 protein reduced with DTT alone, (E & H) hGrpEL1 protein reduced with MsrB2 (F & I) hGrpEL1 protein reduced with MsrB3 (G & J) hGrpEL1 protein reduced with Mxr2 (H) hGrpEL1 protein reduced with MsrA. (K) **Steady state ATPase activity.** Hsp70 ATPase activity was performed as mentioned in material and methods. hGrpEL1 protein was treated with or without H_2O_2 (5 mM) for 2 hours and then followed by incubation with different Msr enzymes for 1 hr. Steady state ATP hydrolysis of Hsp70 was monitored by analyzing the released ^{32}Pi in the presence or absence of hGrpEL1 protein that was oxidized and reduced with Msr enzymes. Bar graphs show means of three independent experiments SD 0.0001

Our *in vitro* results efficiently determine that R type of Msrs interacting with oxidized hGrpEL1 and ably reduce Met-SO at Met146. We asked the question whether the reduced hGrpEL1 able to functionally complement the ATPase stimulating activity on yHsp70. We performed ATPase cycle of recombinant yHsp70 by using recombinant hGrpEL1 with or without treatment with H_2O_2 as described in the methods. In another set, we reduced the oxidized hGrpEL1 by incubating with different Msrs prior to performing yHsp70 ATPase activity assay. Hsp70 alone shows a low intrinsic ATPase activity and the addition of hGrpEL1 stimulates ATPase activity of Hsp70 by five folds while oxidized hGrpEL1 does not stimulate the activity. Incubation of oxidized hGrpEL1 with R type of Msrs (MsrB2, MsrB3 and yMxr2) could able to restore the function competently (Fig. 3.5K). However, pretreatment of oxidized hGrpEL1 with S epimer reducing enzyme MsrA does not restore the ATPase stimulation activity on Hsp70. These results strongly support that R epimer reducing enzymes play a major role in the biogenesis of hGrpEL1 during oxidative stress.

3.3.5 Human GrpEL1 M146L functionally complements the oxidative sensitive phenotype of *mxr2Δ in vivo*

So far our study shows that human hGrpEL1 gene complements the function of MGE1 both *in vitro* and *in vivo*. Further, hGrpEL1 mutant is resistant oxidative stress like Mge1-155L in stimulating ATPase activity on Hsp70 *in vitro*. We have shown that oxidation resistant mutant Mge1-M155L supports the growth of *mxr2*Δ under different oxidative stress conditions. To further understand whether hGrpEL1 M146L can functionally complement the deletion of MXR2, we generated a yeast strain that ectopically expressing either wild type hGrpEL1 or hGrpEL1 M146L in *mxr2*Δ strain background as described in the methods and compared the growth phenotype with

wild type BY4741 strain in presence and absence of H_2O_2. Yeast strains expressing wild type and mutant hGrpEL1 grow normally in absence of H_2O_2 while hGrpEL1-M146L mutant displayed better growth phenotype in presence of H_2O_2 (Fig. 3.6A).

Fig. 3.6

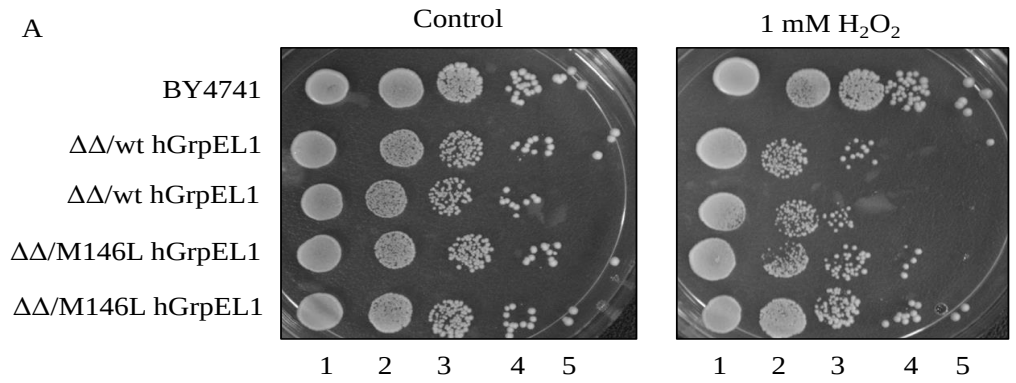

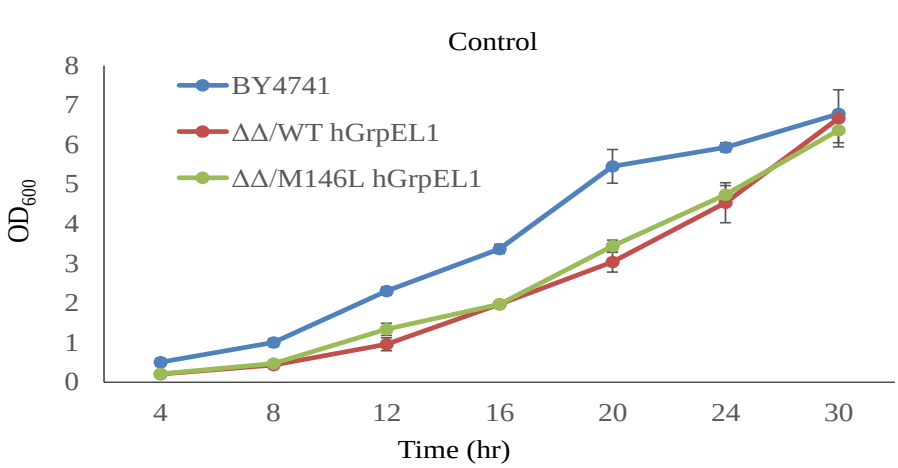

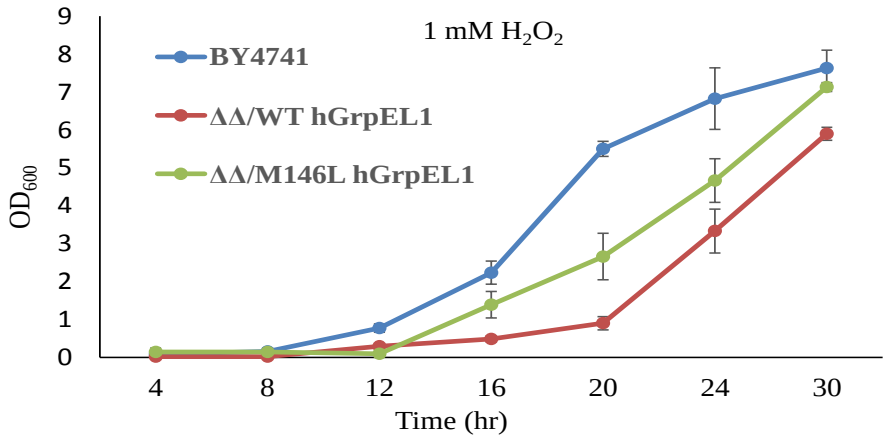

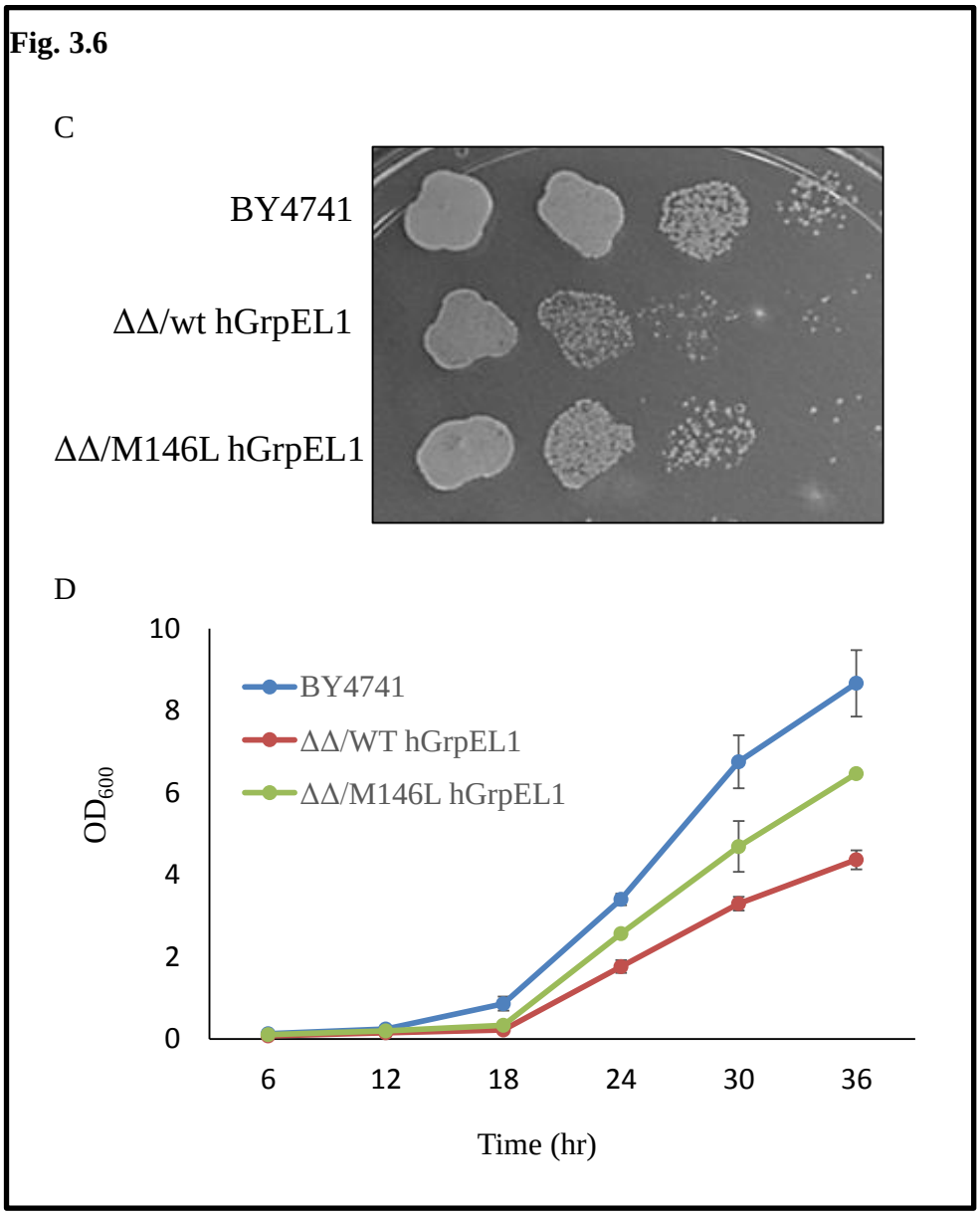

Figure 3.6 Yeast cells expressing human GrpEL1 M146L are resistance to oxidative stress

Yeast strains expressing WT human GrpEL1 and hGrpEL1-M146L mutant in *mxr2*Δ background were analyzed for the tolerance of oxidative stress. BY4741 parent strain was used as a control. Overnight grown cultures were normalized to OD_{600} 0.5 and spotted on YPD plated with or without H_2O_2. (A) YPD -/+ 1 mM H_2O_2, (B) YPGE. Liquid growth assay was performed in YPD +/- H_2O_2 (C) and YPGE (D) by taking OD values at different time intervals and plotted a growth curve from three independent cultures.

Similar growth resistant phenotype of hGrpEL1 M146L was observed in YPD liquid cultures with H_2O_2 (Fig. 3.6B). These results indicate hGrpEL1 is oxidatively sensitive *in vivo* and conserved Met mutant plays a major role in protecting GrpE mediated Hsp70 chaperone functions. We have shown earlier that *mxr2*Δ strain fails to grow on non-fermentable carbon sources while Mge1-M155L can grow efficiently like BY4741. Similarly, we find that hGrpEL1 M146L able to grow on non-fermentable carbon source when compared to the strain expressing WT hGrpEL1 in *mxr2*Δ strain background (Fig. 3.6C &D). These results further strengthen our notion that GrpE is critical in regulation of Hsp70 chaperone system during oxidative stress. Further, our study demonstrate that Msrs mediated redox regulation cycle is conserved across evolution.

3.4 Discussion

Molecular Chaperones are crucial components for cellular protein homeostasis. Chaperones are highly conserved across evolution and they comprise of distinct subunit components. Most of the chaperones assist in protein folding by utilizing ATP as energy source [135], [155]. Certain chaperones display stress dependent expression and also regulated by post translational modifications. Very few chaperones have been reported to be regulated through reversible oxidative modifications at cysteine or methionine residue. It has been shown that thermal stress induces the expression Hsp33 gene and also regulates its activity through redox mechanism by disulfide bond formation at zinc binding site [156], [157]. In eukaryotes redox modifications at Cys residues of cytosolic Hsp70 and Hsp90 chaperones causes the inactivation of chaperones and induction of unfolding protein response (UPR) [158], [159]. In addition, Met and Cys oxidation in eye lens proteins α-Crystallins thought to be one of the major cause of eye defects (cataract) due to loss of α-Crystallins function in protein folding [160], [161].

Hsp70 chaperone system is also required for mitochondrial proteostasis, iron sulfur cluster biogenesis and mtDNA maintenance. In the Hsp70 chaperone complex, GrpE is the only component which can respond to thermal and oxidative stress. Hsp70 ATPase cycle known to regulate through Met mediated redox modifications of Mge1 [103], [146]. During oxidative stress Met in Mge1 gets oxidized and reduces the ATPase stimulating activity on Hsp70. Methionine sulfoxide reductase 2 restores the activity of Mge1 by reducing it. hGrpEL1 a mammalian homologue of Mge1 also responds to oxidative stress by dissociating dimeric form into monomer. In this chapter, we show that hGrpEL1 modulates the ATPase activity of Hsp70 during oxidative stress (Fig. 3.1E). Our results also display hGrpEL1 able to complement MGE1 deletion indicating that it is probably playing a similar role in in regulating different Hsp70 chaperones that are present in yeast mitochondria (Fig. 3.2). Further, oxidation resistant mutant hGrpEL1-M146L is able to rescue the growth defect of *mxr2*Δ strain in presence of H_2O_2 indicating the conserved role of hGrpEL1 during oxidative stress (Fig. 3.6).

Msrs act as antioxidants to regulate various biological process. These proteins preferentially show high activity towards Met-SO in unfolded proteins. Although, Met-R-SO and Met-S-SO reducing enzymes are present in human mitochondria there are few reports depicting the specificity of Msrs reduction towards protein bound Met-SO. Our previous and current *in vitro* data suggest that hGrpEL1/Mge1 is specifically reduced by R epimer reducing enzymes. Although both methionines in hGrpEL1 are oxidized *in vitro*, MsrB isoform shows high specificity towards M146 SO when compared to Met44 SO in reducing the sulfoxide. Yeast cells fails to grow in the absence MsrB on non-fermentable carbon sources or under oxidative conditions which further signifies the importance of R type Msrs (Fig. 3.3). We show that only R type of human Msr isoforms can complement the loss of yMxr2 to support the mitochondrial biogenesis. Further over-expression

of MsrB in yeast protects the cells from aging under calorie restriction suggesting that important collaborative role of chaperones and antioxidant proteins in mitochondria.

Mitochondria accounts for 90% of total cellular ROS. ROS in optimal level can regulate the protein functions, however, excessive ROS can damage various biomolecules. Imbalance in ROS production could be due to dysfunctional mitochondria or environmental factors or decreased antioxidant capacity of cell [117], [140]. Methionine oxidation, loss of Msrs and increased mitochondrial ROS is major cause of several neurological disorders like Parkinson's and Alzheimer's disease including aging [120], [122]. We hypothesize that hGrpEL1 oxidation might be playing a key role in Msr associated pathologies during aging due to its multifactorial role in mitochondrial biogenesis. Age dependent accumulation of ROS or decreased antioxidant property or altered Msrs activities could leads to increased Met-SO of hGrpEL1. Met oxidation of Mge1/hGrpEL1 leads to defective chaperones system and protein homeostasis which may be the reason for progress of several pathological mitochondrial associated disorders. Recent studies suggest that mitochondrial biogenesis primarily regulated through mitochondrial protein import machinery. Mitochondrial GrpE probably act like a redox sensor and that transduce appropriate signals for mitochondrial protein homeostasis.

Bibliography

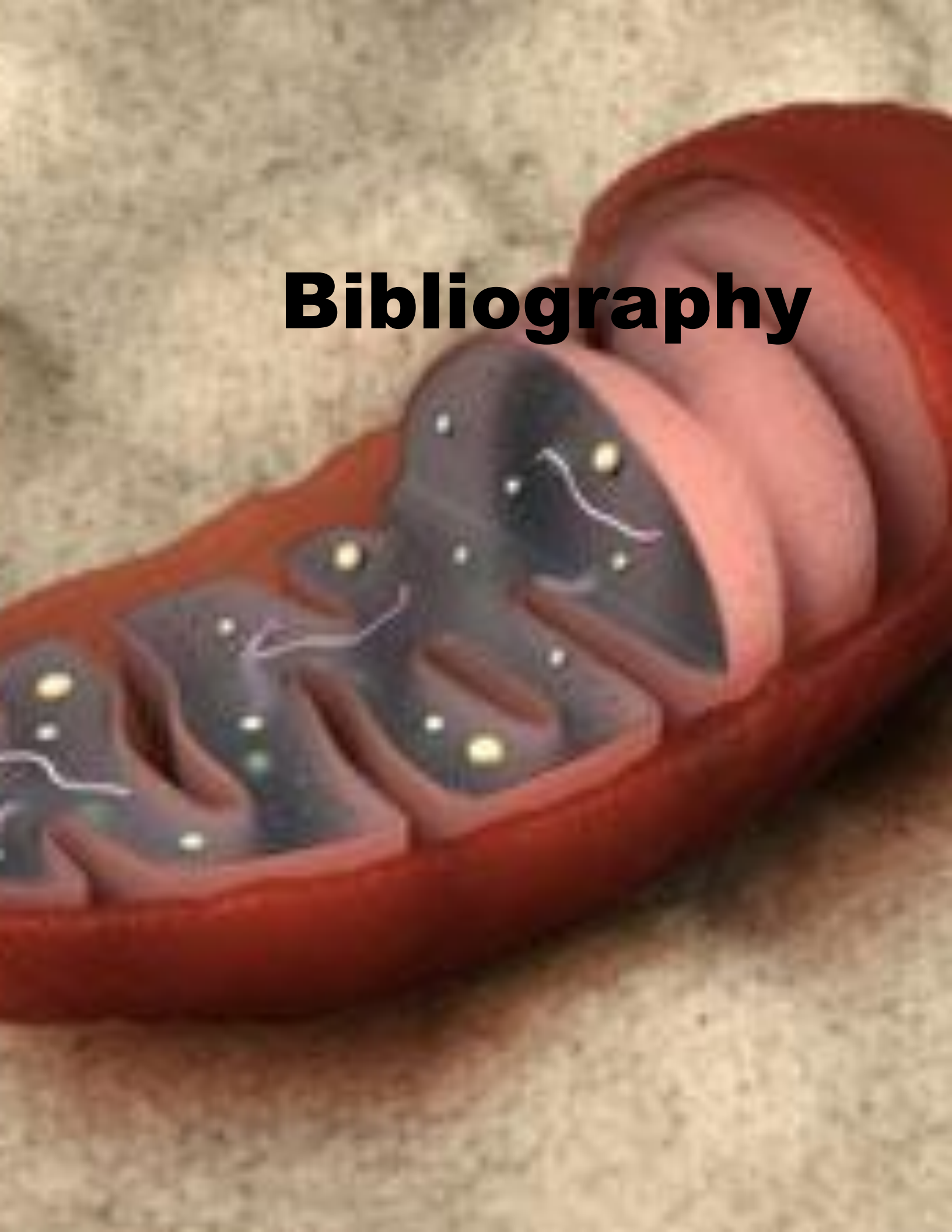

[1] D. C. Wallace, “Mitochondria and cancer,” *Nat. Rev. Cancer*, vol. 12, no. 10, pp. 685–698, Oct. 2012.

[2] S. W. G. Tait and D. R. Green, “Mitochondria and cell death: outer membrane permeabilization and beyond,” *Nat. Rev. Mol. Cell Biol.*, vol. 11, no. 9, pp. 621–632, Sep. 2010.

[3] K. Henze and W. Martin, “Evolutionary biology: Essence of mitochondria,” *Nature*, vol. 426, no. 6963, pp. 127–128, Nov. 2003.

[4] J. N. Timmis, M. A. Ayliffe, C. Y. Huang, and W. Martin, “Endosymbiotic gene transfer: organelle genomes forge eukaryotic chromosomes,” *Nat. Rev. Genet.*, vol. 5, no. 2, pp. 123–135, Feb. 2004.

[5] D. Speijer, “How the mitochondrion was shaped by radical differences in substrates: What carnitine shuttles and uncoupling tell us about mitochondrial evolution in response to ROS,” *BioEssays News Rev. Mol. Cell. Dev. Biol.*, vol. 36, no. 7, pp. 634–643, Jul. 2014.

[6] H. Chen and D. C. Chan, “Mitochondrial dynamics–fusion, fission, movement, and mitophagy–in neurodegenerative diseases,” *Hum. Mol. Genet.*, vol. 18, no. R2, pp. R169–R176, Oct. 2009.

[7] C. Gerbeth, D. Mikropoulou, and C. Meisinger, “From inventory to functional mechanisms: regulation of the mitochondrial protein import machinery by phosphorylation,” *FEBS J.*, vol. 280, no. 20, pp. 4933–4942, Oct. 2013.

[8] T. G. Frey and C. A. Mannella, “The internal structure of mitochondria,” *Trends Biochem. Sci.*, vol. 25, no. 7, pp. 319–324, Jan. 2000.

[9] A. Sickmann, J. Reinders, Y. Wagner, C. Joppich, R. Zahedi, H. E. Meyer, B. Schönfisch, I. Perschil, A. Chacinska, B. Guiard, P. Rehling, N. Pfanner, and C. Meisinger, “The proteome of Saccharomyces cerevisiae mitochondria,” *Proc. Natl. Acad. Sci. U. S. A.*, vol. 100, no. 23, pp. 13207–13212, Nov. 2003.

[10] S. E. Calvo and V. K. Mootha, “The mitochondrial proteome and human disease,” *Annu. Rev. Genomics Hum. Genet.*, vol. 11, pp. 25–44, 2010.

[11] A. Chacinska, C. M. Koehler, D. Milenkovic, T. Lithgow, and N. Pfanner, “Importing mitochondrial proteins: machineries and mechanisms,” *Cell*, vol. 138, no. 4, pp. 628–644, Aug. 2009.

[12] F. U. Hartl, “Molecular chaperones in cellular protein folding,” *Nature*, vol. 381, no. 6583, pp. 571–580, Jun. 1996.

[13] A. S. Savel’ev, L. A. Novikova, I. E. Kovaleva, V. N. Luzikov, W. Neupert, and T. Langer, “ATP-dependent Proteolysis in Mitochondria m-AAA PROTEASE AND PIM1 PROTEASE

EXERT OVERLAPPING SUBSTRATE SPECIFICITIES AND COOPERATE WITH THE mtHsp70 SYSTEM," *J. Biol. Chem.*, vol. 273, no. 32, pp. 20596–20602, Aug. 1998.

[14] F. R. Jornayvaz and G. I. Shulman, "Regulation of mitochondrial biogenesis," *Essays Biochem.*, vol. 47, pp. 69–84, 2010.

[15] T. Wenz, "Regulation of mitochondrial biogenesis and PGC-1α under cellular stress," *Mitochondrion*, vol. 13, no. 2, pp. 134–142, Mar. 2013.

[16] S. Leigh-Brown, J. A. Enriquez, and D. T. Odom, "Nuclear transcription factors in mammalian mitochondria," *Genome Biol.*, vol. 11, no. 7, p. 215, Jul. 2010.

[17] K. Szczepanek, E. J. Lesnefsky, and A. C. Larner, "Multi-Tasking: Nuclear Transcription Factors with Novel Roles in the Mitochondria," *Trends Cell Biol.*, vol. 22, no. 8, pp. 429–437, Aug. 2012.

[18] U. Ahting, M. Thieffry, H. Engelhardt, R. Hegerl, W. Neupert, and S. Nussberger, "Tom40, the Pore-Forming Component of the Protein-Conducting Tom Channel in the Outer Membrane of Mitochondria," *J. Cell Biol.*, vol. 153, no. 6, pp. 1151–1160, Jun. 2001.

[19] K. Gabriel, B. Egan, and T. Lithgow, "Tom40, the import channel of the mitochondrial outer membrane, plays an active role in sorting imported proteins," *EMBO J.*, vol. 22, no. 10, pp. 2380–2386, May 2003.

[20] D. Mokranjac and W. Neupert, "The many faces of the mitochondrial TIM23 complex," *Biochim. Biophys. Acta BBA - Bioenerg.*, vol. 1797, no. 6–7, pp. 1045–1054, Jun. 2010.

[21] H. Yamamoto, M. Esaki, T. Kanamori, Y. Tamura, S. ichi Nishikawa, and T. Endo, "Tim50 is a subunit of the TIM23 complex that links protein translocation across the outer and inner mitochondrial membranes," *Cell*, vol. 111, no. 4, pp. 519–528, Nov. 2002.

[22] D. Mokranjac and W. Neupert, "Thirty years of protein translocation into mitochondria: Unexpectedly complex and still puzzling," *Biochim. Biophys. Acta BBA - Mol. Cell Res.*, vol. 1793, no. 1, pp. 33–41, Jan. 2009.

[23] M. Krayl, J. H. Lim, F. Martin, B. Guiard, and W. Voos, "A cooperative action of the ATP-dependent import motor complex and the inner membrane potential drives mitochondrial preprotein import," *Mol. Cell. Biol.*, vol. 27, no. 2, pp. 411–425, Jan. 2007.

[24] P. Kovermann, K. N. Truscott, B. Guiard, P. Rehling, N. B. Sepuri, H. Müller, R. E. Jensen, R. Wagner, and N. Pfanner, "Tim22, the essential core of the mitochondrial protein insertion complex, forms a voltage-activated and signal-gated channel," *Mol. Cell*, vol. 9, no. 2, pp. 363–373, Feb. 2002.

[25] C. M. Koehler, M. P. Murphy, N. A. Bally, D. Leuenberger, W. Oppliger, L. Dolfini, T. Junne, G. Schatz, and E. Or, "Tim18p, a new subunit of the TIM22 complex that mediates insertion of imported proteins into the yeast mitochondrial inner membrane," *Mol. Cell. Biol.*, vol. 20, no. 4, pp. 1187–1193, Feb. 2000.

[26] C. Schulz, A. Schendzielorz, and P. Rehling, “Unlocking the presequence import pathway,” *Trends Cell Biol.*, vol. 25, no. 5, pp. 265–275, May 2015.

[27] K. Model, C. Meisinger, T. Prinz, N. Wiedemann, K. N. Truscott, N. Pfanner, and M. T. Ryan, “Multistep assembly of the protein import channel of the mitochondrial outer membrane,” *Nat. Struct. Biol.*, vol. 8, no. 4, pp. 361–370, Apr. 2001.

[28] J. Melin, C. Schulz, L. Wrobel, O. Bernhard, A. Chacinska, O. Jahn, B. Schmidt, and P. Rehling, “Presequence recognition by the tom40 channel contributes to precursor translocation into the mitochondrial matrix,” *Mol. Cell. Biol.*, vol. 34, no. 18, pp. 3473–3485, Sep. 2014.

[29] A. B. Harbauer, M. Opalińska, C. Gerbeth, J. S. Herman, S. Rao, B. Schönfisch, B. Guiard, O. Schmidt, N. Pfanner, and C. Meisinger, “Mitochondria. Cell cycle-dependent regulation of mitochondrial preprotein translocase,” *Science*, vol. 346, no. 6213, pp. 1109–1113, Nov. 2014.

[30] A. I. Padrão, R. Vitorino, J. A. Duarte, R. Ferreira, and F. Amado, “Unraveling the phosphoproteome dynamics in mammal mitochondria from a network perspective,” *J. Proteome Res.*, vol. 12, no. 10, pp. 4257–4267, Oct. 2013.

[31] P. A. Grimsrud, J. J. Carson, A. S. Hebert, S. L. Hubler, N. M. Niemi, D. J. Bailey, A. Jochem, D. S. Stapleton, M. P. Keller, M. S. Westphall, B. S. Yandell, A. D. Attie, J. J. Coon, and D. J. Pagliarini, “A quantitative map of the liver mitochondrial phosphoproteome reveals posttranslational control of ketogenesis,” *Cell Metab.*, vol. 16, no. 5, pp. 672–683, Nov. 2012.

[32] X. Zhao, I. R. León, S. Bak, M. Mogensen, K. Wrzesinski, K. Højlund, and O. N. Jensen, “Phosphoproteome analysis of functional mitochondria isolated from resting human muscle reveals extensive phosphorylation of inner membrane protein complexes and enzymes,” *Mol. Cell. Proteomics MCP*, vol. 10, no. 1, p. M110.000299, Jan. 2011.

[33] V. L. Hewitt, E. Heinz, M. Shingu-Vazquez, Y. Qu, B. Jelicic, T. L. Lo, T. H. Beilharz, G. Dumsday, K. Gabriel, A. Traven, and T. Lithgow, “A model system for mitochondrial biogenesis reveals evolutionary rewiring of protein import and membrane assembly pathways,” *Proc. Natl. Acad. Sci. U. S. A.*, vol. 109, no. 49, pp. E3358–3366, Dec. 2012.

[34] D. A. Hood, P. J. Adhihetty, M. Colavecchia, J. W. Gordon, I. Irrcher, A.-M. Joseph, S. T. Lowe, and A. A. Rungi, “Mitochondrial biogenesis and the role of the protein import pathway,” *Med. Sci. Sports Exerc.*, vol. 35, no. 1, pp. 86–94, Jan. 2003.

[35] B. Bukau and A. L. Horwich, “The Hsp70 and Hsp60 chaperone machines,” *Cell*, vol. 92, no. 3, pp. 351–366, Feb. 1998.

[36] U. Jakob and J. Buchner, “Assisting spontaneity: the role of Hsp90 and small Hsps as molecular chaperones,” *Trends Biochem. Sci.*, vol. 19, no. 5, pp. 205–211, May 1994.

[37] Y. E. Kim, M. S. Hipp, A. Bracher, M. Hayer-Hartl, and F. Ulrich Hartl, “Molecular Chaperone Functions in Protein Folding and Proteostasis,” *Annu. Rev. Biochem.*, vol. 82, no. 1, pp. 323–355, 2013.

[38] B. Singh, H. V. Patel, R. G. Ridley, K. B. Freeman, and R. S. Gupta, “Mitochondrial import of the human chaperonin (HSP60) protein,” *Biochem. Biophys. Res. Commun.*, vol. 169, no. 2, pp. 391–396, Jun. 1990.

[39] K. Liberek, A. Lewandowska, and S. Ziętkiewicz, “Chaperones in control of protein disaggregation,” *EMBO J.*, vol. 27, no. 2, pp. 328–335, Jan. 2008.

[40] P. Faou and N. J. Hoogenraad, “Tom34: A cytosolic cochaperone of the Hsp90/Hsp70 protein complex involved in mitochondrial protein import,” *Biochim. Biophys. Acta BBA - Mol. Cell Res.*, vol. 1823, no. 2, pp. 348–357, Feb. 2012.

[41] K. Luce, A. C. Weil, and H. D. Osiewacz, “Mitochondrial protein quality control systems in aging and disease,” *Adv. Exp. Med. Biol.*, vol. 694, pp. 108–125, 2010.

[42] F. Gerdes, T. Tatsuta, and T. Langer, “Mitochondrial AAA proteases — Towards a molecular understanding of membrane-bound proteolytic machines,” *Biochim. Biophys. Acta BBA - Mol. Cell Res.*, vol. 1823, no. 1, pp. 49–55, Jan. 2012.

[43] K. S. Makarova and N. V. Grishin, “Thermolysin and mitochondrial processing peptidase: how far structure-functional convergence goes,” *Protein Sci. Publ. Protein Soc.*, vol. 8, no. 11, pp. 2537–2540, Nov. 1999.

[44] O. Gakh, P. Cavadini, and G. Isaya, “Mitochondrial processing peptidases,” *Biochim. Biophys. Acta BBA - Mol. Cell Res.*, vol. 1592, no. 1, pp. 63–77, Sep. 2002.

[45] J. K. Ngo, L. C. D. Pomatto, and K. J. A. Davies, “Upregulation of the mitochondrial Lon Protease allows adaptation to acute oxidative stress but dysregulation is associated with chronic stress, disease, and aging,” *Redox Biol.*, vol. 1, no. 1, pp. 258–264, 2013.

[46] Y. Matsushima and L. S. Kaguni, “Matrix proteases in mitochondrial DNA function,” *Biochim. Biophys. Acta*, vol. 1819, no. 9–10, pp. 1080–1087, Oct. 2012.

[47] B. R. Francis and P. E. Thorsness, “Hsp90 and mitochondrial proteases Yme1 and Yta10/12 participate in ATP synthase assembly in Saccharomyces cerevisiae,” *Mitochondrion*, vol. 11, no. 4, pp. 587–600, Jul. 2011.

[48] G. Steglich, W. Neupert, and T. Langer, “Prohibitins regulate membrane protein degradation by the m-AAA protease in mitochondria,” *Mol. Cell. Biol.*, vol. 19, no. 5, pp. 3435–3442, May 1999.

[49] H.-J. Park, Y.-M. Seong, J.-Y. Choi, S. Kang, and H. Rhim, “Alzheimer’s disease-associated amyloid beta interacts with the human serine protease HtrA2/Omi,” *Neurosci. Lett.*, vol. 357, no. 1, pp. 63–67, Feb. 2004.

[50] S. Sekine, Y. Kanamaru, M. Koike, A. Nishihara, M. Okada, H. Kinoshita, M. Kamiyama, J. Maruyama, Y. Uchiyama, N. Ishihara, K. Takeda, and H. Ichijo, “Rhomboid protease PARL mediates the mitochondrial membrane potential loss-induced cleavage of PGAM5,” *J. Biol. Chem.*, vol. 287, no. 41, pp. 34635–34645, Oct. 2012.

[51] V. N. Kotiadis, M. R. Duchen, and L. D. Osellame, "Mitochondrial quality control and communications with the nucleus are important in maintaining mitochondrial function and cell health," *Biochim. Biophys. Acta BBA - Gen. Subj.*, vol. 1840, no. 4, pp. 1254–1265, Apr. 2014.

[52] P. Mitchell and J. Moyle, "Chemiosmotic Hypothesis of Oxidative Phosphorylation," *Nature*, vol. 213, no. 5072, pp. 137–139, Jan. 1967.

[53] J. A. Smeitink, J. L. Loeffen, R. H. Triepels, R. J. Smeets, J. M. Trijbels, and L. P. van den Heuvel, "Nuclear genes of human complex I of the mitochondrial electron transport chain: state of the art," *Hum. Mol. Genet.*, vol. 7, no. 10, pp. 1573–1579, 1998.

[54] E. Fernández-Vizarra, V. Tiranti, and M. Zeviani, "Assembly of the oxidative phosphorylation system in humans: what we have learned by studying its defects," *Biochim. Biophys. Acta*, vol. 1793, no. 1, pp. 200–211, Jan. 2009.

[55] L. A. Gómez, J. S. Monette, J. D. Chavez, C. S. Maier, and T. M. Hagen, "Supercomplexes of the Mitochondrial Electron Transport Chain Decline in the Aging Rat Heart," *Arch. Biochem. Biophys.*, vol. 490, no. 1, pp. 30–35, Oct. 2009.

[56] T. A. Rouault and W.-H. Tong, "Iron-sulphur cluster biogenesis and mitochondrial iron homeostasis," *Nat. Rev. Mol. Cell Biol.*, vol. 6, no. 4, pp. 345–351, Apr. 2005.

[57] R. Dutkiewicz, J. Marszalek, B. Schilke, E. A. Craig, R. Lill, and U. Mühlenhoff, "The Hsp70 chaperone Ssq1p is dispensable for iron-sulfur cluster formation on the scaffold protein Isu1p," *J. Biol. Chem.*, vol. 281, no. 12, pp. 7801–7808, Mar. 2006.

[58] I. Ferecatu, S. Gonçalves, M.-P. Golinelli-Cohen, M. Clémancey, A. Martelli, S. Riquier, E. Guittet, J.-M. Latour, H. Puccio, J.-C. Drapier, E. Lescop, and C. Bouton, "The diabetes drug target MitoNEET governs a novel trafficking pathway to rebuild an Fe-S cluster into cytosolic aconitase/iron regulatory protein 1," *J. Biol. Chem.*, vol. 289, no. 41, pp. 28070–28086, Oct. 2014.

[59] O. Stehling and R. Lill, "The Role of Mitochondria in Cellular Iron–Sulfur Protein Biogenesis: Mechanisms, Connected Processes, and Diseases," *Cold Spring Harb. Perspect. Biol.*, vol. 5, no. 8, p. a011312, Aug. 2013.

[60] C. T. Moraes, "What regulates mitochondrial DNA copy number in animal cells?," *Trends Genet. TIG*, vol. 17, no. 4, pp. 199–205, Apr. 2001.

[61] D. Bogenhagen and D. A. Clayton, "Mouse L cell mitochondrial DNA molecules are selected randomly for replication throughout the cell cycle," *Cell*, vol. 11, no. 4, pp. 719–727, Aug. 1977.

[62] H. A. L. Tuppen, E. L. Blakely, D. M. Turnbull, and R. W. Taylor, "Mitochondrial DNA mutations and human disease," *Biochim. Biophys. Acta BBA - Bioenerg.*, vol. 1797, no. 2, pp. 113–128, Feb. 2010.

[63] S. I. Liochev, "Reactive oxygen species and the free radical theory of aging," *Free Radic. Biol. Med.*, vol. 60, pp. 1–4, Jul. 2013.

[64] M. P. Murphy, “How mitochondria produce reactive oxygen species,” *Biochem. J.*, vol. 417, no. 1, pp. 1–13, Jan. 2009.

[65] L. Bleier and S. Dröse, “Superoxide generation by complex III: from mechanistic rationales to functional consequences,” *Biochim. Biophys. Acta*, vol. 1827, no. 11–12, pp. 1320–1331, Dec. 2013.

[66] T. Finkel, “Signal transduction by reactive oxygen species,” *J. Cell Biol.*, vol. 194, no. 1, pp. 7–15, Jul. 2011.

[67] R. S. Balaban, S. Nemoto, and T. Finkel, “Mitochondria, oxidants, and aging,” *Cell*, vol. 120, no. 4, pp. 483–495, Feb. 2005.

[68] H. Kharrazi, A. Vaisi-Raygani, Z. Rahimi, H. Tavilani, M. Aminian, and T. Pourmotabbed, “Association between enzymatic and non-enzymatic antioxidant defense mechanism with apolipoprotein E genotypes in Alzheimer disease,” *Clin. Biochem.*, vol. 41, no. 12, pp. 932–936, Aug. 2008.

[69] M. Morel, A. Kohler, F. Martin, E. Gelhaye, and N. Rouhier, “Comparison of the thiol-dependent antioxidant systems in the ectomycorrhizal Laccaria bicolor and the saprotrophic Phanerochaete chrysosporium,” *New Phytol.*, vol. 180, no. 2, pp. 391–407, 2008.

[70] A. R. Parker, P. N. Petluru, V. L. Nienaber, J. Badger, B. D. Leverett, K. Jair, V. Sridhar, C. Logan, P. Y. Ayala, H. Kochat, and F. H. Hausheer, “Cysteine specific targeting of the functionally distinct peroxiredoxin and glutaredoxin proteins by the investigational disulfide BNP7787,” *Mol. Basel Switz.*, vol. 20, no. 3, pp. 4928–4950, 2015.

[71] H. D. Teixeira, R. I. Schumacher, and R. Meneghini, “Lower intracellular hydrogen peroxide levels in cells overexpressing CuZn-superoxide dismutase,” *Proc. Natl. Acad. Sci. U. S. A.*, vol. 95, no. 14, pp. 7872–7875, Jul. 1998.

[72] N. Rouhier and J.-P. Jacquot, “Molecular and catalytic properties of a peroxiredoxin–glutaredoxin hybrid from Neisseria meningitidis,” *FEBS Lett.*, vol. 554, no. 1–2, pp. 149–153, Nov. 2003.

[73] N. Rouhier, E. Gelhaye, and J. P. Jacquot, “Glutaredoxin-dependent peroxiredoxin from poplar: protein-protein interaction and catalytic mechanism,” *J. Biol. Chem.*, vol. 277, no. 16, pp. 13609–13614, Apr. 2002.

[74] T. Finkel and N. J. Holbrook, “Oxidants, oxidative stress and the biology of ageing,” *Nature*, vol. 408, no. 6809, pp. 239–247, Nov. 2000.

[75] B. S. Berlett and E. R. Stadtman, “Protein Oxidation in Aging, Disease, and Oxidative Stress,” *J. Biol. Chem.*, vol. 272, no. 33, pp. 20313–20316, Aug. 1997.

[76] C. C. Winterbourn and M. B. Hampton, “Thiol chemistry and specificity in redox signaling,” *Free Radic. Biol. Med.*, vol. 45, no. 5, pp. 549–561, Sep. 2008.

[77] T. Ida, T. Sawa, H. Ihara, Y. Tsuchiya, Y. Watanabe, Y. Kumagai, M. Suematsu, H. Motohashi, S. Fujii, T. Matsunaga, M. Yamamoto, K. Ono, N. O. Devarie-Baez, M. Xian, J. M. Fukuto, and T. Akaike, "Reactive cysteine persulfides and S-polythiolation regulate oxidative stress and redox signaling," *Proc. Natl. Acad. Sci.*, vol. 111, no. 21, pp. 7606–7611, May 2014.

[78] C. E. Paulsen and K. S. Carroll, "Cysteine-Mediated Redox Signaling: Chemistry, Biology, and Tools for Discovery," *Chem. Rev.*, vol. 113, no. 7, pp. 4633–4679, Jul. 2013.

[79] C. Klomsiri, P. A. Karplus, and L. B. Poole, "Cysteine-Based Redox Switches in Enzymes," *Antioxid. Redox Signal.*, vol. 14, no. 6, pp. 1065–1077, Mar. 2011.

[80] R. Brigelius-Flohé and L. Flohé, "Basic Principles and Emerging Concepts in the Redox Control of Transcription Factors," *Antioxid. Redox Signal.*, vol. 15, no. 8, pp. 2335–2381, Oct. 2011.

[81] H. Liu, R. Colavitti, I. I. Rovira, and T. Finkel, "Redox-Dependent Transcriptional Regulation," *Circ. Res.*, vol. 97, no. 10, pp. 967–974, Nov. 2005.

[82] D. Trachootham, W. Lu, M. A. Ogasawara, N. R.-D. Valle, and P. Huang, "Redox Regulation of Cell Survival," *Antioxid. Redox Signal.*, vol. 10, no. 8, pp. 1343–1374, Aug. 2008.

[83] H. Ruan, X. D. Tang, M.-L. Chen, M.-L. A. Joiner, G. Sun, N. Brot, H. Weissbach, S. H. Heinemann, L. Iverson, C.-F. Wu, T. Hoshi, M.-L. Chen, M. A. Joiner, and S. H. Heinemann, "High-quality life extension by the enzyme peptide methionine sulfoxide reductase," *Proc. Natl. Acad. Sci. U. S. A.*, vol. 99, no. 5, pp. 2748–2753, Mar. 2002.

[84] G. V. Kryukov, R. A. Kumar, A. Koc, Z. Sun, and V. N. Gladyshev, "Selenoprotein R is a zinc-containing stereo-specific methionine sulfoxide reductase," *Proc. Natl. Acad. Sci. U. S. A.*, vol. 99, no. 7, pp. 4245–4250, Apr. 2002.

[85] J. Moskovitz, "Methionine sulfoxide reductases: ubiquitous enzymes involved in antioxidant defense, protein regulation, and prevention of aging-associated diseases," *Biochim. Biophys. Acta*, vol. 1703, no. 2, pp. 213–219, Jan. 2005.

[86] E. P. Skaar, D. M. Tobiason, J. Quick, R. C. Judd, H. Weissbach, F. Etienne, N. Brot, and H. S. Seifert, "The outer membrane localization of the Neisseria gonorrhoeae MsrA/B is involved in survival against reactive oxygen species," *Proc. Natl. Acad. Sci. U. S. A.*, vol. 99, no. 15, pp. 10108–10113, Jul. 2002.

[87] L. A. Denkel, S. A. Horst, S. F. Rouf, V. Kitowski, O. M. Böhm, M. Rhen, T. Jäger, and F.-C. Bange, "Methionine Sulfoxide Reductases Are Essential for Virulence of Salmonella Typhimurium," *PLoS ONE*, vol. 6, no. 11, p. e26974, Nov. 2011.

[88] S. J. Sasindran, S. Saikolappan, and S. Dhandayuthapani, "Methionine sulfoxide reductases and virulence of bacterial pathogens," *Future Microbiol.*, vol. 2, no. 6, pp. 619–630, Dec. 2007.

[89] A. Koc, A. P. Gasch, J. C. Rutherford, H.-Y. Kim, and V. N. Gladyshev, "Methionine sulfoxide reductase regulation of yeast lifespan reveals reactive oxygen species-dependent and -independent components of aging," *Proc. Natl. Acad. Sci. U. S. A.*, vol. 101, no. 21, pp. 7999–8004, May 2004.

[90] J. Moskovitz, B. S. Berlett, J. M. Poston, and E. R. Stadtman, "The yeast peptide-methionine sulfoxide reductase functions as an antioxidant in vivo," *Proc. Natl. Acad. Sci. U. S. A.*, vol. 94, no. 18, pp. 9585–9589, Sep. 1997.

[91] A. Kaya, A. Koc, B. C. Lee, D. E. Fomenko, M. Rederstorff, A. Krol, A. Lescure, and V. N. Gladyshev, "Compartmentalization and regulation of mitochondrial function by methionine sulfoxide reductases in yeast," *Biochemistry (Mosc.)*, vol. 49, no. 39, pp. 8618–8625, Oct. 2010.

[92] H.-Y. Kim and V. N. Gladyshev, "Methionine sulfoxide reduction in mammals: characterization of methionine-R-sulfoxide reductases," *Mol. Biol. Cell*, vol. 15, no. 3, pp. 1055–1064, Mar. 2004.

[93] L. Tarrago, A. Kaya, E. Weerapana, S. M. Marino, and V. N. Gladyshev, "Methionine sulfoxide reductases preferentially reduce unfolded oxidized proteins and protect cells from oxidative protein unfolding," *J. Biol. Chem.*, vol. 287, no. 29, pp. 24448–24459, Jul. 2012.

[94] S. Boschi-Muller, A. Gand, and G. Branlant, "The methionine sulfoxide reductases: Catalysis and substrate specificities," *Arch. Biochem. Biophys.*, vol. 474, no. 2, pp. 266–273, Jun. 2008.

[95] R. G. Midwinter, F.-C. Cheah, J. Moskovitz, M. C. Vissers, and C. C. Winterbourn, "IkappaB is a sensitive target for oxidation by cell-permeable chloramines: inhibition of NF-kappaB activity by glycine chloramine through methionine oxidation," *Biochem. J.*, vol. 396, no. 1, pp. 71–78, May 2006.

[96] R.-J. Hung, C. S. Spaeth, H. G. Yesilyurt, and J. R. Terman, "SelR reverses Mical-mediated oxidation of actin to regulate F-actin dynamics," *Nat. Cell Biol.*, vol. 15, no. 12, pp. 1445–1454, Dec. 2013.

[97] M. A. Ciorba, S. H. Heinemann, H. Weissbach, N. Brot, and T. Hoshi, "Modulation of potassium channel function by methionine oxidation and reduction," *Proc. Natl. Acad. Sci. U. S. A.*, vol. 94, no. 18, pp. 9932–9937, Sep. 1997.

[98] J. R. Erickson, M. A. Joiner, X. Guan, W. Kutschke, J. Yang, C. V. Oddis, R. K. Bartlett, J. S. Lowe, S. E. O'Donnell, N. Aykin-Burns, M. C. Zimmerman, K. Zimmerman, A.-J. L. Ham, R. M. Weiss, D. R. Spitz, M. A. Shea, R. J. Colbran, P. J. Mohler, and M. E. Anderson, "A dynamic pathway for calcium-independent activation of CaMKII by methionine oxidation," *Cell*, vol. 133, no. 3, pp. 462–474, May 2008.

[99] D. A. Capdevila, W. A. Marmisollé, F. Tomasina, V. Demicheli, M. Portela, R. Radi, and D. H. Murgida, "Specific methionine oxidation of cytochrome c in complexes with zwitterionic lipids by hydrogen peroxide: potential implications for apoptosis," *Chem. Sci.*, vol. 6, no. 1, pp. 705–713, Dec. 2014.

[100] A. Drazic, H. Miura, J. Peschek, Y. Le, N. C. Bach, T. Kriehuber, and J. Winter, "Methionine oxidation activates a transcription factor in response to oxidative stress," *Proc. Natl. Acad. Sci. U. S. A.*, vol. 110, no. 23, pp. 9493–9498, Jun. 2013.

[101] S. Luo and R. L. Levine, "Methionine in proteins defends against oxidative stress," *FASEB J.*, vol. 23, no. 2, pp. 464–472, Feb. 2009.

[102] B. Szczesny, T. K. Hazra, J. Papaconstantinou, S. Mitra, and I. Boldogh, "Age-dependent deficiency in import of mitochondrial DNA glycosylases required for repair of oxidatively damaged bases," *Proc. Natl. Acad. Sci. U. S. A.*, vol. 100, no. 19, pp. 10670–10675, Sep. 2003.

[103] A. Marada, P. K. Allu, A. Murari, B. PullaReddy, P. Tammineni, V. R. Thiriveedi, J. Danduprolu, and N. B. V. Sepuri, "Mge1, a nucleotide exchange factor of Hsp70, acts as an oxidative sensor to regulate mitochondrial Hsp70 function," *Mol. Biol. Cell*, vol. 24, no. 6, pp. 692–703, Mar. 2013.

[104] T. Langer, C. Lu, H. Echols, J. Flanagan, M. K. Hayer, and F. U. Hartl, "Successive action of DnaK, DnaJ and GroEL along the pathway of chaperone-mediated protein folding," *Nature*, vol. 356, no. 6371, pp. 683–689, Apr. 1992.

[105] S. A. Knight, N. B. Sepuri, D. Pain, and A. Dancis, "Mt-Hsp70 homolog, Ssc2p, required for maturation of yeast frataxin and mitochondrial iron homeostasis," *J. Biol. Chem.*, vol. 273, no. 29, pp. 18389–18393, Jul. 1998.

[106] D. M. Cyr, T. Langer, and M. G. Douglas, "DnaJ-like proteins: molecular chaperones and specific regulators of Hsp70," *Trends Biochem. Sci.*, vol. 19, no. 4, pp. 176–181, Apr. 1994.

[107] X. Zhu, X. Zhao, W. F. Burkholder, A. Gragerov, C. M. Ogata, M. E. Gottesman, and W. A. Hendrickson, "Structural analysis of substrate binding by the molecular chaperone DnaK," *Science*, vol. 272, no. 5268, pp. 1606–1614, Jun. 1996.

[108] F. U. Hartl and M. Hayer-Hartl, "Molecular chaperones in the cytosol: from nascent chain to folded protein," *Science*, vol. 295, no. 5561, pp. 1852–1858, Mar. 2002.

[109] M. Blamowska, W. Neupert, and K. Hell, "Biogenesis of the mitochondrial Hsp70 chaperone," *J. Cell Biol.*, vol. 199, no. 1, pp. 125–135, Oct. 2012.

[110] K. Mapa, M. Sikor, V. Kudryavtsev, K. Waegemann, S. Kalinin, C. A. M. Seidel, W. Neupert, D. C. Lamb, and D. Mokranjac, "The conformational dynamics of the mitochondrial Hsp70 chaperone," *Mol. Cell*, vol. 38, no. 1, pp. 89–100, Apr. 2010.

[111] J. F. Swain, G. Dinler, R. Sivendran, D. L. Montgomery, M. Stotz, and L. M. Gierasch, "Hsp70 chaperone ligands control domain association via an allosteric mechanism mediated by the interdomain linker," *Mol. Cell*, vol. 26, no. 1, pp. 27–39, Apr. 2007.

[112] C. Harrison, "GrpE, a nucleotide exchange factor for DnaK," *Cell Stress Chaperones*, vol. 8, no. 3, pp. 218–224, Jul. 2003.

[113] B. Westermann, C. Prip-Buus, W. Neupert, and E. Schwarz, “The role of the GrpE homologue, Mge1p, in mediating protein import and protein folding in mitochondria,” *EMBO J.*, vol. 14, no. 14, pp. 3452–3460, Jul. 1995.

[114] C. J. Harrison, M. Hayer-Hartl, M. Di Liberto, F. Hartl, and J. Kuriyan, “Crystal structure of the nucleotide exchange factor GrpE bound to the ATPase domain of the molecular chaperone DnaK,” *Science*, vol. 276, no. 5311, pp. 431–435, Apr. 1997.

[115] S. Laloraya, P. J. Dekker, W. Voos, E. A. Craig, and N. Pfanner, “Mitochondrial GrpE modulates the function of matrix Hsp70 in translocation and maturation of preproteins.,” *Mol. Cell. Biol.*, vol. 15, no. 12, pp. 7098–7105, Dec. 1995.

[116] S. Sakuragi, Q. Liu, and E. Craig, “Interaction between the nucleotide exchange factor Mge1 and the mitochondrial Hsp70 Ssc1,” *J. Biol. Chem.*, vol. 274, no. 16, pp. 11275–11282, Apr. 1999.

[117] S. Orrenius, V. Gogvadze, and B. Zhivotovsky, “Mitochondrial oxidative stress: implications for cell death,” *Annu. Rev. Pharmacol. Toxicol.*, vol. 47, pp. 143–183, 2007.

[118] R. L. Levine, J. Moskovitz, and E. R. Stadtman, “Oxidation of methionine in proteins: roles in antioxidant defense and cellular regulation,” *IUBMB Life*, vol. 50, no. 4–5, pp. 301–307, Nov. 2000.

[119] X.-H. Zhang and H. Weissbach, “Origin and evolution of the protein-repairing enzymes methionine sulphoxide reductases,” *Biol. Rev. Camb. Philos. Soc.*, vol. 83, no. 3, pp. 249–257, Aug. 2008.

[120] S. P. Gabbita, M. Y. Aksenov, M. A. Lovell, and W. R. Markesbery, “Decrease in peptide methionine sulfoxide reductase in Alzheimer’s disease brain,” *J. Neurochem.*, vol. 73, no. 4, pp. 1660–1666, Oct. 1999.

[121] M. Kantorow, J. R. Hawse, T. L. Cowell, S. Benhamed, G. O. Pizarro, V. N. Reddy, and J. F. Hejtmancik, “Methionine sulfoxide reductase A is important for lens cell viability and resistance to oxidative stress,” *Proc. Natl. Acad. Sci. U. S. A.*, vol. 101, no. 26, pp. 9654–9659, Jun. 2004.

[122] C. B. Glaser, G. Yamin, V. N. Uversky, and A. L. Fink, “Methionine oxidation, alpha-synuclein and Parkinson’s disease,” *Biochim. Biophys. Acta*, vol. 1703, no. 2, pp. 157–169, Jan. 2005.

[123] J. Styskal, F. A. Nwagwu, Y. N. Watkins, H. Liang, A. Richardson, N. Musi, and A. B. Salmon, “Methionine sulfoxide reductase A affects insulin resistance by protecting insulin receptor function,” *Free Radic. Biol. Med.*, vol. 56, pp. 123–132, Mar. 2013.

[124] P. Tammineni, C. Anugula, F. Mohammed, M. Anjaneyulu, A. C. Larner, and N. B. V. Sepuri, “The import of the transcription factor STAT3 into mitochondria depends on GRIM-19, a component of the electron transport chain,” *J. Biol. Chem.*, vol. 288, no. 7, pp. 4723–4732, Feb. 2013.

[125] G. Wright, K. Terada, M. Yano, I. Sergeev, and M. Mori, "Oxidative stress inhibits the mitochondrial import of preproteins and leads to their degradation," *Exp. Cell Res.*, vol. 263, no. 1, pp. 107–117, Feb. 2001.

[126] J. P. Grimshaw, I. Jelesarov, H. J. Schönfeld, and P. Christen, "Reversible thermal transition in GrpE, the nucleotide exchange factor of the DnaK heat-shock system," *J. Biol. Chem.*, vol. 276, no. 9, pp. 6098–6104, Mar. 2001.

[127] M. P. Mayer and B. Bukau, "Hsp70 chaperones: Cellular functions and molecular mechanism," *Cell. Mol. Life Sci.*, vol. 62, no. 6, pp. 670–684, Mar. 2005.

[128] T. Lutz, B. Westermann, W. Neupert, and J. M. Herrmann, "The mitochondrial proteins Ssq1 and Jac1 are required for the assembly of iron sulfur clusters in mitochondria," *J. Mol. Biol.*, vol. 307, no. 3, pp. 815–825, Mar. 2001.

[129] R. D. Gietz and R. A. Woods, "Transformation of yeast by lithium acetate/single-stranded carrier DNA/polyethylene glycol method," *Methods Enzymol.*, vol. 350, pp. 87–96, 2002.

[130] Y. Meyer, B. B. Buchanan, F. Vignols, and J.-P. Reichheld, "Thioredoxins and glutaredoxins: unifying elements in redox biology," *Annu. Rev. Genet.*, vol. 43, pp. 335–367, 2009.

[131] R. Pamplona and D. Costantini, "Molecular and structural antioxidant defenses against oxidative stress in animals," *Am. J. Physiol. Regul. Integr. Comp. Physiol.*, vol. 301, no. 4, pp. R843–863, Oct. 2011.

[132] L. Packschies, H. Theyssen, A. Buchberger, B. Bukau, R. S. Goody, and J. Reinstein, "GrpE accelerates nucleotide exchange of the molecular chaperone DnaK with an associative displacement mechanism," *Biochemistry (Mosc.)*, vol. 36, no. 12, pp. 3417–3422, Mar. 1997.

[133] A. F. Mehl, L. D. Heskett, S. S. Jain, and B. Demeler, "Insights into dimerization and four-helix bundle formation found by dissection of the dimer interface of the GrpE protein from Escherichia coli," *Protein Sci. Publ. Protein Soc.*, vol. 12, no. 6, pp. 1205–1215, Jun. 2003.

[134] B. Wu, D. Ang, M. Snavely, and C. Georgopoulos, "Isolation and characterization of point mutations in the Escherichia coli grpE heat shock gene.," *J. Bacteriol.*, vol. 176, no. 22, pp. 6965–6973, Nov. 1994.

[135] P. De Los Rios and P. Goloubinoff, "Protein folding: Chaperoning protein evolution," *Nat. Chem. Biol.*, vol. 8, no. 3, pp. 226–228, Mar. 2012.

[136] O. Iosefson, S. Sharon, P. Goloubinoff, and A. Azem, "Reactivation of protein aggregates by mortalin and Tid1--the human mitochondrial Hsp70 chaperone system," *Cell Stress Chaperones*, vol. 17, no. 1, pp. 57–66, Jan. 2012.

[137] R. Rosenzweig, S. Moradi, A. Zarrine-Afsar, J. R. Glover, and L. E. Kay, "Unraveling the mechanism of protein disaggregation through a ClpB-DnaK interaction," *Science*, vol. 339, no. 6123, pp. 1080–1083, Mar. 2013.

[138] H. S. Marinho, C. Real, L. Cyrne, H. Soares, and F. Antunes, "Hydrogen peroxide sensing, signaling and regulation of transcription factors," *Redox Biol.*, vol. 2, pp. 535–562, 2014.

[139] A. Acharya, I. Das, D. Chandhok, and T. Saha, "Redox regulation in cancer," *Oxid. Med. Cell. Longev.*, vol. 3, no. 1, pp. 23–34, 2010.

[140] T. C. Squier, "Oxidative stress and protein aggregation during biological aging," *Exp. Gerontol.*, vol. 36, no. 9, pp. 1539–1550, Sep. 2001.

[141] L. Ferder, L. A. Romano, L. B. Ercole, I. Stella, and F. Inserra, "Biomolecular changes in the aging myocardium: the effect of enalapril," *Am. J. Hypertens.*, vol. 11, no. 11 Pt 1, pp. 1297–1304, Nov. 1998.

[142] E.-M. Hanschmann, J. R. Godoy, C. Berndt, C. Hudemann, and C. H. Lillig, "Thioredoxins, glutaredoxins, and peroxiredoxins--molecular mechanisms and health significance: from cofactors to antioxidants to redox signaling," *Antioxid. Redox Signal.*, vol. 19, no. 13, pp. 1539–1605, Nov. 2013.

[143] A. Koc and V. N. Gladyshev, "Methionine Sulfoxide Reduction and the Aging Process," *Ann. N. Y. Acad. Sci.*, vol. 1100, no. 1, pp. 383–386, Apr. 2007.

[144] F. Cabreiro, C. R. Picot, B. Friguet, and I. Petropoulos, "Methionine Sulfoxide Reductases," *Ann. N. Y. Acad. Sci.*, vol. 1067, no. 1, pp. 37–44, May 2006.

[145] S. K. Sharma, P. De los Rios, P. Christen, A. Lustig, and P. Goloubinoff, "The kinetic parameters and energy cost of the Hsp70 chaperone as a polypeptide unfoldase," *Nat. Chem. Biol.*, vol. 6, no. 12, pp. 914–920, Dec. 2010.

[146] P. K. Allu, A. Marada, Y. Boggula, S. Karri, T. Krishnamoorthy, and N. B. V. Sepuri, "Methionine sulfoxide reductase 2 reversibly regulates Mge1, a cochaperone of mitochondrial Hsp70, during oxidative stress," *Mol. Biol. Cell*, vol. 26, no. 3, pp. 406–419, Feb. 2015.

[147] A. V. Goswami, B. Chittoor, and P. D'Silva, "Understanding the Functional Interplay between Mammalian Mitochondrial Hsp70 Chaperone Machine Components," *J. Biol. Chem.*, vol. 285, no. 25, pp. 19472–19482, Jun. 2010.

[148] K. Cai, R. O. Frederick, J. H. Kim, N. M. Reinen, M. Tonelli, and J. L. Markley, "Human Mitochondrial Chaperone (mtHSP70) and Cysteine Desulfurase (NFS1) Bind Preferentially to the Disordered Conformation, Whereas Co-chaperone (HSC20) Binds to the Structured Conformation of the Iron-Sulfur Cluster Scaffold Protein (ISCU)," *J. Biol. Chem.*, vol. 288, no. 40, pp. 28755–28770, Oct. 2013.

[149] H.-Y. Kim and J.-R. Kim, "Thioredoxin as a reducing agent for mammalian methionine sulfoxide reductases B lacking resolving cysteine," *Biochem. Biophys. Res. Commun.*, vol. 371, no. 3, pp. 490–494, Jul. 2008.

[150] F. L. Aachmann, G.-H. Kwak, R. Del Conte, H.-Y. Kim, V. N. Gladyshev, and A. Dikiy, "Structural and biochemical analysis of mammalian methionine sulfoxide reductase B2," *Proteins*, vol. 79, no. 11, pp. 3123–3131, Nov. 2011.

[151] X. Liang, A. Kaya, Y. Zhang, D. T. Le, D. Hua, and V. N. Gladyshev, "Characterization of methionine oxidation and methionine sulfoxide reduction using methionine-rich cysteine-free proteins," *BMC Biochem.*, vol. 13, no. 1, p. 21, Oct. 2012.

[152] O. Deloche and C. Georgopoulos, "Purification and biochemical properties of Saccharomyces cerevisiae's Mge1p, the mitochondrial cochaperone of Ssc1p," *J. Biol. Chem.*, vol. 271, no. 39, pp. 23960–23966, Sep. 1996.

[153] E. Ikeda, S. Yoshida, H. Mitsuzawa, I. Uno, and A. Toh-e, "YGE1 is a yeast homologue of Escherichia coli grpE and is required for maintenance of mitochondrial functions," *FEBS Lett.*, vol. 339, no. 3, pp. 265–268, Feb. 1994.

[154] H. K. Khor, M. E. Jacoby, T. C. Squier, G. C. Chu, and D. Chelius, "Identification of methionine sulfoxide diastereomers in immunoglobulin gamma antibodies using methionine sulfoxide reductase enzymes," *mAbs*, vol. 2, no. 3, pp. 299–308, Jun. 2010.

[155] F. U. Hartl, A. Bracher, and M. Hayer-Hartl, "Molecular chaperones in protein folding and proteostasis," *Nature*, vol. 475, no. 7356, pp. 324–332, Jul. 2011.

[156] B. Raman, L. V. Siva Kumar, T. Ramakrishna, and C. Mohan Rao, "Redox-regulated chaperone function and conformational changes of Escherichia coli Hsp33," *FEBS Lett.*, vol. 489, no. 1, pp. 19–24, Jan. 2001.

[157] J. Graumann, H. Lilie, X. Tang, K. A. Tucker, J. H. Hoffmann, J. Vijayalakshmi, M. Saper, J. C. Bardwell, and U. Jakob, "Activation of the redox-regulated molecular chaperone Hsp33--a two-step mechanism," *Struct. Lond. Engl. 1993*, vol. 9, no. 5, pp. 377–387, May 2001.

[158] M. Mollapour and L. Neckers, "Post-translational modifications of Hsp90 and their contributions to chaperone regulation," *Biochim. Biophys. Acta BBA - Mol. Cell Res.*, vol. 1823, no. 3, pp. 648–655, Mar. 2012.

[159] W. B. Pratt, Y. Morishima, H.-M. Peng, and Y. Osawa, "Role of the Hsp90/Hsp70-Based Chaperone Machinery in Making Triage Decisions When Proteins Undergo Oxidative and Toxic Damage," *Exp. Biol. Med. Maywood NJ*, vol. 235, no. 3, pp. 278–289, Mar. 2010.

[160] R. Michael and A. J. Bron, "The ageing lens and cataract: a model of normal and pathological ageing," *Philos. Trans. R. Soc. B Biol. Sci.*, vol. 366, no. 1568, pp. 1278–1292, Apr. 2011.

[161] M. H. Garner and A. Spector, "Selective oxidation of cysteine and methionine in normal and senile cataractous lenses.," *Proc. Natl. Acad. Sci. U. S. A.*, vol. 77, no. 3, pp. 1274–1277, Mar. 1980.

Publications

Mge1, a nucleotide exchange factor of Hsp70, acts as an oxidative sensor to regulate mitochondrial Hsp70 function

Adinarayana Marada, Praveen Kumar Allu, Anjaneyulu Murari, BhoomiReddy PullaReddy, Prasad Tammineni, Venkata Ramana Thiriveedi, Jayasree Danduprolu, and Naresh Babu V. Sepuri
Department of Biochemistry, School of Life Sciences, University of Hyderabad, Hyderabad 500046, India

ABSTRACT **Despite the growing evidence of the role of oxidative stress in disease, its molecular mechanism of action remains poorly understood. The yeast *Saccharomyces cerevisiae* provides a valuable model system in which to elucidate the effects of oxidative stress on mitochondria in higher eukaryotes. Dimeric yeast Mge1, the cochaperone of heat shock protein 70 (Hsp70), is essential for exchanging ATP for ADP on Hsp70 and thus for recycling of Hsp70 for mitochondrial protein import and folding. Here we show an oxidative stress–dependent decrease in Mge1 dimer formation accompanied by a concomitant decrease in Mge1–Hsp70 complex formation in vitro. The Mge1-M155L substitution mutant stabilizes both Mge1 dimer and Mge1–Hsp70 complex formation. Most important, the Mge1-M155L mutant rescues the slow-growth phenomenon associated with the wild-type Mge1 strain in the presence of H_2O_2 in vivo, stimulation of the ATPase activity of Hsp70, and the protein import defect during oxidative stress in vitro. Furthermore, cross-linking studies reveal that Mge1–Hsp70 complex formation in mitochondria isolated from wild-type Mge1 cells is more susceptible to reactive oxygen species compared with mitochondria from Mge1-M155L cells. This novel oxidative sensor capability of yeast Mge1 might represent an evolutionarily conserved function, given that human recombinant dimeric Mge1 is also sensitive to H_2O_2.**

Monitoring Editor
Ramanujan S. Hegde
National Institutes of Health

Received: Oct 5, 2012
Revised: Jan 8, 2013
Accepted: Jan 14, 2013

INTRODUCTION

Mitochondria are essential organelles involved in many cellular processes, such as energy metabolism and apoptosis. Although the mitochondrion has its own genome, it depends on the nucleus for optimal functioning (Chacinska *et al.*, 2009). Based on their signal sequence, mitochondrial proteins encoded by nuclear DNA are targeted to different subcompartments of mitochondria through a translocase system present on outer and inner mitochondrial membranes known as the translocase of outer membrane (TOM) and translocase of inner membrane (TIM) complexes, respectively (Schulke *et al.*, 1997, 1999; Endo *et al.*, 2003; Kutik *et al.*, 2007; Neupert and Herrmann, 2007). Targeting of precursor protein to the matrix involves an interplay among many proteins; however, the final step of this process is mediated by Tim44 and a translocation motor that contains mitochondrial heat shock protein 70 (mHsp70), Pam16, Pam18, and the nucleotide exchange factor Mge1 (Azem *et al.*, 1997; Mokranjac *et al.*, 2007; Stojanovski *et al.*, 2007; Schiller *et al.*, 2008). Hsp70, in combination with Tim44, binds to the emerging end of the transit peptide from the TIM channel in an ATP-dependent manner, and the ATPase cycle of mHsp70 leads to pulling or vectorial translocation of preproteins across the inner mitochondrial membrane (Matouschek *et al.*, 2000; Okamoto *et al.*, 2002; Liu *et al.*, 2003). Mge1, a component of this translocation motor, accelerates the exchange of ATP for ADP on mHsp70 and promotes a change from the high–substrate affinity conformation of mHsp70 to a lower–substrate affinity form with a concomitant release of precursor protein from mHsp70 to begin the next round of translocation

This article was published online ahead of print in MBoC in Press (http://www.molbiolcell.org/cgi/doi/10.1091/mbc.E12-10-0719) on January 23, 2013.

Address correspondence to: Naresh Babu V. Sepuri (nareshuohyd@gmail.com or nbvssl@uohyd.ernet.in).

Abbreviations used: Ccpo, cytochrome *c* peroxidase; DHFR, dihydrofolate reductase; HSP 70, heat shock protein 70; ROS, reactive oxygen species; Tim, translocase of inner membrane; Tom, translocase of outer membrane.

Supplemental Material can be found at:
http://www.molbiolcell.org/content/suppl/2013/01/21/mbc.E12-10-0719v1.DC1.html

Methionine sulfoxide reductase 2 reversibly regulates Mge1, a cochaperone of mitochondrial Hsp70, during oxidative stress

Praveen Kumar Allu, Adinarayana Marada, Yerranna Boggula, Srinivasu Karri, Thanuja Krishnamoorthy, and Naresh Babu V. Sepuri
Department of Biochemistry, School of Life Sciences, University of Hyderabad, Gachibowli, Hyderabad 500046, India

ABSTRACT **Peptide methionine sulfoxide reductases are conserved enzymes that reduce oxidized methionines in protein(s). Although these reductases have been implicated in several human diseases, there is a dearth of information on the identity of their physiological substrates. By using *Saccharomyces cerevisiae* as a model, we show that of the two methionine sulfoxide reductases (MXR1, MXR2), deletion of mitochondrial MXR2 renders yeast cells more sensitive to oxidative stress than the cytosolic MXR1. Our earlier studies showed that Mge1, an evolutionarily conserved nucleotide exchange factor of Hsp70, acts as an oxidative sensor to regulate mitochondrial Hsp70. In the present study, we show that Mxr2 regulates Mge1 by selectively reducing MetO at position 155 and restores the activity of Mge1 both in vitro and in vivo. Mge1 M155L mutant rescues the slow-growth phenotype and aggregation of proteins of *mxr2*Δ strain during oxidative stress. By identifying the first mitochondrial substrate for Mxrs, we add a new paradigm to the regulation of the oxidative stress response pathway.**

Monitoring Editor
Thomas D. Fox
Cornell University

Received: Sep 13, 2014
Revised: Nov 17, 2014
Accepted: Nov 20, 2014

INTRODUCTION

Persistent oxidative stress is responsible for several neurological disorders, heart failure, and ageing (Finkel and Holbrook, 2000; Orrenius *et al.*, 2007). To combat oxidative stress, cellular systems have evolved several antioxidant defensive mechanisms. Methionine sulfoxide reductases (Msrs) are among the important regulators of oxidative stress (Levine *et al.*, 2000). These enzymes reduce either free or protein-bound oxidized methionine in a thioredoxin and thioredoxin reductase–dependent mechanism to prevent the accumulation of oxidized proteins and amino acids. In yeast, they are three methionine sulfoxide reductases, known as fRMsr, Mxr1/MsrA, and Mxr2/MsrB. The first is responsible for reducing free methionine sulfoxide (free Met-SO), and the last two are involved in the reduction of oxidized methionine present in proteins (Boschi-Muller *et al.*, 2008; Le *et al.*, 2009). Oxidation of methionine can produce a diastereomeric mixture of R and S methionine sulfoxide forms. Mxr1 apparently plays a role in reducing the S form of sulfoxide, whereas Mxr2 acts specifically on R sulfoxides. The mechanism of action of these enzymes has been well characterized in vitro using reconstitution assays containing purified Mxrs (Boschi-Muller *et al.*, 2008; Tarrago *et al.*, 2012). Homologues of Mxr proteins are present across evolution and have been found to play an essential role in the prevention of oxidative damage to proteins mediated by reactive oxygen species (ROS) in bacterial, plant, and animal cells (Zhang and Weissbach, 2008). These enzymes have been implicated in ageing and age-related disorders such as Alzheimer and Parkinson disease, cataract development, and insulin resistance (Gabbita *et al.*, 1999; Kantorow *et al.*, 2004; Glaser *et al.*, 2005; Styskal *et al.*, 2013). Despite their clinical relevance, there is a paucity of information on the identity of the physiological substrates of Mxrs and their regulation. Several reports suggest NF-κBα, potassium channel, and calmodulin as possible substrates of Mxrs (Ciorba *et al.*, 1997; Midwinter *et al.*, 2006; Erickson *et al.*, 2008). In a recent report, SelR, a homologue of MsrB in *Drosophila*, was shown to reduce the oxidized R form of methionine in actin and thereby regulate actin polymerization (Hung *et al.*, 2013). In mammals, MsrA has two isoforms present in mitochondria and cytosol, whereas MsrB has multiple isoforms

This article was published online ahead of print in MBoC in Press (http://www.molbiolcell.org/cgi/doi/10.1091/mbc.E14-09-1371) on November 26, 2014.

Address correspondence to: Naresh Babu V. Sepuri (nareshuohyd@gmail.com, nbvssl@uohyd.ernet.in).

Abbreviations used: Hsp70, heat shock protein 70; MALDI-TOF, matrix-assisted laser desorption/ionization time-of-flight; Mge1, mitochondrial GrpE; Mxr, methionine sulfoxide reductase; Tim23, translocase of inner membrane 23.

Supplemental Material can be found at:
http://www.molbiolcell.org/content/suppl/2014/11/24/mbc.E14-09-1371v1.DC1.html

Plagiarism report

Methionine Sulfoxide Reductase mediated Redox regulation of mitochondrial GrpE

by Allu Praveen Kumar

Methionine Sulfoxide Reductase mediated Redox regulation of mitochondrial GrpE

ORIGINALITY REPORT

9%	6%	7%	1%
SIMILARITY INDEX	INTERNET SOURCES	PUBLICATIONS	STUDENT PAPERS

PRIMARY SOURCES

	edoc.ub.uni-muenchen.de	
1	Internet Source	1%
2	www.ncbi.nlm.nih.gov	
	Internet Source	<1%
	www.molbiolcell.org	
3	Internet Source	<1%
4	ec.asm.org	
	Internet Source	<1%